Waseda University
Doctoral Dissertation

Multi-Carrier Transmission Techniques toward Flexible and Efficient Wireless Communication Systems

高効率適応無線通信システムに向けたマルチキャリア伝送方式に関する研究

February 2008

Graduate School of
Global Information and Telecommunication Studies

Ryota Kimura
木村 亮太

Acknowledgement

This dissertation completes achievements of my research activities at Graduate School of Global Information and Telecommunication Studies, Waseda University, Japan, under the supervision of Prof. Shigeru Shimamoto. I would like to deeply thank to Prof. Shimamoto for his guidance and encouragement. I also would like to express my gratitude to Prof. Mitsuji Matsumoto, Prof. Yoshiaki Tanaka and Prof. Takuro Sato for their supervision for this dissertation. In addition, I would like to thank to members of Shimamoto Laboratory for their continuous supports.

A part of this dissertation includes achievements of my researches at Graduate School of Science and Engineering, Chuo University, Japan, under the supervision of Prof. Shoji Shinoda. I really appreciate Prof. Shinoda for his helpful support in my master course life. I also would like to thank to Prof. Hiroshi Shirai and members of Shinoda Laboratory for their kind encouragements.

A part of this dissertation also includes achievements of my researches at National Institute of Information and Communications Technology, Japan, under the supervision of Dr. Hiroshi Harada. I would like to appreciate Dr. Harada for giving me opportunities to deeply study on the area of wireless communications. I am also grateful to Dr. Shuzo Kato for his unwavering leadership in our standardization activities.

Through my research activities, I have received incredible amount of benefit from research experts in the area of wireless communication. In addition to those I appreciate above, I would like to express my appreciation to Dr. Hiroshi Takano of Japan Patent Office, Prof. Seiichi Sampei of Osaka University, Prof. Masahiro Umehira of Ibaraki University, Dr. Yozo Shoji and Dr. Ryuhei Funada of National Institute of Information and Communications Technology and Dr. Kazuyuki Shimezawa of Chuo University (now he is with Sharp Corporation) for their valuable discussions.

Finally, I would like to show my respect for my parents, Naomi and Akio, who

always understand my things.

This work was partly supported by the 21st Century Center of Excellent Program in Waseda University: Productive ICT Academia Program, and Research Fellowship of Japan Society for the Promotion of Science.

Contents

List of Figures

List of Tables

Chapter 1

Introduction

1.1 Current State of Wireless Communication Systems

Recent growths of information technologies have been changing the social infrastructure and human lifestyle. One of the important elements of IT is networking technology connecting computers, servers and information devices. Broadband wired infrastructures, such as community antenna television (CATV), digital subscriber lines (DSLs) and optical fiber, are very popular in urban areas and are providing hundred-Mbps class services. Because of such infrastructures, many people enjoy web-browsing, e-mail, chat, on-line game, video streaming and the other various multimedia entertainments.

The culture of mobile and wireless communication has been also popular since late 1990s. Actually, the second generation mobile communication systems, such as global system for mobile communication (GSM), personal digital communications (PDC) and personal handy-phone system (PHS), are spread over the world. Then, the third generation mobile communication systems called as International Mobile Telecommunication 2000 (IMT-2000) has been launched since 2001 first in Japan. Wideband code division multiple access (W-CDMA) [2], CDMA2000 [3] and time-division CDMA (TD-CDMA) [4] are the representatives of IMT-2000. These systems provide several Mbps of maximum data rate for the outdoor users. Moreover, their advanced systems such as high-speed packet access (HSPA) [5] will provide up to several tens Mbps of data rate.

From the point of indoor environments, wireless local area network (WLAN) systems have succeeded to open the wireless market [6],[7]. The WLAN standards of the Institute of Electrical and Electronics Engineers (IEEE) 802.11a/b/g [8],[9]

can provide 54 Mbps of maximum data rate. They can configure the office and in-home networks easily. Almost all the latest models of laptop computers include WLAN chips as standard equipments.

Moreover, new concepts are coming, those are wireless personal area networks (WPANs) and wireless body area networks (BANs). The target of WPANs is communicating devices in very short range of areas, up to several meters [25]–[27]. The various data rate of WPANs will be prepared for widely assumed situations, for example, very low speed communication with very low power consumption for sensor networks, and ultra high speed communication up to several Gbps for in-home connections among set-top boxes, audio equipments and screens. WBANs are much shorter range and lower power consumption communication around the human body. They sometimes use the human body itself as a transmission medium [28]. The promising application of WBANs is medical and health solution, which monitors physical conditions by using wearable devices, implant medical devices and so on. Some task groups of IEEE802.15 have been discussing the establishment of WPANs and WBANs standards. Ultra-wideband (UWB) [29], [30] and millimeter-wave technologies [31]–[34] have attracted attention in the IEEE802.15 standardization body.

1.2 MC Transmission Comes on

From the past, single-carrier (SC) transmission techniques are mainly adopted as physical (PHY) layer specifications of wireless systems [35]. The SC transmission techniques are very simple and sufficient for narrowband access where transmitted signals suffer from flat fading. However, recent wireless systems desire higher data rate with using broadband channels. The SC transmission techniques are often insufficient for such a broadband access where transmitted signals suffer from inter-symbol interference (ISI) and frequency selective fading. To overcome ISI and frequency selective fading, the SC transmission techniques require some equalization techniques such as decision feedback equalization and maximum likelihood sequence estimation [35]–[40]. Such equalization techniques increase high complexity of signal processing and then increase the size and cost of hardware.

Multi-carrier (MC) transmission [43]–[47] came on as alternative PHY techniques. The MC transmission techniques provide high spectral efficiency and flexibility of spectral management to wireless systems. In addition, it also provides

robustness against inter-symbol interference (ISI) with helps of guard interval (GI) and frequency-domain signal processing. The MC transmission techniques can overcome the weakness of SC ones by the above features. In other words, it can be seen that the MC transmission is more suitable for the broadband access than the SC transmission. Actually, since late 1990s, the MC transmission techniques have adopted for some practical wireless systems such as digital broadcasting and WLAN described above.

1.3 Current and Future Problems around Multi-Carrier Transmission Techniques

The next generation IT has been moving toward "ubiquitous world [1]." The goal of ubiquitous world is connecting all people, computers, information devices and any other objects whenever and wherever via incognizant networks. From the point of wireless networks, the existing wireless technologies must be not enough to realize and satisfy the ubiquitous world. Thus, the wireless researchers and developers have to address higher speed, spectral efficient and flexible communication systems. It is generally said that the fourth generation mobile systems, or IMT-Advanced named by International Telecommunication Union (ITU) Radiocommunication Sector (ITU-R) [24], should provide 100 Mbps of data rate in highly mobile environments and 1 Gbps of that in static environments [16]–[23]. In the development of mobile communication systems, several standardization bodies, such as the Third Generation Partnership Project (3GPP), 3GPP2, IEEE802.16 and IEEE802.20, have been discussing evolved wireless access toward IMT-Advanced [2], [3], [10]–[15].

There are the following three problems related to the development of flexible and efficient wireless communication systems with MC transmission techniques:

Problem (1): What air interface is suitable for the next generation mobile communication systems?

Problem (2): Can the choice of existing duplex schemes satisfy the requirements of future wireless communication systems for eternity?

Problem (3): How should we consider the relationship between the SC and MC transmission techniques for building wireless system standards?

1.3.1 Candidates of Air Interface for Next Generation Mobile Communication Systems

As mentioned above, CDMA is adopted for the PHY layer air interface of IMT-2000 systems. Meanwhile, orthogonal frequency division multiplexing (OFDM) [44], [45], which is based on the MC transmission techniques, is adopted for that of IEEE802.11a/g based WLAN systems. The MC transmission techniques also have attracted much attention for the PHY air interface of IMT-Advanced because of the features of them. In early 2000s, orthogonal frequency and code division multiplexing (OFCDM) [20], [48]–[50] was proposed for bridging between CDMA and OFDM. It can be seen that the main concept of OFCDM is similar to that of CDMA in a sense. Users' signals are multiplexed in the code-domain in OFCDM as well as in CDMA. In addition, single frequency reuse also is realized by the spreading codes. The proposal of OFCDM focused on a seamless PHY interface between multi-cell and hot-spot systems by introducing variable spreading factor. One of significant problems of OFCDM is inter-code interference, which is caused even in single cell configuration. Two dimensional code allocation was proposed for mitigating the impact of inter-code interference [20], [48]–[50]. However, this allocation algorithm has to consider the cell configuration, the number of active users, interference affect and so on. It will be too complicated in the broadband mobile communication systems. It is unassured that OFCDM will maximize the ability of MC transmission technique for realizing the mobile communication systems.

Orthogonal frequency division multiple access (OFDMA) is another air interface based on the MC based multiple access schemes [44], [46], [53]–[57]. OFDMA employs its flexibility of spectral resource management for the multiple access. The users' signals are multiplexed in the frequency-domain by using orthogonal and narrowband sub-carriers. Because of the orthogonal sub-carriers, OFDMA improves the spectral efficiency more than frequency division multiple access (FDMA). The most advantage of OFDMA is multi-user diversity effect brought by adaptive bit, power and user allocation [173]–[177]. This diversity is more effective in the broadband wireless access systems in which signals will suffer from frequency-selective fading. It will be difficult for OFCDM to obtain such a diversity effect because all signals are overlapped over the frequency-domain. Thus, it can be said that OFDMA uses the ability of MC transmission techniques more effectively than OFCDM and that OFDMA is a powerful candidate for the future mobile communication systems.

1.3.2 Duplexing Scheme for Future Wireless Communication Systems

Duplexing is the key factor of wireless communication systems as well as multiplexing and multiple access. Duplexing prepares forward and reverse link channels which user terminals (UTs) use to communicate each other. Frequency division duplex (FDD) and time division duplex (TDD) have been adopted to the existing wireless communication systems for a long time [35]. FDD is the most popular duplex scheme in the current wireless access systems. In the FDD systems, UT can easily separate desired and undesired signals by a band pass filter because the duplex channels consist of different frequency bands. Moreover, FDD requires no particular synchronization between the forward and reverse link channels. TDD is another famous scheme. In the TDD systems, UTs share the same frequency band but use different time slots to receive the forward link signals and transmit the reverse link ones. The capacity of TDD is variable by changing the number of slots assigned to the forward and reverse links. Then, TDD is more suitable for the wireless systems with asymmetric traffics.

Compared to multiplexing and multiple access, duplexing itself is hardly treated as the research topic in these days. Proposals of Hybrid FDD and TDD schemes can be found for flexible wireless communication systems [178]–[180]. However, no new concept of duplexing itself has appears. It is unassured that the choice of FDD or TDD will satisfy the requirements of future wireless communication systems. And then, a novel duplexing scheme must be needed to realize more flexible and efficient systems.

1.3.3 Two-Party Standoff in Standardization Activities

Recently, standardization activities have been regarded as important factors to open new wireless markets and to get big business there. However, there is a serious problem, that is, several major promotion groups get into a tangle in the standardization activities. For example, TGn Sync [187] and WWiSE [188] competed to get the majority in the IEEE802.11n Task Group. Similarly, one group promoting an OFDM based UWB [189], and another group promoting a direct-spreading based UWB competed in the IEEE802.15.3a Task Group. Such standoff would delay the status of standardization activities, and then they would prevent the open of new market. In addition, such delays uselessly waste development costs and human resources. Unfortunately, the IEEE802.15.3a was broken up by

such standoff.

The MC transmission techniques must have met the similar conflictions during standardization activities. Actually, the standoff of IEEE802.15.3a can be seen as that between the MC and SC techniques in a sense. All the proposers, supporters and attendees should consider avoiding the fruitless standoff.

1.4 Construction of Dissertation

To solve the problems mentioned above, this dissertation investigates wide topics of MC transmission techniques. For Problem (1), Chapter 3 proposes new algorithms with the combination of OFDM and multi-input multi-output (MIMO) technologies, that is, MIMO-OFDM. Moreover, Chapter 4 proposes solutions for avoiding multiple access interference (MAI) in OFDMA reverse link. For Problem (2), Chapter 5 proposes a novel concept of duplexing scheme based on the MC transmission, multi-carrier division duplex (MCDD). For Problem (3), Chapter 6 analyzes recent issues and solutions related to wireless system standardization through the case-study of IEEE802.15.3c. This dissertation could show helpful conclusions to build flexible and efficient wireless communication systems by investigating from technical issues to strategic business.

The rest of this dissertation is organized as follows. Chapter 2 introduces the basis of MC transmission techniques. The major features of MC techniques are high spectral efficiency, robustness against ISI channels, and flexibility of spectral resource management. The chapter mathematically shows the signal of MC system through transmitter, multi-path channel and receiver. In addition, the major issues of MC techniques, channel estimation (CE), forward error correction (FEC) and interleaving, time and frequency synchronization, Doppler effect and peak-to-average power ratio (PAPR), are also introduced. After the introduction, comparison of the features of SC and MC transmission techniques, and that of the features of OFCDM and OFDMA are addressed. This chapter would help to smoothly understand the following chapters in this dissertation.

Chapter 3 presents new algorithms of signal detection and channel estimation for MIMO-OFDM. The MIMO technologies have also attracted considerable attention in the area of wireless communication. They employ multiple antennas at either or both transmitter and receiver sides and then maximally use spatial multiplexing and spatial diversity gains in a wireless channel. The most important advantage of MIMO is increasing data rate without extension of spec-

trum. Moreover, OFDM is very suitable for combination of MIMO because the frequency-domain signal processing of OFDM essentially enables MIMO to execute both signal detection and equalization at the same time. The WLAN standard of IEEE802.11n has adopted the MIMO-OFDM technology to increase maximum data rate and spectral efficiency. And then, the next generation mobile communication systems would adopt the MIMO-OFDM technologies. There are two main issues of MIMO-OFDM in the mobile situation, those are, robustness against fast time-varying fading channel and complexity reduction for signal detection algorithm. This chapter provides solutions to these issues. First, sequentially-updated channel estimation (SUCE) tracks the variation of fading channel and estimates channel frequency response over a packet. Second, multiple-QR-decomposition assisted group detection (Multi-QRD-GD) decomposes and equalizes the spatially-multiplexed signal with complexity-reduced and parallelized algorithm. One more advantage of proposed algorithms is reducing not only computational complexity but also processing latency in the receiver. The processing latency often degrades the performances of channel estimation and signal detection in the mobile situation because the variation of fading induces estimation errors between the estimated channel response and actual response. With the help of parallelized signal processing, the proposed algorithms minimize such estimation errors even in the mobile situation. Computer simulation shows that the proposed algorithms outperform to existing ones in a highly mobile fading environment.

Chapter 4 proposes solutions for avoiding MAI in OFDMA reverse link. In OFDMA, available sub-carriers are divided into independent sets. These sets are the unit of frequency resource allocation for UTs. Basically, different set is assigned to UTs and each set keeps the orthogonality each other. However, some impaired factors, time misalignment due to propagation delays, lose the orthogonality among UTs and then induce MAI. Because of MAI, the performance of OFDMA reverse link is degraded drastically. To avoid MAI due to the propagation delays, time alignment control (TAC) is proposed for OFDM reverse link in Chapter 4. In TAC, AP estimates the amounts of propagation delays for each UT in a period of initial connection. After that, AP informs the estimates of propagation delays of UTs. UTs adjust their transmit timing according to the estimates from AP in the following periods. The advantage of TAC is avoiding MAI without extension of GI. Moreover, the complexity reduction scheme is also proposed for TAC of OFDMA in this chapter.

Chapter 5 presents a novel concept of duplexing scheme based on the MC transmission, MCDD. MCDD employs the feature of flexibility and extend it to

the duplex scheme. A significant issue of MCDD is inter-link interference (ILI) occurring among the duplex channels. In Chapter 5 proposes time-spreading technique to MCDD to reduce the impact of ILI. By using the time-spreading technique, the duplex channels keep the orthogonality each other. In addition, reuse of spreading codes is investigated in Chapter 5. Because the time-spreading technique inherently decreases the maximum data rate of MCDD, the spreading factor should be small as possible. The reuse of spreading codes avoids to decreasing the maximum data rate while it still reduces ILI. The MC based wireless system could be more flexible and efficient by introducing MCDD and by combining multiplexing, multiple access and duplexing together.

Chapter 6 analyzes recent issues and solutions related to wireless system standardization. Recently, several major promotion groups get into a tangle in the standardization activities. In this chapter, two examples of standoff in IEEE802.11n and IEEE802.15.3a are first introduced. Then, a latest standardization activity of IEEE802.15.3c Task Group (TG3c), which aims at the establishing millimeter-wave based WPAN systems, is introduced. There was two major concepts of system, SC and MC based systems, in the TG3c activity. Then, a technical solution, "Common Mode," was proposed for bridging between the SC and MC. Finally, Common Mode helped to bring the SC and MC based systems to a single system specification. Through the analysis of TG3c activity, what is important for succeeding at the establishment of wireless system standard is addressed.

The last chapter concludes remarkable outcomes of this work and presents an outlook for the MC based wireless communication.

The author desires that this dissertation would be worthful and helpful for the evolution of future wireless communication systems.

Chapter 2

Multi-Carrier Transmission Techniques and Their Features

Summary

In this chapter, the basis of MC transmission techniques is introduced. The MC transmission provides high spectral efficiency and flexibility of spectral management to wireless systems. In addition, it also provides robustness against ISI with helps of GI and frequency-domain signal processing. In this chapter, comparison between the MC and SC transmission techniques and that between OFDMA and OFCDM are also achieved. This chapter would help to smoothly understand the following chapters in this dissertation.

2.1 Multi-Carrier Transmission

2.1.1 Basis

MC transmission [43],[44],[46],[47] is based on frequency-domain parallel transmission. It employs orthogonal sub-carriers for the parallel transmission. Figure 2.1 illustrates the sub-carrier allocation of MC transmission. Because the sub-carriers are spectrally overlapped each other, the MC transmission achieves high spectral efficiency. Fast Fourier transform (FFT) and inverse FFT (IFFT) operations are available for generating the sub-carrier signals easily.

Figure 2.2 is a basic configuration of transmitter. An original bit stream is converted to K-parallel streams, where K is the number of sub-carriers. At each sub-carrier, the bit stream is modulated onto phase shift keying (PSK) or quadra-

ture amplitude modulation (QAM) symbols. Generally, Gray coded modulation is applied to these PSK and QAM to minimize amount of bit errors. After modulation, the IFFT operation generates time-domain wave form, which is called as time-domain symbol hereafter. Then, GI is added to each time-domain symbol. Let $S(d,k)$ be the d-th modulated symbol on the k-th sub-carrier. The l-th sample in the d-th time-domain symbol $s(d,l)$ ($l = 0, \cdots, G+F-1$) is expressed by

$$s(d,l) = \sum_{k=0}^{K-1} S(d,k) e^{j2\pi k(l-G)/F}, \tag{2.1}$$

where F is the IFFT and FFT points and G is the GI points. Average symbol power σ_S^2 is defined by $\sigma_S^2 = \left\langle |S(d,k)|^2 \right\rangle$, where the operator $\langle a \rangle$ indicates average of a. Equation (2.1) means that GI is a copy of last G samples of the corresponding time-domain symbol. When the sub-carrier separation is Δ_F, the sample duration Δ_T is $1/\Delta_F$ and the time-symbol period including GI T is $(G+F)\Delta_T$. The baseband packet signal $x(t)$ is expressed by

$$x(t) = \sum_{d=0}^{D-1} \sum_{l=0}^{G+F-1} s(d,l)\delta(t - d(G+F-1) - l), \tag{2.2}$$

$$\delta(t) = \begin{cases} 1 & t = 0 \\ 0 & \text{otherwise} \end{cases}. \tag{2.3}$$

In (2.2), D is the number of time-domain symbols per packet. Finally, the baseband signal is converted to an analog and radio frequency (RF) signal and transmitted.

The transmitted signal suffers from a multi-path fading channel. The multi-path channel is modeled as a discrete complex filter. In this chapter, a time-invariant multi-path channel is assumed for sake of simplicity. The channel impulse response $h(t)$ is expressed by

$$h(t) = \sum_{\tau=0}^{T_{CH}} \alpha_\tau \delta(t - \tau), \tag{2.4}$$

where T_{CH} is the channel length and α_τ is the complex coefficient of the τ-th path. If a mobile fading channel is assumed, amplitude and phase of α_τ are characterized by Rayleigh and uniform distributions, respectively. In basic design of OFDM, the length of GI is equal to or longer than the assumed channel length to avoid ISI and ICI due to the channel.

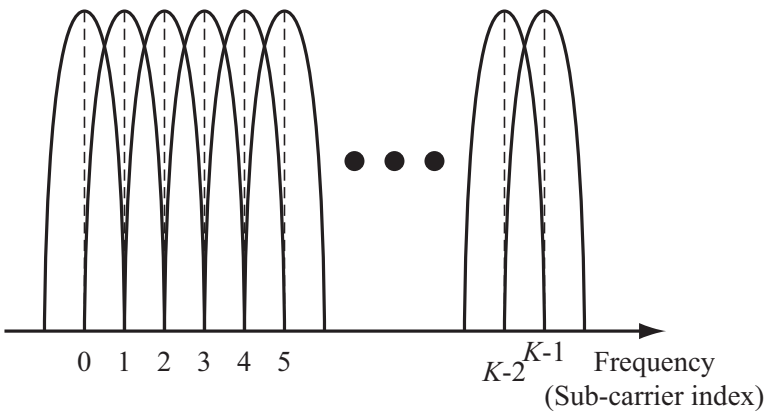

Figure 2.1: Sub-carrier allocation of MC transmission.

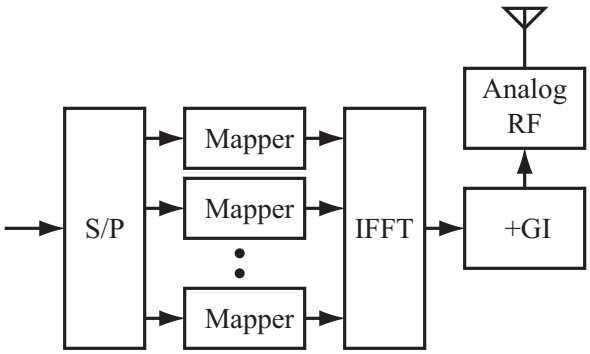

S/P: serial-to-parallel converter,
IFFT: inverse fast Fourier transform,
GI: guard interval, RF: radio frequency

Figure 2.2: Configuration of MC transceiver.

Figure 2.3 illustrates a configuration of receiver. Passing through the multi-path channel, the signal arrives at the receiver. The received analog and RF signal is first converted to digital baseband signal. The received baseband signal $y(t)$ is expressed by

$$y(t) = \sum_{\tau=0}^{T_{CH}-1} h(\tau)x(t-\tau) + n(t), \tag{2.5}$$

where $n(t)$ is additive white Gaussian noise (AWGN) with zero mean and σ_N^2 variance. Next, GI is removed from each received time-domain symbol. The remaining symbols are converted to sub-carrier symbols by FFT operation. Let $r(d,l)$ be the l-th sample in the d-th received time-domain symbol for $l = 0, \cdots, F-1$. The received symbol on the k-th sub-carrier $R(d,k)$ is expressed by

$$\begin{aligned} R(d,k) &= \frac{1}{F}\sum_{l=0}^{F-1} r(d,l)e^{-j2\pi kl/F} \\ &= H(k)S(d,k) + \Gamma(d,k) + \Xi(d,k) + N(d,k), \end{aligned} \tag{2.6}$$

where

$$H(k) = \sum_{l=0}^{F-1} h(l)e^{-j2\pi kl/F}, \tag{2.7}$$

$$\Gamma(d,k) = \sum_{l=0}^{F-1}\sum_{l'=l+G+1}^{T_{CH}-1} h(l')s(d-1, G+F-l')e^{-j2\pi kl/F}, \tag{2.8}$$

$$\Xi(d,k) = -\sum_{l=0}^{F-1}\sum_{l'=l+G+1}^{T_{CH}-1} h(l')s(d, F-l')e^{-j2\pi kl/F}, \tag{2.9}$$

and

$$N(d,k) = \sum_{l=0}^{F-1} n(d,l)e^{-j2\pi kl/F}. \tag{2.10}$$

In (2.6), $\Gamma(d,k)$ and $\Xi(d,k)$ are ISI and ICI components due to the multi-path delay, respectively. It is noted that when the length of GI is equal to or longer than the channel delay, i.e. $G \geq T_{CH}-1$, these ISI and ICI components disappear in the received symbols. The following explanation in this chapter assumes the length of GI is enough long to avoid ISI and ICI.

An attractive feature of MC transmission is to simplify equalization in the frequency-domain. This fact is led from (2.6). Let $\hat{H}(d,k)$ be an estimate of $H(d,k)$. A simple zero-forcing (ZF) method equalizes $R(d,k)$ by $\hat{H}(d,k)$ as follow:

$$\begin{aligned}\hat{S}(d,k) &= \frac{\hat{H}(d,k)^*}{\left|\hat{H}(d,k)\right|^2}R(d,k) \\ &= S(d,k) + \frac{\hat{H}(d,k)^*}{\left|\hat{H}(d,k)\right|^2}N(d,k),\end{aligned} \tag{2.11}$$

where a^* indicates complex conjugate of a. ZF does not consider noise effect, and it causes noise enhancement like the second term of (2.11). Another minimum mean square error (MMSE) method considers minimizing the noise enhancement. MMSE method equalizes $R(d,k)$ as follow:

$$\hat{S}(d,k) = \frac{\hat{H}(d,k)^*}{\left|\hat{H}(d,k)\right|^2 + 1/\mathrm{SNR}}R(d,k), \tag{2.12}$$

where SNR means signal-to-noise power ratio which is equivalent to σ_S^2/σ_N^2. It is known that MMSE method outperforms to ZF one, and that MMSE one has to estimate SNR. The transmitted bit stream is decided from the equalized symbols $\hat{S}(d,k)$.

2.1.2 Features

2.1.2.1 Guard Interval and Frequency-Domain Processing

Figure 2.4 explains the impact of GI. A time-domain symbol consists of an effective data symbol and GI periods. The aim of GI is avoiding ISI due to multi-path fading channels. If no GI is inserted to the OFDM symbol, delayed signals induce ISI and ICI after the FFT operation in the receiver side [157]–[160]. The impacts of ISI and ICI spread over the frequency-domain as illustrated in (2.6). GI holds the periodicity of time-domain symbol even in the multi-path channel. Then, no interference occurs after the FFT operation and the simple frequency-domain equalization can be introduced such as (2.11) and (2.12). It should be noted that the length of GI is generally decided by the maximum or root mean square delay time of assumed propagation characteristics [6]–[9], [11], [12].

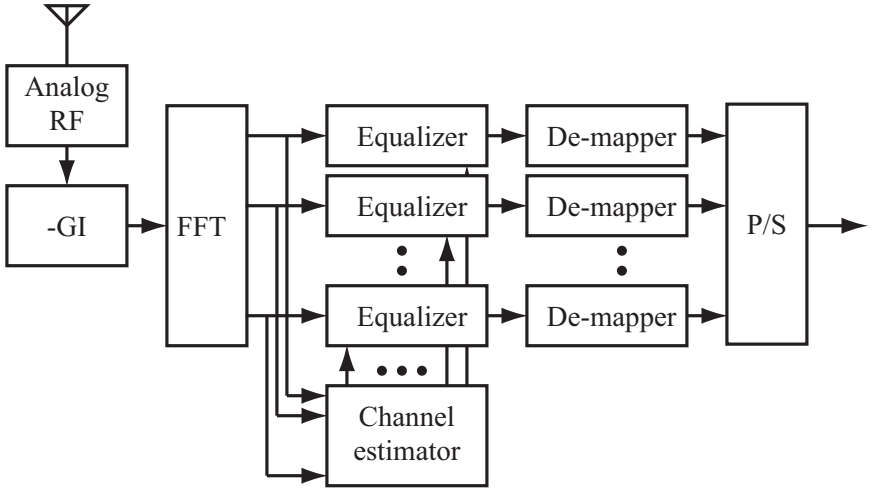

RF: radio frequency, GI: guard interval,
FFT: fast Fourier transform, P/S: parallel-to-serial converter

Figure 2.3: Configuration of MC receiver.

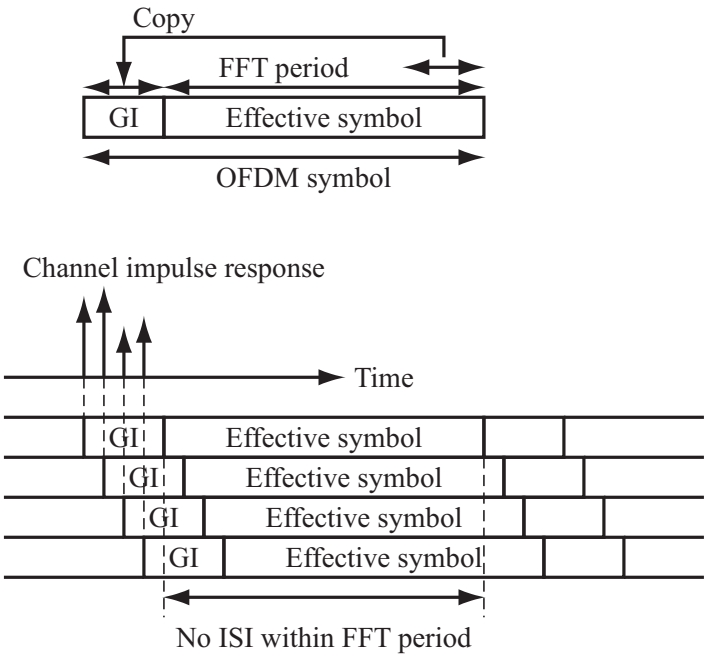

Figure 2.4: Impact of gurad interval.

2.1.2.2 Sub-Carrier Based Resource Control

As above-mentioned, the MC techniques employ the parallel and orthogonal sub-carriers in the frequency-domain. It means that the MC techniques can control bit, power and user allocation sub-carrier-by-sub-carrier.

The designs of MC systems usually focus on multi-path propagation environments. In such environments, the characteristics of channel response have frequency-selectivity. Thus, the optimal modulation parameter is different sub-carrier-by-sub-carrier. MC based adaptive modulation and coding (AMC) is a famous way to improve spectral efficiency and to reduce redundant power mis-allocation by taking the frequency-selectivity into account [153], [171], [172]. Moreover, AMC can solve the design of OFDM based single frequency reuse systems [153], [172].

OFDMA is an MC based multiple access scheme [44], [46], [53]–[57]. In OFDMA, an individual set of sub-carriers is assigned to corresponding user. The orthogonality among the users is held in the frequency-domain because of the different sub-carriers. Similar to OFDM, OFDMA achieves higher spectral efficiency than conventional frequency division multiple access (FDMA). In the OFDMA systems, sub-carrier allocation is decided by channel frequency response use-by-user. Thus, OFDMA can improve spectral efficiency by assigning a set of sub-carriers to a user whose channel response on those sub-carriers is the best among all users. This kind of effect is called as multi-user diversity. AMC and multi-user diversity have a strong relationship from the point of sub-carrier control in OFDMA [173]–[177].

2.1.3 Major Issues in Multi-Carrier Transmission Techniques

2.1.3.1 Channel Estimation

Channel estimation (CE) is necessary to equalize the received symbols in the frequency-domain [58]–[64]. Typically, CE is categorized to two cases, pilot symbol assisted CE and blind CE. The blind CE requires no pilot symbols and thus improves frame efficiency. However, it requires a huge amount of computational complexity compared to the pilot symbol assisted CE. The existing and currently discussed MC based systems employ the pilot symbol assisted CE for simplicity. There are mainly three patterns of pilot symbol allocation as illustrated in Fig. 2.5. The preamble pattern allocates the pilot symbols over the frequency-axis at a certain time. This is most used for packet based wireless systems. The tone

pattern allocates the pilot symbols along the time-axis at certain sub-carriers. The WLAN standard of IEEE802.11 uses both preamble and tone pilot patterns. The scattered pattern is used in terrestrial digital broadcasting. The following chapters in this dissertation also use the preamble patterns for the pilot symbols assisted CE.

2.1.3.2 Forward Error Correction and Interleaving

Forward error correction (FEC) is a very important technique to improve error probability of wireless link performance [66]–[68]. The basis of FEC is to add redundant bits into original information bits in a transmitter side, and to correct bit errors in a decoder of receiver side. General digital communication systems employ FEC techniques, for example, satellite communication systems employ convolutional codes and wideband code division multiple access (W-CDMA) as IMT-2000 employs turbo codes. The performance characteristics depend on the types of FEC techniques, and some FEC techniques are weak to burst errors. The burst errors dominate in possible error patterns in wireless fading channels. Thus, FEC techniques are generally employed with interleaving techniques. The interleaving techniques randomize the burst errors caused by the fading channels. Especially in MC systems, frequency-domain interleaving is effective to improve the performance of FEC techniques [65]. Actually, IEEE802.11a/g/n WLANs employ convolutional codes with frequency interleaving.

2.1.3.3 Time and Frequency Synchronization

Synchronization issues have been treated in many literatures [69]–[84]. It is especially known that time and frequency synchronization are very important for the MC transmission.

Because the MC transmission employs FFT to convert time-domain symbols to corresponding frequency-domain symbols. Thus, the receiver has to accurately set the FFT timing to the time-domain symbols. Inaccurate FFT timing equivalently reduces the length of GI and then causes ISI in a sense.

Transmitter and receiver use local oscillators to up-convert a baseband signal to a RF signal and to down-convert a RF signal to a baseband signal, respectively. The local oscillators should generate correct carrier frequency. However, it is very difficult for them to generate the correct frequency and it might need huge costs. Thus, there would often be frequency offset between transmitter and receiver. This

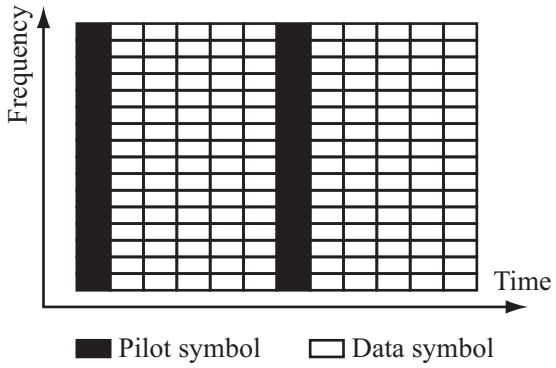

(a) Preamble pattern

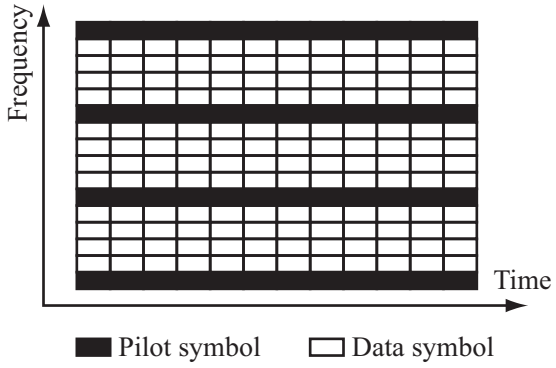

(b) Tone pattern

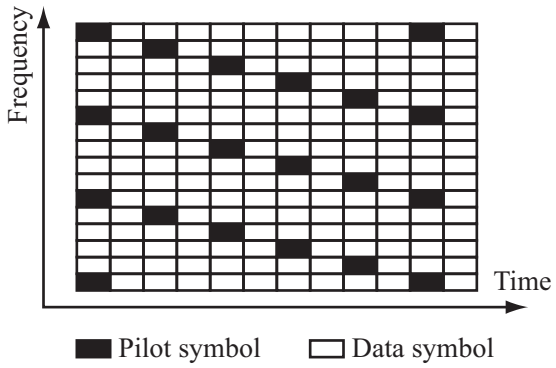

(c) Scattered pattern

Figure 2.5: Pilot symbol allocation.

frequency offset loses the orthogonality among sub-carriers and causes ICI in the MC systems.

Usually, synchronization is acquired by known pilot symbols and GIs. When the pilot symbols are employed for synchronization, the design of pilot symbols is very important to acquire required performances of systems.

2.1.3.4 Inter-Carrier Interference Due to Doppler Effect

In a mobile environment, received signals suffer from Doppler effect. In the frequency-domain, the signal spectrum is spread by Doppler effect. Doppler effect also causes ICI in the MC systems [85]–[90]. The impact of ICI depends on relationship between a velocity of terminal and sub-carrier separation.

2.1.3.5 Peak-to-Average Power Ratio

An MC signal consists of the sum of sub-carrier signals. It is well-known that peak-to-average power ratio (PAPR) of MC signal is higher than that of SC signal. PAPR for a signal $s(t)$ is defined by

$$\mathrm{PAPR} = \frac{\max\left\{|s(t)|^2\right\}}{\left\langle |s(t)|^2 \right\rangle}. \tag{2.13}$$

High PAPR requires linearity of power amplifier and high-resolution of analog-to-digital converter (ADC) and digital-to-analog converter (DAC). For example, in the standardization bodies, the definitions of power amplifier is provided for the system evaluation [96]. Such amplifier, ADC and DAC increase power consumption and implementation cost. The PAPR issue is significant especially for reverse link transmission of cellular system because the batteries of terminal are limited. Some reduction techniques are proposed for PAPR issue, such as phase control [95], pre-coding [91], [93] and clipping [92], [94] of signal in transmitter side. However, these techniques also cause bit error degradation.

2.2 Comparison of Single- and Multi-Carrier Transmission Techniques

Table 2.1 compares the features of SC and MC transmission techniques. As mentioned above, the MC transmission provides the high spectral efficiency, ISI im-

Table 2.1: Major features of single- and multi-carrier transmission.

	SC	MC
Spectral efficiency	Low	High
ISI equalization	High complex (but FDE is available)	Simple (FDE is available)
Flexible spectral management	Hard	Possible
PAPR	Low	High
Hardware cost	Low	High

munity and flexible spectral resource management. Is is hard for the SC transmission to obtain such features. However, it is noted that the SC transmission has its advantages compared to the MC one. PAPR of SC is lower than that of MC, and then the SC one is more robust against nonlinearity effect, such as power amplifier and analog-to-digital converter. And then, the hardware cost of SC is clearly reasonable if no equalizer is implemented in the terminal. Moreover, frequency-domain equalization (FDE) has been available for the SC transmission to combat the ISI channels [41], [42]. This is a fact that the SC transmission techniques have been alternative of MC ones in some wireless system which are operating not only in line-of-sight (LOS) envinronments but also in non LOS (NLOS) environments [196], [199].

2.3 Comparison of OFCDM and OFDMA

The features of OFCDM [20], [48]–[50] and OFDMA [44], [46], [53]–[57] are compared in this section. Through this comparison, the reason why this dissertation focuses on OFDMA based wireless systems is clarified. Table 2.2 lists the major features of OFCDM and OFDMA. The biggest difference between OFCDM and OFDMA is their multiple access schemes. It can be considered that the concept of OFCDM is derived from CDMA in a sense. OFCDM multiplexes users' signals in the code-domain like CDMA. It enables single-frequency reuse by the help of codes as well. In OFCDM, inter-code interference is a significant issue. This kind of interference occurs even in single-cell environments. Thus, some countermeasures such as two-dimensional spreading [51], [52] and interference cancellers are required for solving such an interference issue.

Table 2.2: Major features of OFCDM and OFDMA.

	OFCDM	OFDMA
Frequency-domain	-	Multiplexing Multiple access
Time-domain	Multiplexing Multiple access	Multiplexing Multiple access
Code-domain	Multiple access	-
Single-frequency reuse	Possible (by codes)	Possible (by adaptive modulation, frequency hopping, etc.)
Multi-user diversity	None	Available

Meanwhile, OFDMA multiplexes users' signals in the frequency-domain. As above-mentioned, OFDMA obtains the frequency and multi-user diversity effects in frequency-selective channel conditions [173]–[177]. In addition, essentially, no interference occurs among users in the single-cell environment because of the orthogonal sub-carriers. An important problem of OFDMA is the way to realize the single-frequency reuse for the mobile communication systems with multi-cell. Recently, it has been clear that sub-carrier based AMC and frequency hopping techniques enable the single-frequency reuse in those systems [54]–[56], [153], [172]. Thus, OFDMA is also a major alternative scheme for the mobile communication systems.

2.4 Conclusion

In this chapter, the basis of MC transmission techniques is introduced. The major features of MC techniques are high spectral efficiency, robustness against ISI channels, and flexibility of frequency resource management. In addition to this introduction, the features of single- and multi-carrier transmission techniques are compared in this chapter. Moreover, those of OFCDM and OFDMA are also compared. The biggest difference between them is multiple access scheme. It is noted that not only OFCDM but also OFDMA is a major alternative scheme for the mobile communication systems. This chapter would help to smoothly understand the following chapters in this dissertation.

Chapter 3

Multi-Input Multi-Output Orthogonal Frequency Division Mutiplexing in a Highly Mobile Fading Channel

Summary

A new MIMO-OFDM system using reduced-complexity-and-latency signal detection and channel estimation is proposed in this chapter. Both the proposed detection and estimation algorithms reduce not only their complexity but also their latency. Reducing latency could avoid the degradation of system performance in an actual mobile fading environment. In this chapter, the bit error rate performance of proposed system is evaluated by computer simulations. The simulation results show that our proposed estimation scheme outperforms conventional minimum mean square error based schemes. They also show that the proposed system outperforms a maximum likelihood detection based system in a mobile fading environment. Moreover, the proposed algorithms require the less complexity than the conventional algorithms.

3.1 Introduction

MIMO [97]–[100], especially MIMO-OFDM [101], [107], is a promising technology to increase spectral efficiency and data rate in a severe multi-path fading channel. Signal detection is a significant issue for MIMO [97], [108]–[123]. Spa-

tial filtering and maximum likelihood detection (MLD) are two representatives of detection algorithms. MLD provides the best performance among them because of the full receiver diversity gain. However, it requires a huge amount of computational complexity. So far, many researches challenged to reduce the MLD's computational complexity [108]–[123].

The demand for the high data rate communication has been increasing not only in a static environment but also in a mobile one. Channel estimation (CE) is an important issue in the mobile and packet based wireless communication [125]–[133]. Typically, pilot symbols are added at a head of a packet and used for CE. However, CE errors commonly occur during the packet period in the mobile environment. The impact of CE errors increases more when the user mobility is higher. Several CE schemes were proposed to track and compensate for the variation of fading. Minimum mean square error based CE (MMSE CE) [134], [135] is well-known as an effective one. Moreover, Refs. [136] and [137] challenged to simplify the original MMSE CE scheme.

However, the previous researches on the signal detection and CE algorithms for MIMO did not treat a latency problem in the signal processing. Reference [126] mentioned that the latency reduces the frequency of CE and then degrades the system performance in the highly mobile environment. Moreover, the accumulated latency totally decreases an actual throughput.

In this chapter, an MIMO-OFDM system using new signal detection and CE is proposed. The aim of proposed system is enhancing the performance in the mobile fading environment and supporting the high-mobility users. Both the signal detection and CE algorithms reduce not only their complexity but also their latency.

The proposed MIMO-OFDM system exploits multiple-QR-decomposition assisted group detection (Multi-QRD-GD) as signal detection. Group detection (GD) itself was already proposed in some past literatures, such as Ref. [110]. GD consists of a sub-space projector and multiple local detectors. Our proposed Multi-QRD-GD uses multiple-QRD as the sub-space projector. By the help of QRD, Multi-QRD-GD can employ successive detection and reduce the complexity in the local detectors. Moreover, Multi-QRD-GD realizes parallel signal processing, and thus reduces the latency.

The proposed system also exploits sequentially-updated channel estimation (SUCE) as channel tracking. SUCE uses co-channel interference (CCI) cancellation and outlier detection. It is based on symbol-by-symbol processing, meanwhile some conventional CE schemes were based on packet-by-packet processing

[129]. Packet-by-packet processing often induces a larger latency than symbol-by-symbol processing, and then decreases an actual data throughput. Moreover, SUCE uses neither FFT nor IFFT operations. Thus, it reduces the complexity and latency compared to the conventional CE algorithms [134]–[137].

3.2 Signal Model

An MIMO-OFDM using K sub-carriers, L transmitter antennas and M receiver antennas is modeled in this chapter. Let $s_l(t,k)$ be a phase shift keying (PSK) or quadrature amplitude modulation (QAM) symbol on the k-th sub-carrier at the discrete time t, transmitted from the l-th antenna. Similarly, let $\boldsymbol{s}(t,k) = [s_1(t,k) \ \cdots \ s_L(t,k)]^T$ be a transmitted symbol vector. The operator $\boldsymbol{a}^T$ means transposition of vector $\boldsymbol{a}$. The transmitted symbols pass through a MIMO channel and then arrive at a receiver. The received symbol vector $\boldsymbol{r}(t,k)$ is expressed as follows:

$$\begin{aligned}\boldsymbol{r}(t,k) &= [r_1(t,k) \ \cdots \ r_M(t,k)]^T \\ &= \boldsymbol{H}(t,k)\boldsymbol{s}(t,k) + \sum_{\substack{k'=0 \\ k'\neq k}}^{K-1} \boldsymbol{H}_C(t,k')\boldsymbol{s}(t,k') + \boldsymbol{n}(t,k),\end{aligned} \tag{3.1}$$

where

$$\boldsymbol{H}(t,k) = [\boldsymbol{h}_1(t,k) \ \cdots \ \boldsymbol{h}_L(t,k)], \tag{3.2}$$

$$\boldsymbol{h}_l(t,k) = [h_{1,l}(t,k) \ \cdots \ h_{M,l}(t,k)]^T, \tag{3.3}$$

$$\boldsymbol{n}(t,k) = [n_1(t,k) \ \cdots \ n_M(t,k)]^T. \tag{3.4}$$

In the above equations, $r_m(t,k)$ is the symbol received by the m-th receiver antenna, $h_{m,l}(t,k)$ is the k-th sub-carrier's channel frequency response (CFR) between the l-th transmitter and the m-th receiver antennas and $n_m(t,k)$ is additive white Gaussian noise (AWGN) with zero mean and σ^2 variance. The second term of the right side in (3.1) indicates an ICI term due to Doppler effect [138]. This ICI term is derived in Appendix A.1. In this chapter, those are assumed that CFR are spatially identical and independent each other, and that no ISI appears because of an enough GI length.

3.3 Multi-QR-Decomposition Assisted Group Detection

Figures 3.1 and 3.2 illustrate the configurations of transmitter and receiver, respectively. And then, Fig. 3.3 illustrates the configuration of Multi-QRD-GD. Multi-QRD-GD consists of a sub-space projector based on multiple-QRD and local detectors. The sub-space projector isolates the received MIMO symbols into G_r sub-groups. The local detectors estimate the transmitted symbols from the isolated sub-groups. In this chapter, the number of sub-groups G_r is fixed to two. In this case, the number of symbols included in each sub-group is $\lfloor L/G_r \rfloor$ or $\lceil L/G_r \rceil$. The operator $\lfloor a \rfloor$ indicates the maximum integer which is equal to or less than a and $\lceil a \rceil$ indicates the minimum integer which is equal to or greater than a. For sake of simplicity, the notation of estimated CFR matrix $\hat{\boldsymbol{H}}(t,k)$ is replaced with $\boldsymbol{H}(t,k)$ in this section.

Before the sub-space projector, adaptive group selection (AGS) is performed with taking the channel condition into account. AGS first measures a relative signal power for the symbol from the l-th transmitter antenna $\gamma_l(t,k)$:

$$\gamma_l(t,k) = \|\boldsymbol{h}_l(t,k)\|^2 . \tag{3.5}$$

After the measurement, AGS prepares parameters $rank(v)(t,k)$ for $v = 1, \cdots, L$, and ranks the indices l based on the descending order of $\gamma_l(t,k)$. For instance, $rank(1)(t,k) = \arg_l \max\{\gamma_l(t,k)\}$ and $rank(L)(t,k) = \arg_l \min\{\gamma_l(t,k)\}$. AGS generates different matrices $\boldsymbol{H}_g(t,k)$ for $g = 1, \cdots, G_r$. $\boldsymbol{H}_g(t,k)$ corresponds to the g-th sub-group and is the column-permutated matrix of $\boldsymbol{H}(t,k)$ according to a rule about $rank(v)(t,k)$ [124]. Hereafter, for ease of explanation, $\boldsymbol{H}_1(t,k) = \boldsymbol{H}(t,k)$ and $\boldsymbol{H}_2(t,k) = [\boldsymbol{h}_{\lceil L/G_r \rceil+1}(t,k) \ \cdots \ \boldsymbol{h}_L(t,k) \ \boldsymbol{h}_1(t,k) \ \cdots \ \boldsymbol{h}_{\lceil L/G_r \rceil}(t,k)]$.

Each generated matrix is decomposed into a unitary matrix and an upper triangular one by QRD. $\boldsymbol{H}_g(t,k)$ is expressed as follows:

$$\boldsymbol{H}_g(t,k) = \boldsymbol{Q}_g(t,k)\boldsymbol{R}_g(t,k), \tag{3.6}$$

where

$$\boldsymbol{Q}_g(t,k) = \begin{bmatrix} q_{1,1,g}(t,k) & \cdots & q_{1,L,g}(t,k) \\ \vdots & \ddots & \vdots \\ q_{M,1,g}(t,k) & \cdots & q_{M,L,g}(t,k) \end{bmatrix}, \tag{3.7}$$

$$\boldsymbol{R}_g(t,k) = \begin{bmatrix} \xi_{1,1,g}(t,k) & \xi_{1,2,g}(t,k) & \cdots & \xi_{1,L,g}(t,k) \\ 0 & \xi_{2,2,g}(t,k) & \cdots & \xi_{2,L,g}(t,k) \\ \vdots & \ddots & \ddots & \vdots \\ 0 & \cdots & \cdots & \xi_{L,L,g}(t,k) \end{bmatrix}. \tag{3.8}$$

After QRD, the sub-space projector obtains vectors $\boldsymbol{z}_g(t,k)$ for $g = 1, \cdots, G_r$:

$$\begin{aligned} \boldsymbol{z}_g(t,k) &= [\ z_{1,g}(t,k) \quad \cdots \quad z_{L,g}(t,k)\ ]^T \\ &= \boldsymbol{Q}_g^H(t,k)\boldsymbol{r}(t,k) \\ &= \boldsymbol{R}_g(t,k)\boldsymbol{s}(t,k) + \tilde{\boldsymbol{n}}_g(t,k), \end{aligned} \tag{3.9}$$

where

$$\begin{aligned} \tilde{\boldsymbol{n}}_g(t,k) &= [\ \tilde{n}_{1,g}(t,k) \quad \cdots \quad \tilde{n}_{L,g}(t,k)\ ]^T \\ &= \boldsymbol{Q}_g^H(t,k)\boldsymbol{n}(t,k). \end{aligned} \tag{3.10}$$

The operator $\boldsymbol{A}^H$ means conjugate transposition of matrix $\boldsymbol{A}$. When $G_r = 2$, the last halves of $\boldsymbol{z}_g(t,k) = \left[z_{\lceil L/G_r \rceil+1,g}(t,k) \ \cdots \ z_{L,g}(t,k)\right]^T$ for $g = 1, 2$ can be expressed

by (3.11) and (3.12), respectively:

$$
\begin{aligned}
&\begin{bmatrix} z_{\lceil L/G_r\rceil+1,1}(t,k) \\ \vdots \\ z_{L,1}(t,k) \end{bmatrix} \\
&= \begin{bmatrix} \xi_{\lceil L/G_r\rceil+1,\lceil L/G_r\rceil+1,1}(t,k) & \cdots & \cdots & \xi_{\lceil L/G_r\rceil+1,L,1}(t,k) \\ 0 & \xi_{\lceil L/G_r\rceil+2,\lceil L/G_r\rceil+2,1}(t,k) & \cdots & \xi_{\lceil L/G_r\rceil+2,L,1}(t,k) \\ \vdots & \ddots & \ddots & \vdots \\ 0 & \cdots & 0 & \xi_{L,L,1}(t,k) \end{bmatrix} \\
&\quad \cdot \begin{bmatrix} s_{\lceil L/G_r\rceil+1}(t,k) \\ \vdots \\ s_L(t,k) \end{bmatrix} + \begin{bmatrix} \tilde{n}_{\lceil L/G_r\rceil+1,1}(t,k) \\ \vdots \\ \tilde{n}_{L,1}(t,k) \end{bmatrix}, \qquad (3.11) \\
&\begin{bmatrix} z_{\lceil L/G_r\rceil+1,2}(t,k) \\ \vdots \\ z_{L,2}(t,k) \end{bmatrix} \\
&= \begin{bmatrix} \xi_{\lceil L/G_r\rceil+1,\lceil L/G_r\rceil+1,2}(t,k) & \cdots & \cdots & \xi_{\lceil L/G_r\rceil+1,L,2}(t,k) \\ 0 & \xi_{\lceil L/G_r\rceil+2,\lceil L/G_r\rceil+2,2}(t,k) & \cdots & \xi_{\lceil L/G_r\rceil+2,L,2}(t,k) \\ \vdots & \ddots & \ddots & \vdots \\ 0 & \cdots & 0 & \xi_{L,L,2}(t,k) \end{bmatrix} \\
&\quad \cdot \begin{bmatrix} s_1(t,k) \\ \vdots \\ s_{\lceil L/G_r\rceil}(t,k) \end{bmatrix} + \begin{bmatrix} \tilde{n}_{\lceil L/G_r\rceil+1,2}(t,k) \\ \vdots \\ \tilde{n}_{L,2}(t,k) \end{bmatrix}. \qquad (3.12)
\end{aligned}
$$

These last halves indicate the sub-groups isolated by the sub-space projector. Actually, the process by (3.9) can be replaced by once matrix multiplication and is not required G_r times any longer (see Appendix A.2).

The output of sub-space projector is fed into the local detectors individually. From (3.11) and (3.12), it is observed that each last half of $\boldsymbol{z}_g(t,k)$ already holds an upper triangular form. Therefore, Multi-QRD-GD can apply successive detection algorithms such as sphere decoding [117] and M-algorithm [115], [116] directly to the local detectors. In this chapter, M-algorithm is applied to the detectors. M-algorithm successively estimates possible transmitted symbols by computing metrics based on squared Euclidean distance. Each local detector consists of multi-stage M-algorithm, where the number of stages is equal to that of symbols included in the corresponding sub-group. Computing the metrics, M-algorithm

restricts the number of metrics surviving from a certain stage to the next stage. Let S_{l_M} be this number at the l_M-th stage. When l_M is zero, S_0 is set to one. The following explains the first sub-group by (3.11) as an example. At the first stage, that is $l_M = 1$, the metrics $\mu_{1,v}(t,k)\,(1 \le v \le SS_0)$ are computed as follow:

$$\mu_{1,v}(t,k) = \left| z_L(t,k) - \xi_{L,L}(t,k)\check{s}_L(t,k) \right|^2. \tag{3.13}$$

The S_{l_M} smallest metrics of SS_{l_M-1} ones get through to the (l_M+1)-th stage as surviving metrics $\Lambda_{l_M,u}(t,k)\,(1 \le u \le S_{l_M})$. After the first stage, the accumulated metrics at the l_M-th stage $\mu_{l_M,v}(t,k)\,(1 \le v \le SS_{l_M-1})$ is computed as follows:

$$\begin{aligned}\mu_{l_M,v}(t,k) = \Bigg| & z_{L-l_M+1}(t,k) - \sum_{p=L-l_M+2}^{L} \xi_{p,p}(t,k)\check{s}_{p,u}(t,k) \\ & - \xi_{L-l_M+1,L-l_M+1}(t,k)\check{s}_{L-l_M+1}(t,k) \Bigg|^2 + \Lambda_{l_M-1,u}(t,k),\end{aligned} \tag{3.14}$$

where $\check{s}_{p,u}(t,k)$ is the candidates of $s_p(t,k)$ used in the calculation of $\Lambda_{l_M,u}(t,k)$. Finishing the computations of the metrics at the final stage, the local detectors generate approximated log-likelihood ratio (LLR) for each transmitted bit $\hat{b}_{l,i}(t,k)(1 \le i \le \sqrt{S})$, which was proposed in Ref. [116], as follows:

$$\hat{b}_{l,i}(t,k) = \sqrt{\mu_{l,i,0,\min}(t,k)} - \sqrt{\mu_{l,i,1,\min}(t,k)}, \tag{3.15}$$

where

$$\mu_{l,i,a,\min}(t,k) = \min\left\{\mu_{l,i,a}(t,k)\right\}, \tag{3.16}$$

and $\mu_{l,i,a}(t,k)$ is the metric computed by the candidate symbol $\check{s}_l(t,k)$ whose $b_{l,i}(t,k)$ is $a(\in \{1,0\})$. LLR are fed into any decoder applied to the system. Then, the transmitted bits are recovered by the decoder.

3.4 Sequentially-Updated Channel Estimation

Figure 3.4 illustrates the configuration of SUCE. The aim of SUCE is tracking the variation of fading and updating estimated CFR. Moreover, SUCE could reduce not only the computational complexity but also the latency by terminating its process within the frequency-domain.

SUCE carries out in parallel according to the related transmitter antennas. After detection and decoding, the decoded bit stream is re-encoded and re-modulated

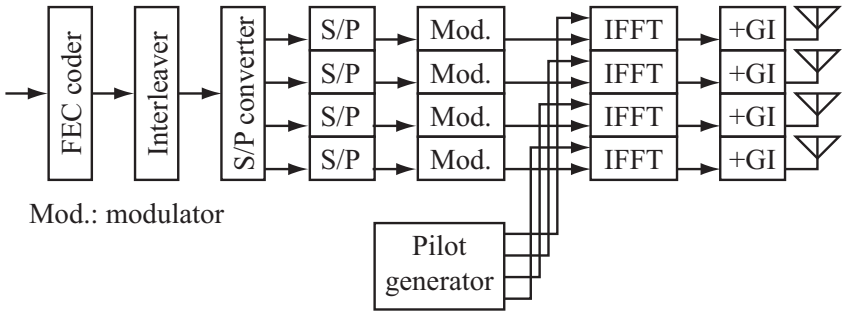

Figure 3.1: Configuration of proposed transmitter.

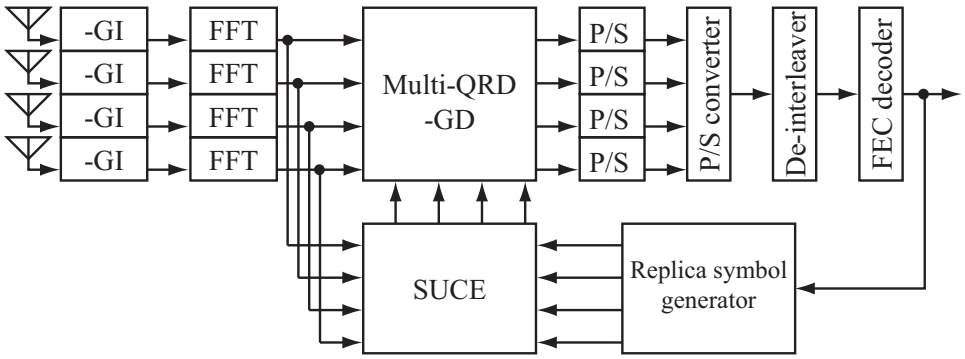

Figure 3.2: Configuration of proposed receiver.

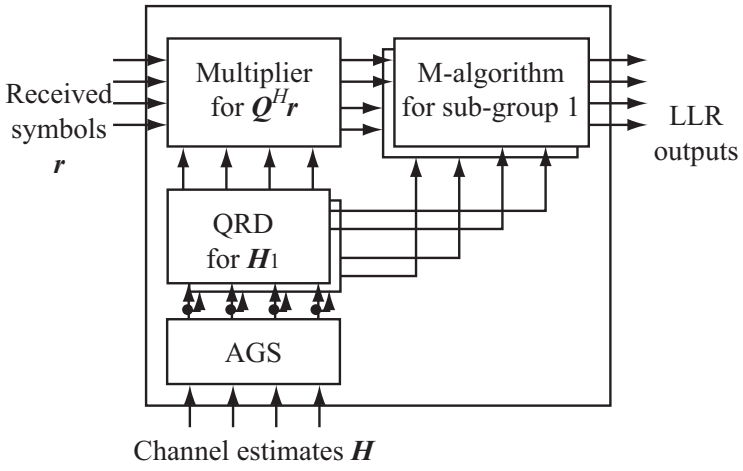

Figure 3.3: Configuration of Multi-QRD-GD block.

onto the decision-feedback symbol vector $\hat{\boldsymbol{s}}(t,k) = [\hat{s}_1(t,k) \cdots \hat{s}_L(t,k)]^T$ by a replica symbol generator. SUCE generates a replica of CCI component related to $s_l(t,k)$, $\boldsymbol{\Gamma}_l(t,k)$:

$$\boldsymbol{\Gamma}_l(t,k) = \hat{\boldsymbol{H}}^{(l)}(t,k)\hat{\boldsymbol{s}}(t,k), \tag{3.17}$$

where $\hat{\boldsymbol{H}}^{(l)}(t,k)$ is the current estimated CFR matrix whose l-th column is replaced by a zero vector. Then, a CCI canceller subtracts the CCI component from the received symbol vector:

$$\boldsymbol{r}_{c,l}(t,k) = \boldsymbol{r}(t,k) - \boldsymbol{\Gamma}_l(t,k). \tag{3.18}$$

After that, a divider obtains temporal estimates of CFR related to the l-th transmitter antenna $\tilde{\boldsymbol{h}}_l(t,k)$:

$$\tilde{\boldsymbol{h}}_l(t,k) = \frac{\hat{s}_l^*(t,k)}{|\hat{s}_l(t,k)|^2}\boldsymbol{r}_{c,l}(t,k), \tag{3.19}$$

where the operator a^* means conjugate of a.

The accuracy of the temporal estimate depends on the magnitude of channel coefficient at each sub-carrier and antenna. Especially, in the mobile environment, it should be considered that the possible magnitude is suddenly decreased down by the time-variation of fading. To avoid the inaccuracy due to such a channel, an outlier detector compares the relative magnitude using the temporal estimate $\tilde{h}_{m,l}(t,k)$ and the current estimate $\hat{h}_{m,l}(t,k)$. The outlier detector outputs $\bar{h}_{m,l}(t,k)$ deciding whether the temporal one is enough reliable or not:

$$\bar{h}_{m,l}(t,k) = \begin{cases} \tilde{h}_{m,l}(t,k) & \left|\tilde{h}_{m,l}(t,k)\right|^2 \geq \lambda_{th}^2 \left|\hat{h}_{m,l}(t,k)\right|^2 \\ \hat{h}_{m,l}(t,k) & \text{otherwise} \end{cases}, \tag{3.20}$$

where λ_{th} is the threshold parameter for this decision.

After the decision, the estimates pass through an average filter to mitigate the noise influence. The filter averages the temporal estimates along the time-axis:

$$\hat{\boldsymbol{H}}(t+1,k) = \begin{cases} \frac{1}{t}\sum_{d=0}^{t+1} \bar{\boldsymbol{H}}(d,k) & t < N_{av} \\ \frac{1}{N_{av}}\sum_{d=t-N_{av}+1}^{t} \bar{\boldsymbol{H}}(d,k) & \text{otherwise} \end{cases}, \tag{3.21}$$

where N_{av} is the number of temporal estimates for average. $\hat{\boldsymbol{H}}(t+1,k)$ is the output of SUCE and used in the signal detection block at the next time $t+1$. SUCE carries out the above steps symbol-by-symbol.

It is noted that estimated CFRs might mismatch with actual CFRs when the latency cannot be ignored. When convolutional coding is used, for example, latency must be caused by a trace-back in a Viterbi decoder. In this case, the scale of latency is determined by the constraint length of the code. Moreover, a latency caused by signal detection would be dominant in the MIMO systems. The actual latency in receivers also depends on capacity and speed of signal processors. It is important to estimate possible latency in the implementation procedure.

3.5 Evaluation and Discussion

3.5.1 Major Parameters

The BER performance of our proposed MIMO-OFDM system in a mobile fading environment is evaluated by computer simulation. Table 3.1 lists the parameters used in the simulation. These parameters follow dynamic parameter controlled orthogonal frequency and time division multiple access (DPC-OF/TDMA) [155]. According to these parameters, the maximum data rate on physical layer are up to 307.2 and 614.4 Mbps at 96 MHz bandwidth when modulation are QPSK and 16QAM, respectively. For the 4x4 MIMO-OFDM system with $G_r = 2$, we use AGS proposed in Ref. [124], where the matrices $\boldsymbol{H}_1(t,k)$ and $\boldsymbol{H}_2(t,k)$ are defined as follows:

$$\boldsymbol{H}_1(t,k) = [\boldsymbol{h}_{rank(3)(t,k)}(t,k)\ \boldsymbol{h}_{rank(2)(t,k)}(t,k)\ \boldsymbol{h}_{rank(4)(t,k)}(t,k)\ \boldsymbol{h}_{rank(1)(t,k)}(t,k)\ ], \tag{3.22}$$

$$\boldsymbol{H}_2(t,k) = [\boldsymbol{h}_{rank(4)(t,k)}(t,k)\ \boldsymbol{h}_{rank(1)(t,k)}(t,k)\ \boldsymbol{h}_{rank(3)(t,k)}(t,k)\ \boldsymbol{h}_{rank(2)(t,k)}(t,k)\ ]. \tag{3.23}$$

In the local detectors, S_1 is set to 4 and 14 for QPSK and 16QAM, respectively [124]. The transmitted packet consists of 2 pilot and 19 data OFDM symbols. The first 2 pilot symbols are used for carrier interferometory based initial CE (see Appendix A.3) [133].

An intentional processing delay is introduced to the following simulations instead of latency to investigate the impact of CE mismatch with respect to fading variation. By introducing T_{dl} in symbol period as the intentional delay, the estimated channel coefficient matrix $\hat{\boldsymbol{H}}(t+1,k)$ is replaced by the next equation:

$$\hat{\boldsymbol{H}}(t+1,k) = \begin{cases} \hat{\boldsymbol{H}}(0,k) & t < T_{dl} \\ \hat{\boldsymbol{H}}(t-T_{dl}+1,k) & \text{otherwise} \end{cases}. \tag{3.24}$$

Table 3.1: Major parameters.

Data rate	307.2 and 614.4 Mbps
Total bandwidth	96 MHz
Number of antennas: (L, M)	$(4, 4)$
Number of sub-carriers: K	768
IFFT/FFT points: F	1024
FEC scheme	Convolutional coding (rate = $1/2$, constraint = 7)/ Soft decision Viterbi decoding
Modulation	QPSK and 16QAM
Effective symbol period	8.0 μsec
GI period	2.0 μsec
Number of pilot symbols	2
Number of data symbols	19
Initial CE	Carrier interferometory pilot [133]
CE update	SUCE and MMSE CE [136], [137]
Signal detection	Multi-QRD-GD, MLD and QRM-MLD [116]
AGS in Multi-QRD-GD	see Ref. [124]
Synchronization	Perfect
Multi-path model	Exponentially decaying 24-path Rayleigh fading
Path duration	62.5 nsec
Maximum delay	1437.5 nsec
RMS delay spread	360 nsec
Maximum Doppler frequency: f_D	300, 500, 800 and 1000 Hz (60, 100, 160 and 200 km/h at 5 GHz)

3.5.2 Parameter Setting for SUCE

Figure 3.5 shows the relationship between BER and the number of averaged symbols N_{av} for SUCE. This figure plots the BER performances with maximum Doppler frequency f_D of 300, 500, 800 and 1000 Hz. Modulation is fixed to QPSK, energy per bit to noise density ratio E_b/N_0 are fixed to 12 and 20 dB, and the intentional delay T_{dl} is fixed to two symbol periods. Figure 3.5 indicates that six and eight of N_{av} improve BER most especially when f_D is relatively high. When N_{av} is small, the impact of instantaneous noise deteriorates the accuracy of CE drastically. On the other hand, when N_{av} is excessively large, the tracking ability is reduced by the temporal average. This trend appears in BER when f_D is higher than 800 Hz.

Figure 3.6 shows the relationship between BER and the threshold parameter λ_{th}. This figure indicates that the BER performances are almost flat over λ_{th} when f_D are 300 and 500 Hz. This reason is that the channel variation is relatively mild in these cases. On the other hand, the BER performances are improved by setting λ_{th} to 0.1, 0.2 and 0.3 when f_D is higher than 800 Hz. This means that the outlier detector is well-performed to avoid the CE errors due to the variation of fading. Figure 3.6 also indicates that the excess threshold parameter increases BER again. This reason is that the outlier detector discards reliable temporal estimates by such a parameter. According to the above results, we choose eight of N_{av} and 0.2 of λ_{th} for the following simulations.

3.5.3 Comparison of Channel Estimation Algorithms

Figures 3.7, 3.8, 3.9 and 3.10 compare the BER performances of SUCE and conventional MMSE CE (see Appendix A.4) [136], [137] when f_D are 300, 500, 800 and 1000 Hz, respectively. Figures 3.7 and 3.8 plot the BER performances of both QPSK and 16QAM, and Figs. 3.9 and 3.10 plot those of QPSK. Moreover, these figures plot the BER performances with both the perfect initial CE and perfect channel tracking for reference. In these figures, labels "MMSE(1)" and "MMSE(2)" indicate MMSE CE using 1.0 and 0.6 of forgetting factors, respectively. All of them use Multi-QRD-GD as the detection algorithm.

From those figures, it is confirmed that SUCE is superior to MMSE CE. SUCE shows no BER floor down to 10^{-5} when modulation is QPSK and f_D is up to 500 Hz. BER of QPSK with SUCE achieves the order of 10^{-5} when f_D is up to 1000 Hz and that of 16QAM achieves the order of 10^{-4} when f_D is up to 300 Hz. In contrast, conventional MMSE CE, especially that with 1.0 of forgetting factor,

induce irreducible BER floors. These are caused by zero padding introduced by (A.18). Zero padding often induces the mismatch between the estimated and actual CFRs when $K < F$ in the multi-carrier systems [139]. It is noted that MMSE CE with 0.6 of forgetting factor slightly improves the BER performances compared to SUCE only in the lower E_b/N_0 region. This reason is that the impact of noise dominates BER in such an E_b/N_0 region. And then, zero padding suppresses the noise. The improvement by zero padding is approximately less than 0.5 dB.

Compared to the perfect performance, the BER degradation of SUCE becomes larger when f_D becomes higher. SUCE (and also MMSE CE) is influenced by error propagations in the process of updating, though the perfect performance suffers from no error propagation, i.e. the perfect tracking. The impact of error propagation is more significant when f_D is higher.

3.5.4 Comparison of Signal Detection Algorithms

Figures 3.11, 3.12, 3.13 and 3.14 compare the BER performances of MLD (see Appendix A.5), MLD with QR-decomposition and M-algorithm (QRM-MLD) [116] with SUCE and Proposed Multi-QRD-GD with SUCE when f_D are 300, 500, 800 and 1000 Hz, respectively. It is noted that Multi-QRD-GD with $G_r = 1$ is reduced to QRM-MLD. The numbers of surviving metrics S_l in QRM-MLD are set to $S_1 = S_2 = S_3 = 4$ for QPSK, and $S_1 = S_2 = S_3 = 10$ for 16QAM. These values make the complexity of QRM-MLD with SUCE to be almost same as that of Multi-QRD-GD with SUCE.

MLD induces significant BER floors especially when f_D is higher than 500 Hz. Although MLD basically obtains the full diversity gain, BER of MLD cannot be improved by only the diversity gain in the highly mobile environments. It is noted that the BER performances of MLD are superior to those of the proposed algorithms only at a low E_b/N_0 region. This reason is that the impact of noise is more significant than that of fading in such an E_b/N_0 region.

Compared to QRM-MLD, Multi-QRD-GD achieves the better BER performances when modulation is QPSK and f_D are 800 and 1000 Hz. The gain between Multi-QRD-GD with SUCE and QRM-MLD with SUCE is approximately 2.8 dB at 10^{-5} of BER when modulation is QPSK and f_D is 800 Hz. Because QRM-MLD is based on the successive detection all in series, it is weak against error propagation due to the CE errors in the highly mobile environments. In other words, when the total complexities of QRM-MLD and Multi-QRD-GD are set to be almost same each other, the decided number of surviving metrics are not enough

for QRM-MLD to obtain the diversity gain. On the other hand, Multi-QRD-GD is based on the successive detection, parts of which are executed in parallel. Thus, the impact of error propagation is mitigated by reducing the number of stages in each local detector. However, it is a fact that Multi-QRD-GD loses a part of diversity gain by adopting the parallel processing. Figures 3.11 and 3.12 show that QRM-MLD is superior to Multi-QRD-GD when modulation is QPSK and f_D are 300 and 500 Hz. These mean that the impact of fading variation is relatively small in such environments, and then QRM-MLD obtains more diversity gain than Multi-QRD-GD. The difference between QRM-MLD with SUCE and Multi-QRD-GD with SUCE is approximately 0.5 dB at 10^{-5} of BER when modulation is QPSK and f_D is 500 Hz.

It is noted that all the algorithms induce irreducible BER floors when modulation is 16QAM. In addition to the inaccuracy of CE, ICI also cannot be ignored for 16QAM. Although all those algorithms induce the irreducible BER floors, proposed Multi-QRD-GD with SUCE achieves the better BER performances than the others.

3.5.5 Impact of Signal Processing Delay

Figure 3.15 shows the impact of intentional delay T_{dl} to BER of the proposed system when modulation is QPSK. f_D are fixed to 500 and 800 Hz. Figure 3.15 indicates that BER degradation due to T_{dl} is more significant when f_D is higher. Even when f_D is 500 Hz, a BER floor is caused by 8 symbols of T_{dl}. When f_D is 800 Hz, the severer BER floor is caused by T_{dl} of 4 symbols. These results imply that the total latency should be small in the MIMO-OFDM systems operating in the highly mobile environments.

3.5.6 Complexity

In this sub-section, we evaluate the computational complexities of proposed algorithms are evaluated. Table 3.2 compares the required numbers of real multiplications per update in MMSE CE [137] and SUCE. We regard one complex multiplication as four real multiplications. From this table, we see that the proposed SUCE requires 23.7 % multiplications of the conventional MMSE CE. In conventional MMSE CE, the FFT and IFFT operations require a great amount of the computations. From the point of complexity in addition to that of BER, it is generally desirable for CE to terminate all the process within the frequency-domain. Table

3.3 compares the required numbers of real multiplications per packet in MLD, QRM-MLD with SUCE and Multi-QRD-GD with SUCE. From Table 3.3, the proposed system requires 54.8 and 0.4 % multiplications of MLD when the modulation scheme is QPSK and 16QAM, respectively. Because the complexity of MLD, especially the metric calculation of that, largely depends on the modulation scheme, the difference of the complexity amount is clearer when the modulation scheme is 16QAM. From these tables, it is confirmed that Multi-QRD-GD and SUCE have the advantages of not only performance but also complexity.

3.6 Conclusion

An MIMO-OFDM system using the reduced-complexity-and-latency signal detection and CE algorithms, those are Multi-QRD-GD and SUCE, is proposed in this chapter. The goal of the proposed system is enhancing the performance in the mobile fading environment and supporting the mobile users. For this goal, the proposed system aims at reducing the latency caused in the receiver as well as reducing the complexity. The computer simulation results show that the proposed system achieves the better BER performance than the conventional schemes in the mobile environment. The proposed system achieves 10^{-5} of BER even when f_D is 1000 Hz, which assumes 200 km/h of vehicle speed at 5 GHz carrier frequency, and modulation is QPSK. Moreover, the proposed system requires less complexity than the conventional schemes. Thus, the proposed system is the better one from the points of not only the performance but also the complexity in the mobile environment.

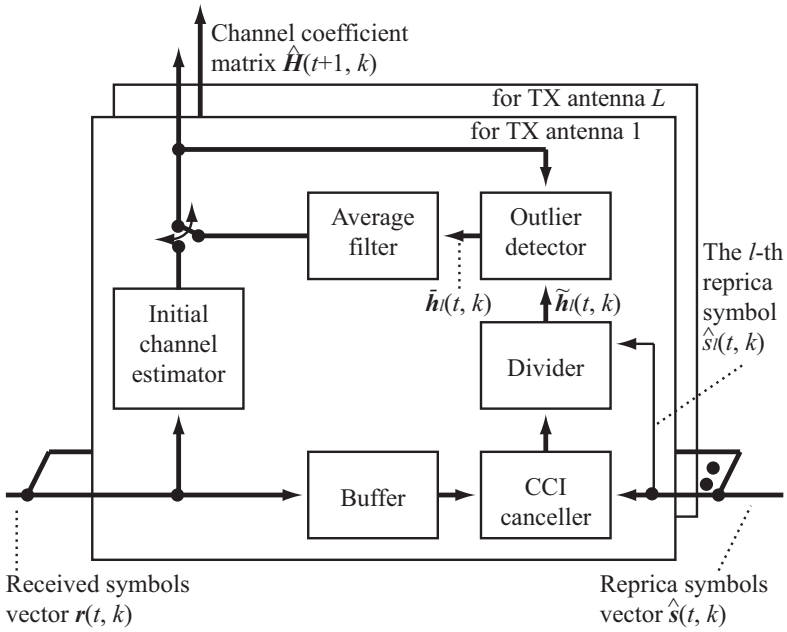

Figure 3.4: Configuration of SUCE block.

Table 3.2: Required numbers of real multiplications per update in the conventional and proposed CE schemes.

	Conventional MMSE CE [137]	Proposed SUCE
Number of real multiplications per update	$4\{(2K + L\log_2 K)LM$ $+(K\log_2 K)LM\}$	$4\{KL(L-1)M$ $+2KLM\}$
Total $(K = 768, L = M = 4)$	1.04×10^6	2.46×10^5

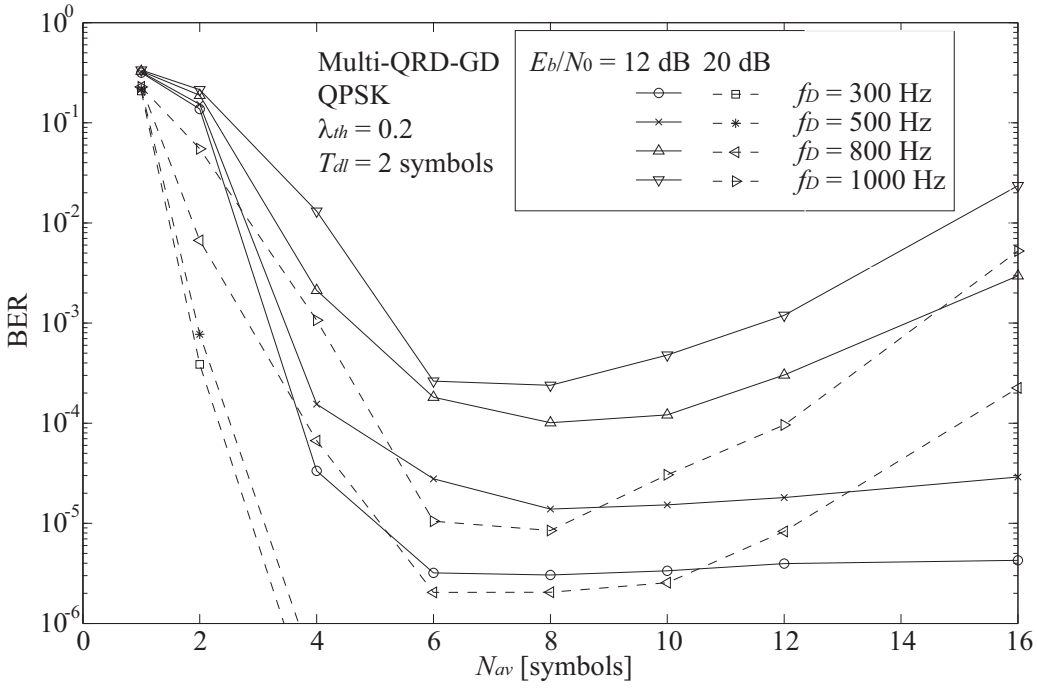

Figure 3.5: Relationship between BER and the number of averaged symbols for SUCE.

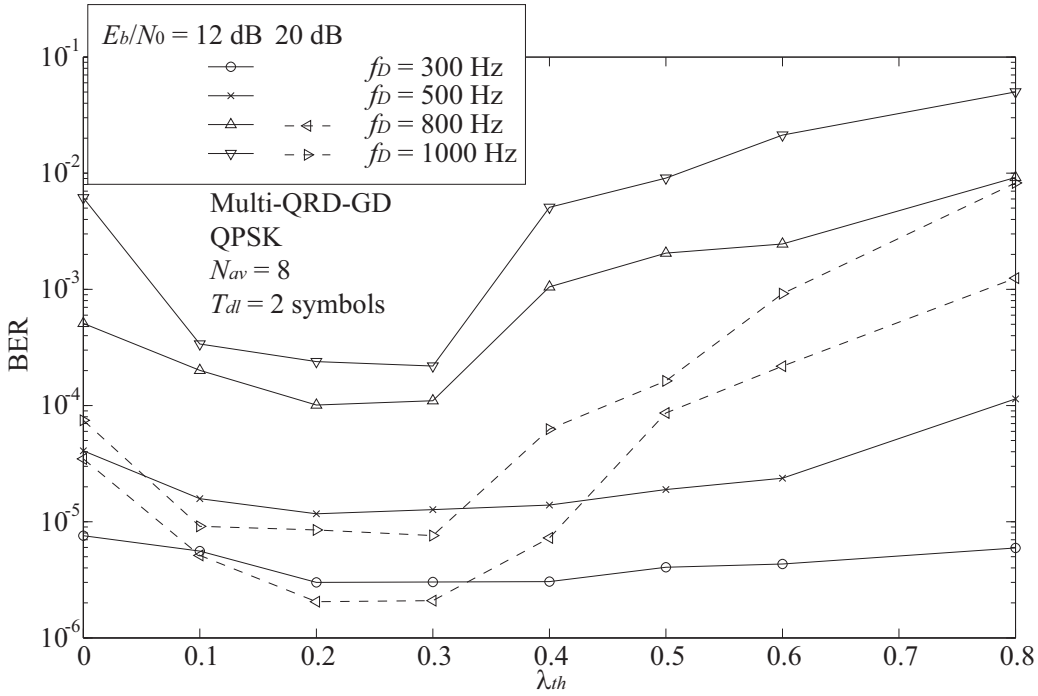

Figure 3.6: Relationship between BER and the threshold parameter for SUCE.

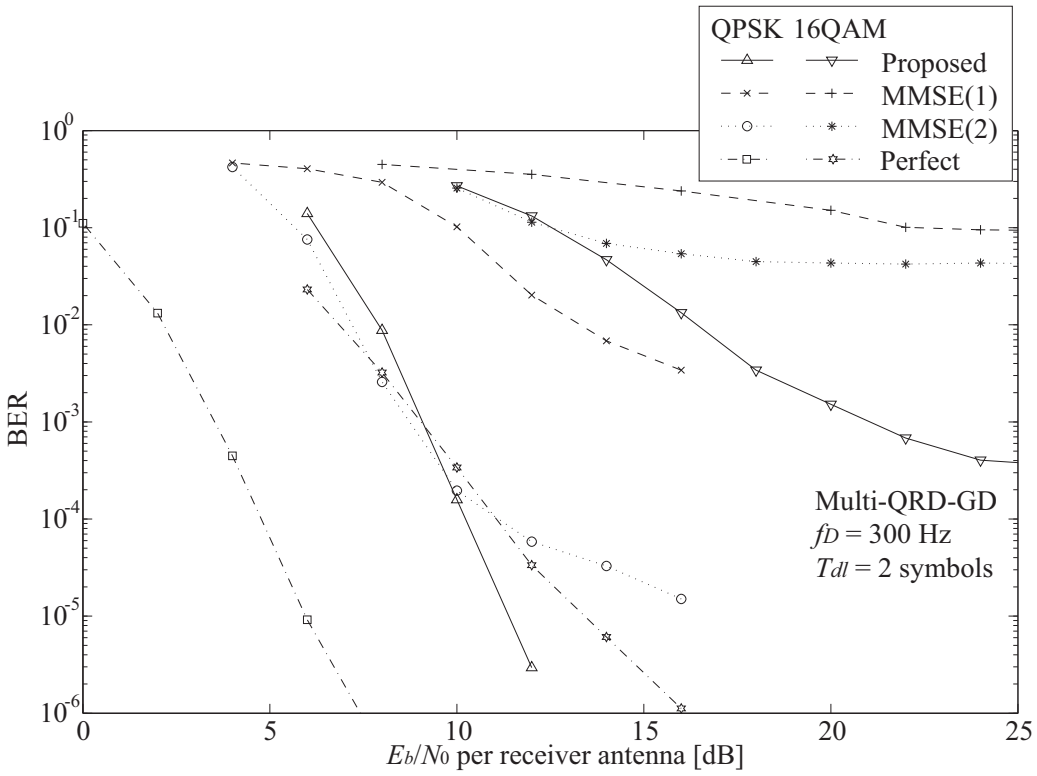

Figure 3.7: BER comparison of CE algorithms when maximum Doppler frequency is 300 Hz.

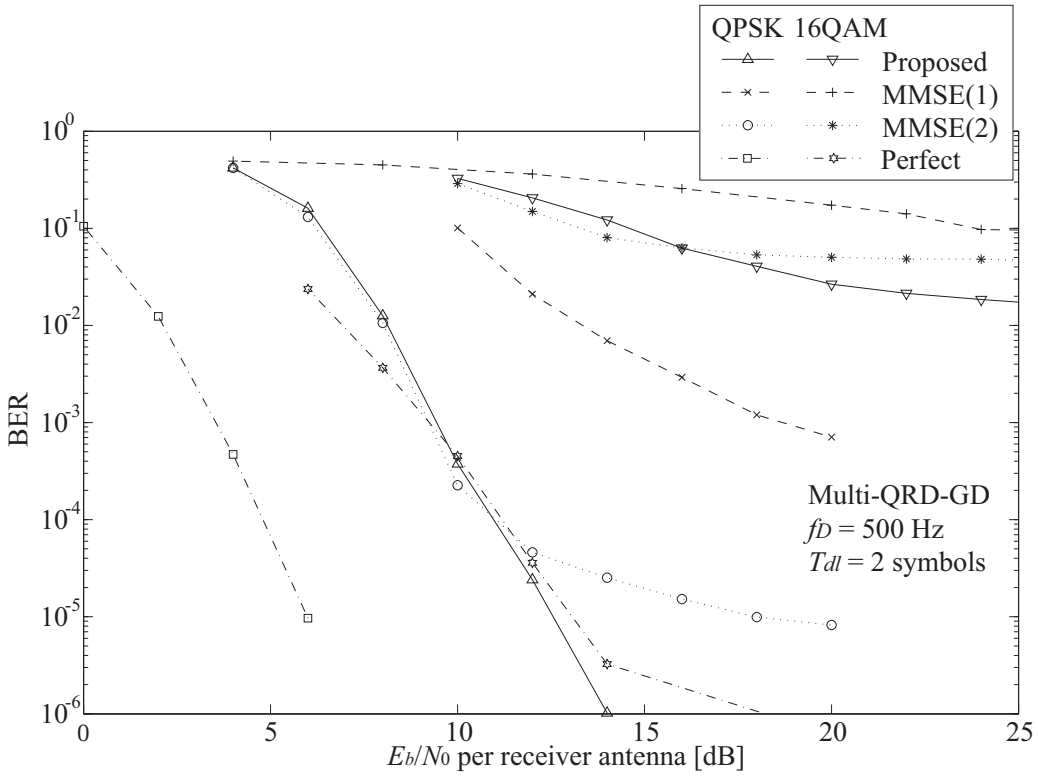

Figure 3.8: BER comparison of CE algorithms when maximum Doppler frequency is 500 Hz.

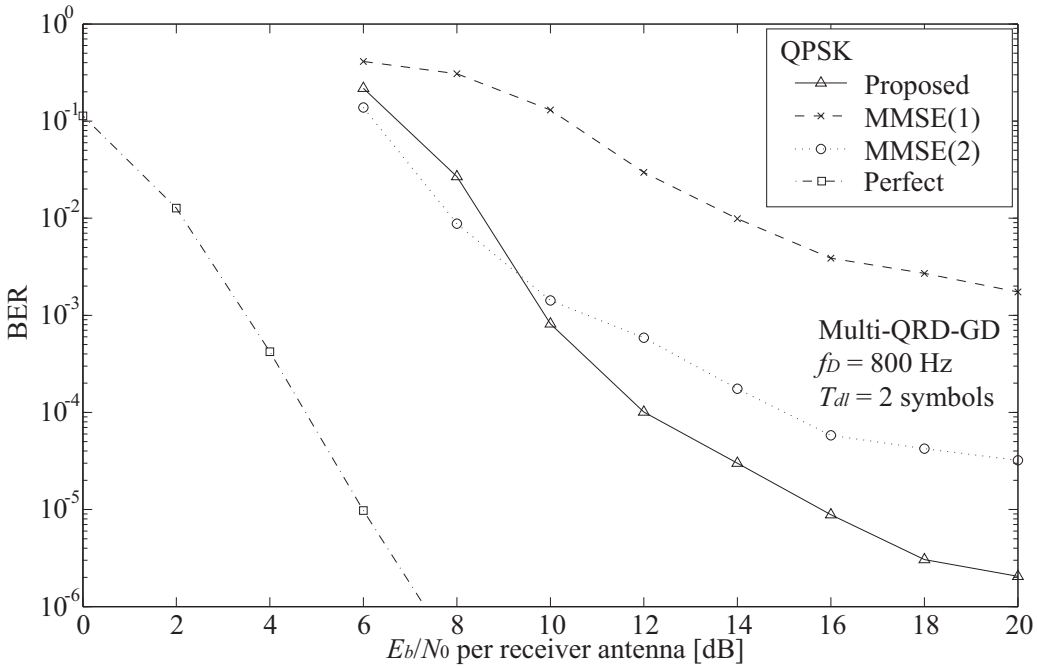

Figure 3.9: BER comparison of CE algorithms when maximum Doppler frequency is 800 Hz.

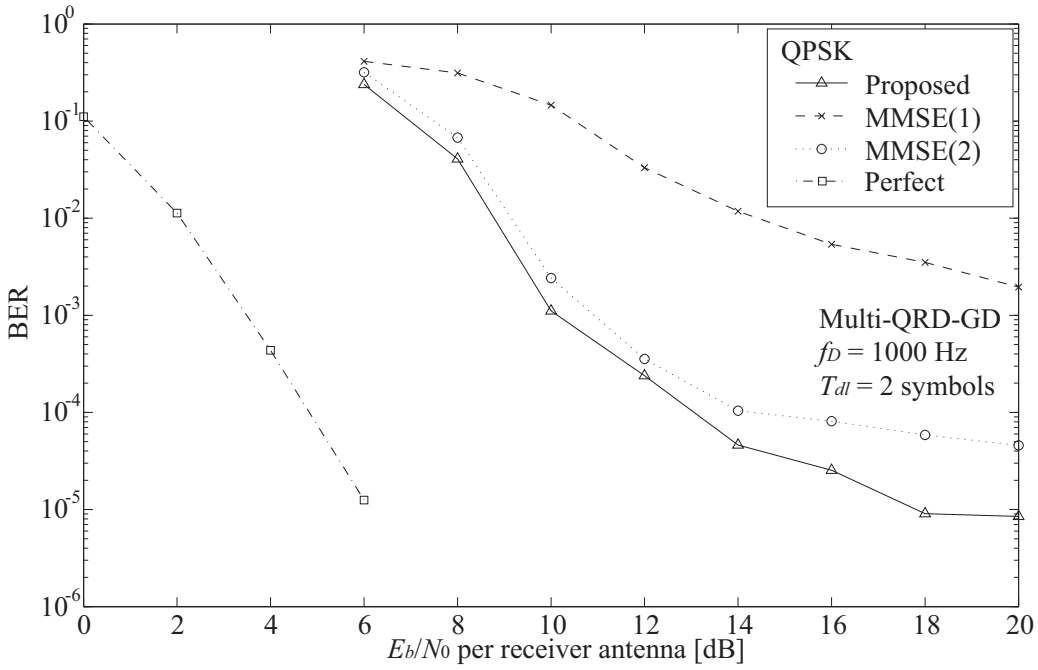

Figure 3.10: BER comparison of CE algorithms when maximum Doppler frequency is 1000 Hz.

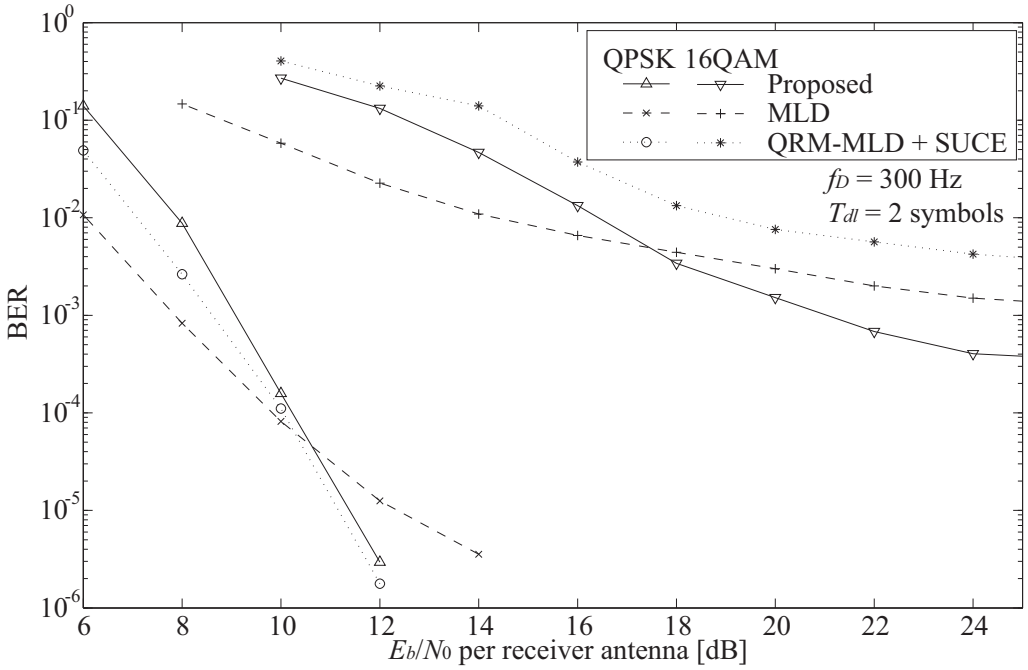

Figure 3.11: BER comparison of the proposed system, MLD and QRM-MLD with SUCE when the maximum Doppler frequency is 300 Hz.

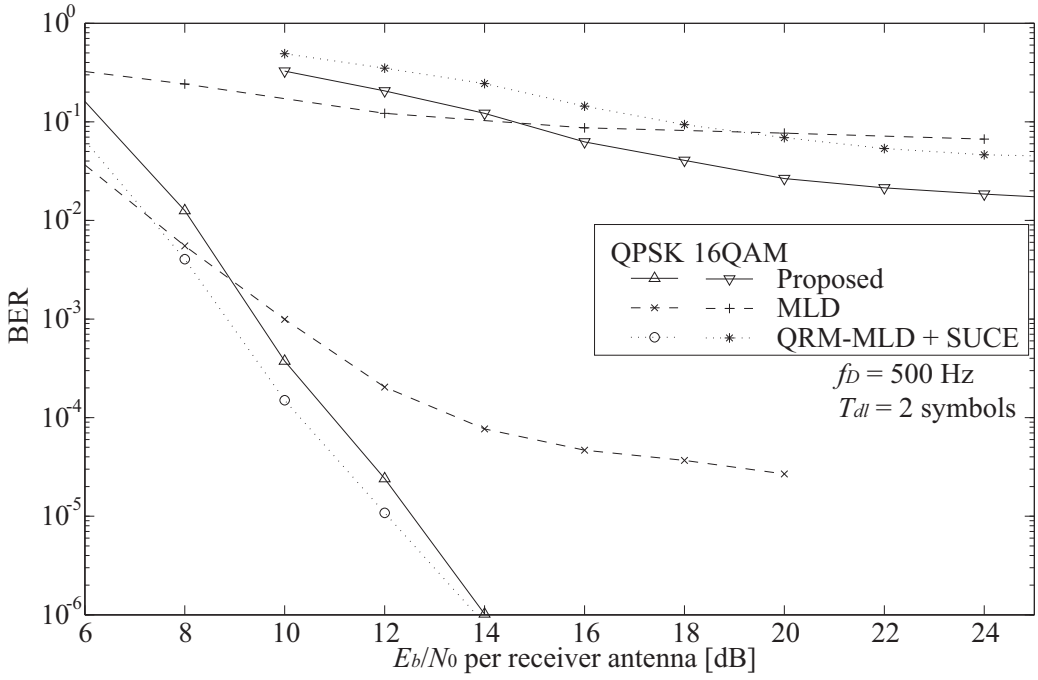

Figure 3.12: BER comparison of the proposed system, MLD and QRM-MLD with SUCE when the maximum Doppler frequency is 500 Hz.

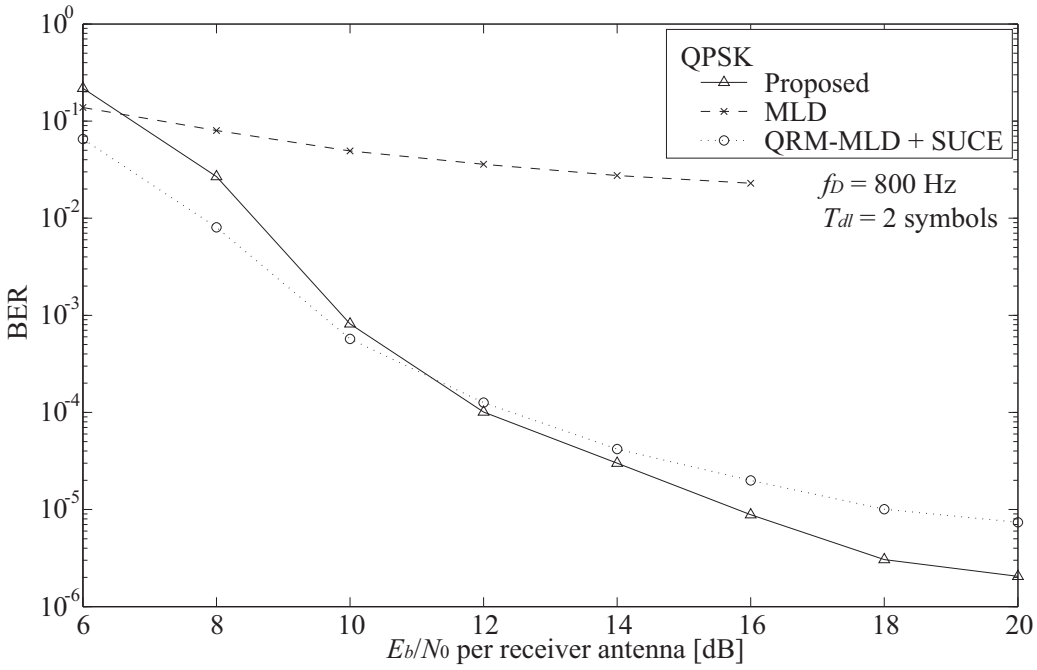

Figure 3.13: BER comparison of the proposed system, MLD and QRM-MLD with SUCE when the maximum Doppler frequency is 800 Hz.

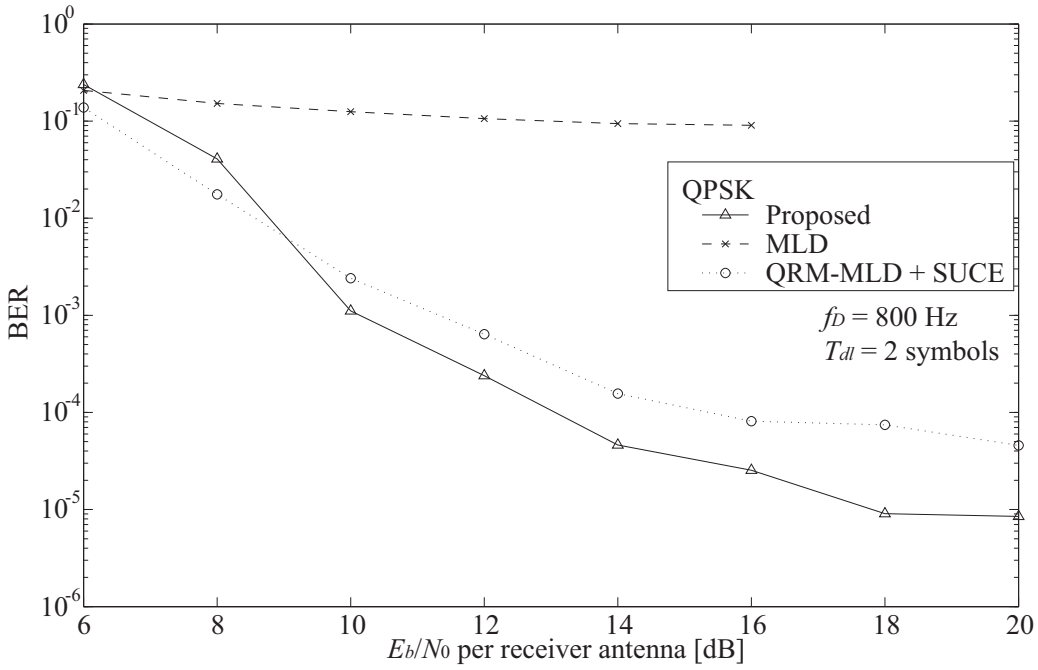

Figure 3.14: BER comparison of the proposed system, MLD and QRM-MLD with SUCE when the maximum Doppler frequency is 1000 Hz.

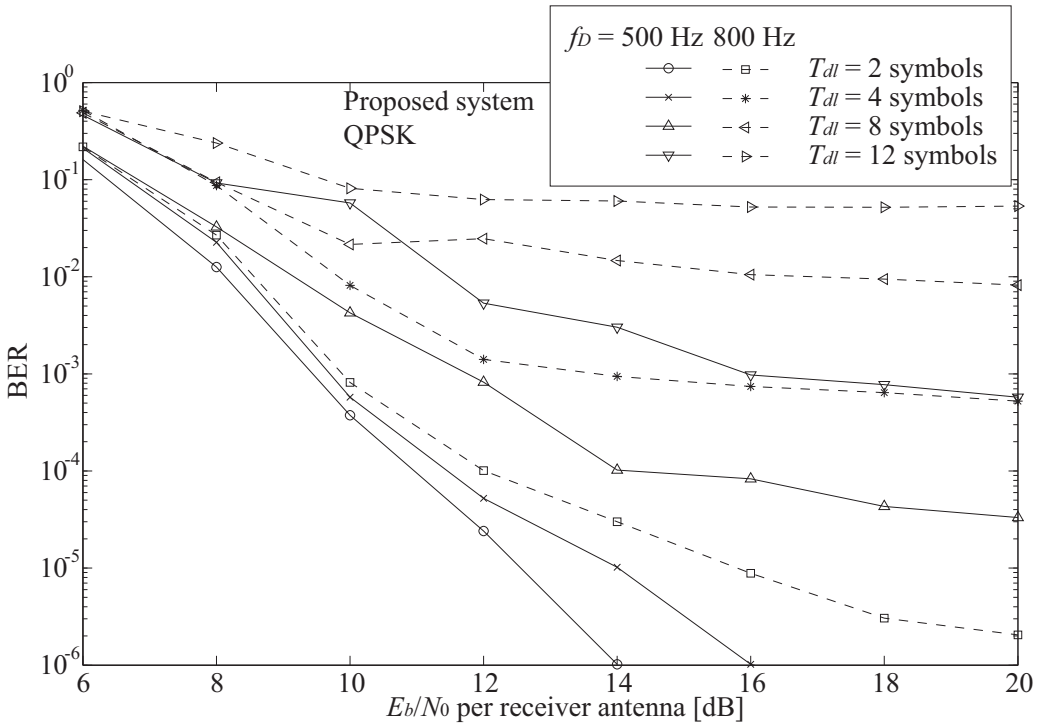

Figure 3.15: Impact of processing delay to BER of the proposed system when modulation is QPSK.

Table 3.3: Required numbers of real multiplications per packet in MLD and proposed system.

		MLD	QRM-MLD & SUCE	Multi-QRD-GD & SUCE
Signal detection	AGS	-	$4LKMD$	$4LKMD$
	QR-decomposition	-	$4L^3KD$	$4G_rL^3KD$
	Computation for $\boldsymbol{Q}^H\boldsymbol{r}$	-	$4L^2KD$	$4L^2KD$
	Replica symbol generation	$4L^2SK$	$2L(L+1)$ $\cdot SKD$	$L(L+2)$ $\cdot SKD$
	Metric computations	$2LS^LKD$	$2\left(1+\sum_{l=1}^{L-1}S_l\right)$ $\cdot SKD$	$2G_r$ $\cdot\left(1+\sum_{l=1}^{L/G_r-1}S_l\right)$ $\cdot SKD$
Channel estimation	CCI cancellation	-	$4KL(L-1)$ $\cdot MD$	$4KL(L-1)$ $\cdot MD$
	Outlier detection	-	$8KLMD$	$8KLMD$
Total ($K=768, L=M=4$, $G_r=2, S=4$(QPSK))		3.01×10^7	1.41×10^7 ($S_{l_M}=4$, $l_M=1,2,3$)	1.65×10^7 ($S_1=4$)
Total ($K=768, L=M=4$, $G_r=2, S=16$(16QAM))		7.65×10^9	3.41×10^7 ($S_{l_M}=10$, $l_M=1,2,3$)	3.36×10^7 ($S_1=14$)

Chapter 4

Time Alignment Control for Otrhogonal Frequency Division Multiple Access Reverse Link

summary

An OFDMA based cellular system is investigated in this chapter. One of the problems of OFDMA is time misalignment of user terminals (UTs) in reverse link transmission. The time misalignment often results in multiple access interference (MAI). To avoid MAI, time alignment control (TAC) is proposed for OFDMA reverse link in this chapter. Moreover, two complexity reduction techniques are also proposed to reduce the implementation cost of TAC. In this chapter, the packet error rate (PER) performances of OFDMA systems with Full-TAC and complexity-reduced TAC (CRTAC) are evaluated by computer simulation. The simulation results show that Full-TAC achieves an equivalent PER performance of ideal time alignment, and that CRTAC also approaches that performance with 1 dB loss when modulation is QPSK and FEC scheme is convolutional coding. In addition, estimation of complexity of TAC shows that CRTAC has the reasonable benefit from the point of implementation.

4.1 Introduction

OFDMA is a promising candidate of PHY specification toward the next generation mobile systems [46],[49],[50],[53]–[57]. In OFDMA, multiple user terminals (UTs) connect with an access point (AP) by using different sub-carriers. On the

reverse link transmissions from UTs to AP in the OFDMA systems, propagation delays (PDs) will be occurred by the UTs' geographical conditions, and they often exceed the length of GI in large areas of communication coverage. In such a case, the differences of PDs induce multiple-access interference (MAI) and degrade the performance of reverse link transmission drastically [144], [147]. In this chapter, TAC is proposed to avoid such MAI. The purposes of TAC are (i) estimating PDs of UTs at AP, (ii) informing those estimates from AP to UTs and (iii) controlling UTs' transmit timings according to those informed estimates. TAC is an effective scheme to improve the performance of reverse link transmission without extending the length of GI. Moreover, complexity reduction techniques are also proposed for TAC in this chapter. These techniques reduce the amount of complex multiplications in the algorithm of TAC.

4.2 System Model of Broadband OFDMA

4.2.1 MAC Layer Protocol

This section introduces a model of broadband OFDMA system [53], [155]. The specification of medium access control (MAC) layer is necessary for investigation of TAC for OFDMA. Packet reservation dynamic time-slot multiple access (PR-DSMA) [150]–[152] is assumed for the specification of MAC protocol.

Figure 4.1 illustrates the reverse and forward link frame formats of PR-DSMA based OFDMA system. This OFDMA system divides and groups all K available sub-carriers into same size blocks, each of which is called "sub-channel block (SCB)." It also divides SCBs into certain periods, and then generates time-slots. UTs simultaneously share these slots, but they employs the different SCBs each other. This system applies frequency division duplex (FDD) to its duplex scheme.

PR-DSMA prepares three types of time-slots in the frames; activation slot (ACTS), message data slot (MDS), and frame control message slot (FCMS). Table 4.1 shows the frame parameters of frame formats of PR-DSMA. PR-DSMA defines the roles of slots as follows:

(1) ACTS is usually located at the beginning of the reverse link frame. It consists of four mini-slots. UTs use ACTSs by random accesses to inform their demands for the registration/elimination and connection setup/release to AP.

(2) MDS is mainly used to transmit data between UTs and AP both in the reverse and forward link frames. In addition, it is also used to transmit AP's

demands for the registration/elimination and connection setup/release in the forward link frame. Moreover, MDS in the reverse link is used to transmit the acknowledgements (ACKs) of the data on the forward link frame.

(3) FCMS is usually allocated at the beginning of the forward link frame. FCMS includes the AP information, slot assignment information of the reverse and forward link frame, and ACKs of the data on the reverse link frame.

PR-DSMA is assumed to connect to transmission control protocol/ Internet protocol (TCP/IP) based upper layers. In PR-DSMA, packet data units transferred from the IP layer are directly segmented and allocated into MDSs in the frames. Hence, PR-DSMA has a high-affinity to the IP networks [151].

4.2.2 UT Transmitter and AP Receiver

Figures 4.2 and 4.3 illustrate configurations of UT transmitter and AP receiver, respectively. The following explains the transmission procedure of UT which uses the b-th SCB. At the UT transmitter, a data bit stream is transferred from the MAC layer with being controlled the transfer timing in accordance with TAC information. After FEC encoding and block interleaving, the interleaved bits is converted to parallel streams on the sub-carriers, and then modulated onto phase shift keying (PSK) or quadrature amplitude modulation (QAM) constellation. Then, OFDM symbols are generated by IFFT. After formatting a slot, the transmitter compensates a carrier frequency offset (CFO) between UT and AP by itself. This CFO can be estimated with utilizing downlink signals from AP. After transmit power control (TPC) to counteract a path loss and shadowing, i.e. slow TPC [35], the slot signal, $s_b(k)$, is transmitted over the air.

Hereafter, the reception procedure of AP is described. At the OFDMA reverse link, AP receives the signals from the multiple UTs simultaneously. The received signal of reverse link, $r(k)$, is given as

$$r(k) = \sum_{b=0}^{B-1} \sum_{p=0}^{P_i-1} h_{p,b}(k)\, s_b\left(k - \tau_{p,b} - \tau_{d,b} + \tilde{\tau}_{d,b}\right) \cdot \exp\left\{ j2\pi(f_{\Delta,b} - \tilde{f}_{\Delta,b})\left(k - \tau_{p,b} - \tau_{d,b} + \tilde{\tau}_{d,b}\right)\right\} + n(k), \tag{4.1}$$

where B is the total number of SCBs, P_b is the total number of paths composing the multi-path channel, $h_{p,b}$ is the channel impulse response (CIR) of the p-th path, $\tau_{p,b}$ is the delay time of the p-th path, $\tau_{d,b}$ is PD due to the geographical condition

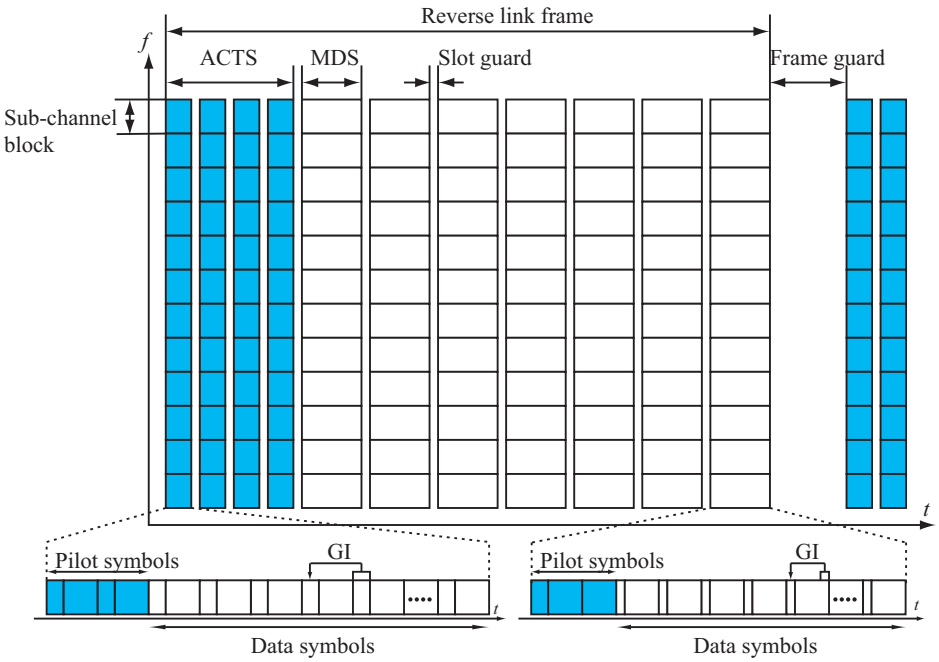

(a) Reverse link

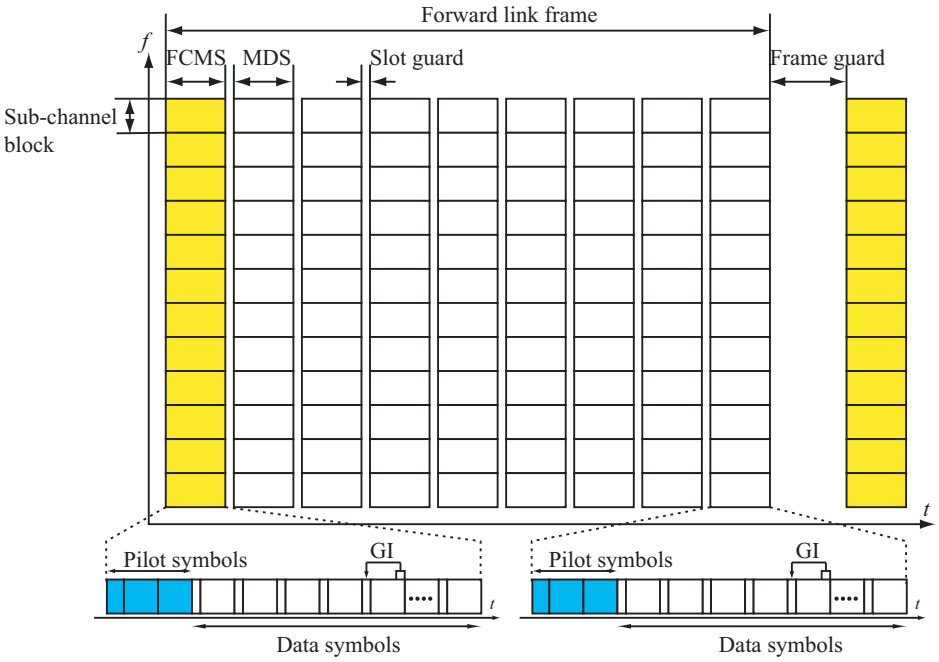

(b) Forward link

Figure 4.1: Frame formats of PR-DSMA.

of UT, $\tilde{\tau}_{d,b}$ is the estimated value of $\tau_{d,b}$, $f_{\Delta,b}$ is CFO between UT and AP, $\tilde{f}_{\Delta,b}$ is the estimated value of $f_{\Delta,b}$, and $n(k)$ is the additive white Gaussian noise (AWGN) component, respectively for the b-th SCB. This chapter assumes that CFOs are ideally compensated by UTs themselves, i.e. $\tilde{f}_{\Delta,b} = f_{\Delta,b}$. In addition, it is noted that $\tilde{\tau}_{d,b} = \tau_{d,b}$ in the ideal TAC.

In AP, the received signal is first fed into PDs estimator and FFT timing synchronizer. These processes are presented in Section 4.3. After the synchronization, GIs are removed from the received OFDM symbols according to the decided FFT timing, and then the remains are converted to the sub-carriers symbols by FFT. The channel frequency responses (CFRs) on all the sub-carriers are initially estimated by employing the received pilot symbols. Next, the channel contaminations which the received data symbols suffer from are compensated by these estimates. After the compensations, soft information weighted by channel state information (CSI) [65] are generated by sub-carrier de-mappers. After the parallel-to-serial (P/S) conversion, de-interleaving, and FEC decoding on each SBC, all data transmitted from the multiple UTs are recovered. It is noted that the proposed OFDMA system exploits SUCE, which is presented in Chapter 3, for improving the transmission performance in highly mobile environments.

4.3 Time Alignment Control

4.3.1 Basic Flow Related to MAC Protocol

Figure 4.4 illustrates the basic flow of TAC. TAC deeply depends on the MAC protocol in the target system. Then, Fig. 4.4 shows TAC combined with PR-DSMA for the proposed PFDMA system. The flow includes the following steps:

Step 1: UTs receive the broadcast-FCMSs, which include the cell information from AP, when they enter into a certain cell or when they want to request their connections to certain AP. Then, each UT obtain the tentative frame timings of the cell, which has independent deviation due to a one-way PD caused by UT's geographical condition. Each UT also estimates its own CFO between AP, $\tilde{f}_{\Delta,b}$, at the same time. This estimated CFO is utilized for self-CFO compensation in the following reverse link transmission (see (4.1)).

Step 2: UTs transmit ACTSs to AP to register themselves and request the assignment of MDSs. At this moment, the arrival timings of these ACTSs at AP

Table 4.1: Frame Parameters in PR-DSMA.

Frame period (reverse/forward link)	2500 μsec (including a frame guard)
ACTS period (reverse link)	500 μsec (including slot guards)
Number of ACTS per frame	1 (4 mini-slots)
MDS period (reverse/forward link)	250 μsec (including a slot guard)
Number of MDS per frame	7 (reverse link) / 8 (forward link)
FCMS period (forward link)	250 μsec (including a slot guard)
Number of FCMS per frame	1

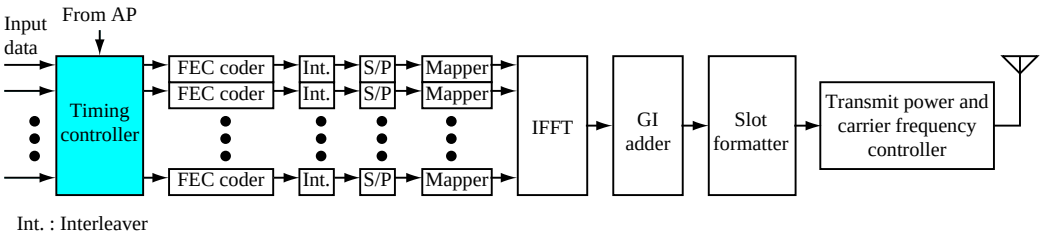

Figure 4.2: Configuration of UT transmitter.

include the different round-trip PDs, $\tau_{d,b}$. AP estimates PDs for all UTs when it receives those ACTSs.

Step 3: After estimating, AP informs UTs of the estimated PDs with the forward link MDSs. These MDSs also include ACKs for the registrations.

Step 4: UTs control their transmit timings of their MDSs according to the informed estimates, $\tilde{\tau}_{d,b}$. These controls align the arrival timings of MDSs at AP. In this chapter, the interval between the receptions of ACTSs and MDSs, T_R (see Fig. 4.4), is called "reception interval."

Step 5: AP can re-estimate PDs with the received MDSs on the reverse link. Receiving the MDSs, AP transmits ACKs and re-estimated PD information with the following FCMSs. UTs obtain the re-estimated information and then update their own transmission timings.

4.3.2 Estimation of Propagation Delay

Figure 4.5 illustrates the configuration of PD estimator and timing synchronizer for Full-TAC. Receiving ACTSs, AP first computes correlations, $P_{c,b}(k)$ for $b = 0, \cdots, B-1$, given as Eq. (4.2):

$$P_{c,b}(k) = \left| \sum_{m=0}^{N_{ref}-1} r\,(k+m)\, c_b^*(m) \right|, \tag{4.2}$$

where $c_b(k)$ is the reference symbol on the b-th SCB which AP prepared in advance, and N_{ref} is the length of $c_b(k)$, respectively. The operator a^* denotes the complex conjugate of a. For Full-TAC, the wave form of reference symbol $c_b(k)$ is same as that of pilot symbol, and N_{ref} is equivalent to the FFT point F. It is noted that the correlations between $c_b(k)$ and $s_{b'}(k)$ for $b \neq b'$ in principle become zero because of their orthogonality when $N_{ref} = F$. $P_{c,b}(k)$ is then equivalent to the magnitude of instantaneous CIR including $\tau_{d,b}$, which the signal on the b-th SCB passed through. To estimate PDs, TAC detects precedent path timings by using $P_{c,b}(k)$ for all SCBs. The precedent path timings $k_{f,b}$ are obtained by the next condition:

$$k_{f,b} = \min\left\{ k_{fc,b} \mid \alpha P_{c,max,b} \leq P_{c,b}(k_{fc,b}) \right\}, \tag{4.3}$$

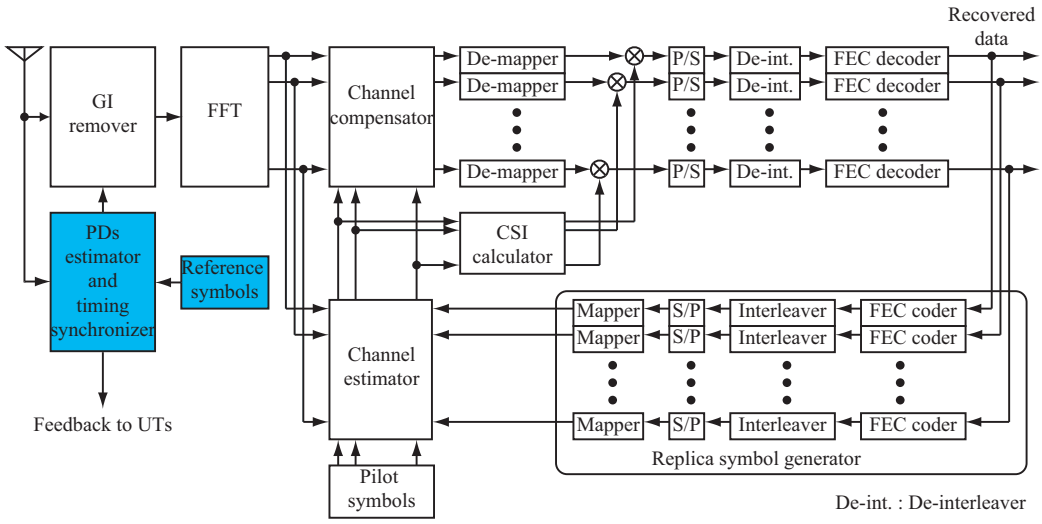

Figure 4.3: Configuration of AP receiver.

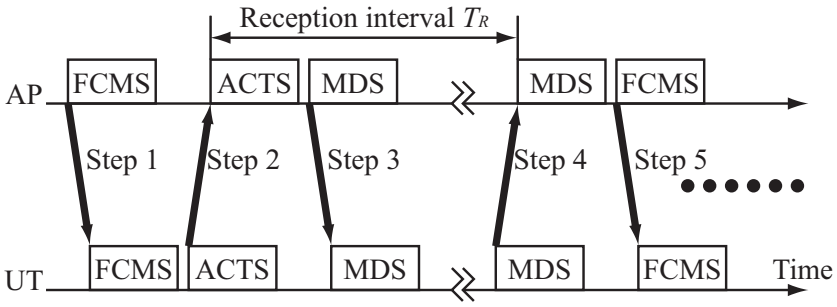

Figure 4.4: Basic flow of TAC.

where

$$P_{c,max,b} = \max\{P_{c,b}(k)\}, \tag{4.4}$$

and $0 \leq \alpha \leq 1$. After that, AP estimates PDs of all UTs, $\tilde{\tau}_{d,b}$, by comparing all $k_{f,b}$ with a desired AP reception time, k_{dr}:

$$\tilde{\tau}_{d,b} = k_{f,b} - k_{dr}. \tag{4.5}$$

Moreover, AP utilizes the precedent path timings for the timing synchronization. AP chooses the fastest timing among the precedent paths k_{fft}:

$$k_{fft} = \min\left\{k_{f,b} \mid 0 \leq b \leq B-1\right\}, \tag{4.6}$$

as the timing of FFT window for demodulating the received OFDM symbols. According to k_{fft}, AP removes GIs from the OFDM symbols and decomposes the sub-carriers data by FFT.

4.4 Complex Reduction Techniques for Time Alignment Control

4.4.1 Simplified Reference Symbols

In this sub-section, simplified reference symbols are presented for reducing the amount of complex multiplications in TAC. The simplified reference symbols are used for computing the cross-correlations like (4.2). These symbols are simplified by "symbol shortening" and "3-level quantization."

In Full-TAC, the reference symbols are identical with the time domain waveform of the transmitted pilot symbols on each SCBs. Thus, the length of reference symbols is equal to the FFT points, i.e. $N_{ref} = F$. To reduce the operations in the computations of cross-correlation, the length of simplified reference symbols are shorter than that of FFT points, that is, $N_{ref} < F$. By symbol shortening, the amount of operations becomes N_{ref}/N_f compared with Full-TAC. However, the orthogonality among the reference symbols is lost by symbol shortening.

The pilot symbols and original reference symbols have continuous waveforms in the time-domain. This means that complex multiplications are necessary in the computations of cross-correlation. The simplified reference symbols $c'_b(k)$ are

quantized onto ±1 and 0 by thresholds $\pm\xi_{I,b}$, that is:

$$\Re\left\{c'_b(k)\right\} = \begin{cases} 1 & \Re\left\{c_b(k)\right\} \geq +\xi_{I,b} \\ 0 & -\xi_{I,b} < \Re\left\{c_b(k)\right\} < +\xi_{I,b} \\ -1 & \Re\left\{c_b(k)\right\} \leq -\xi_{I,b} \end{cases} . \tag{4.7}$$

The operator $\Re\{a\}$ means the real part of complex number a. Similarly, the imaginary parts of the reference symbols $\Im\left\{c'_b(k)\right\}$ are quantized by the same manner of (4.7) with the thresholds $\pm\xi_{Q,b}$. This quantization practically replaces the multipliers to inverters in the matched filters, as illustrated in Fig. 4.7. Generally, the inverter consists of simple bit-operations while the multiplier requires a large and complex digital signal processing (DSP). It is noted that it was proposed for the OFDM timing synchronization to quantize the reference symbol onto ±1 (i.e. $\xi_{I,b}, \xi_{Q,b} = 0$ in (4.7), or 2-level quantization) [73]. The samples with small amplitudes in the reference symbols have less influence in the calculated correlations. 3-level quantization eliminates the influences of such samples by quantizing onto 0s. The amplitudes 0s reduce the amount of inverters from the matched filters. Thus, 3-level quantization reduces the complexity of TAC and the DSP circuits of correlators.

In this chapter, N_{ref} is set to 64, and the thresholds $\xi_{I,b}$ and $\xi_{Q,b}$ are set to the values in Table 4.2. These thresholds restrict the number of 0s in each real and imaginary parts of reference symbols to approximately a third of N_{ref} when $N_{ref} = 64$.

Figure 4.8 illustrates examples of correlation characteristics on a certain SCB. This figure compares three types of characteristics, (Fig. 4.8(a)) the original reference symbol, (Fig. 4.8(b)) the shortened and non-quantized reference symbol, and (Fig. 4.8(c)) the shortened and quantized reference symbol. Figure 4.8 indicates that the symbol shortening drastically reduces the orthogonality between the pilot and reference symbols and blur out the peak in the correlation, while the original symbol can obtain the distinct peak. In addition, this figure also indicates that the correlation by the 3-level quantized symbol is slightly blur compared to that by non-quantized one when $N_{ref} = 64$.

4.4.2 2-Step Precedent Path Detection

It is noted that the accuracy of estimated CIR, which the cross-correlation implies, is degraded by the use of simplified reference symbols. Due to this degradation, the precedent path detection given by (4.3) induces the significant detection errors

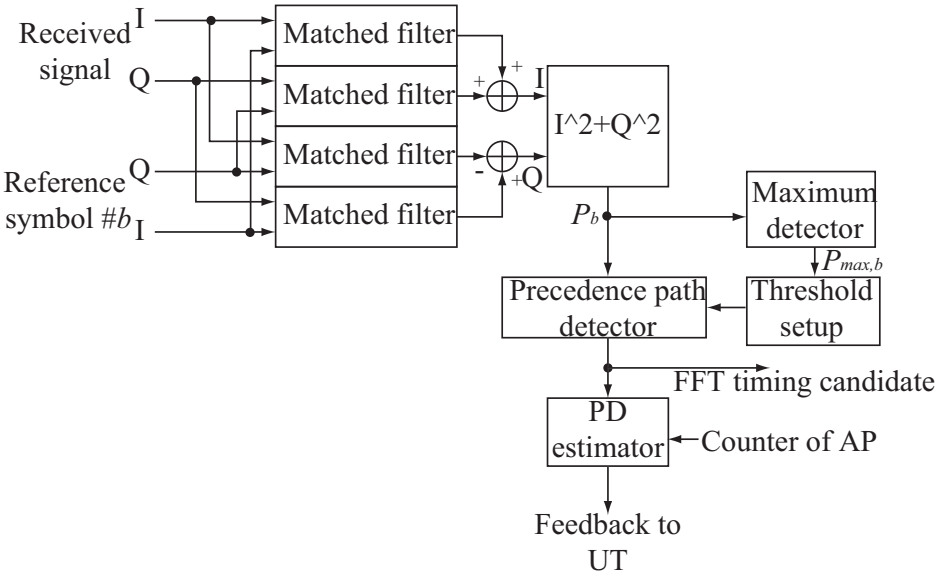

Figure 4.5: Configuration of PD estimator and timing synchronizer.

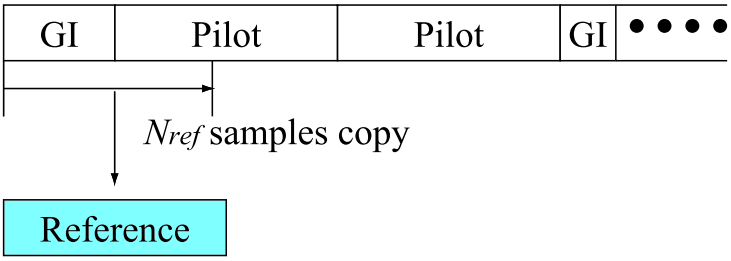

Figure 4.6: Structure of reference symbol.

Table 4.2: Example of threshold values for 3-level quantization.

SCB: b	$(\xi_{I,b}, \xi_{Q,b})$	SCB: b	$(\xi_{I,b}, \xi_{Q,b})$
1	(0.0019, 0.0019)	7	(0.0008, 0.0015)
2	(0.0038, 0.0040)	8	(0.0042, 0.0037)
3	(0.0019, 0.0020)	9	(0.0015, 0.0014)
4	(0.0038, 0.0039)	10	(0.0034, 0.0036)
5	(0.0019, 0.0017)	11	(0.0016, 0.0019)
6	(0.0038, 0.0041)	12	(0.0030, 0.0035)

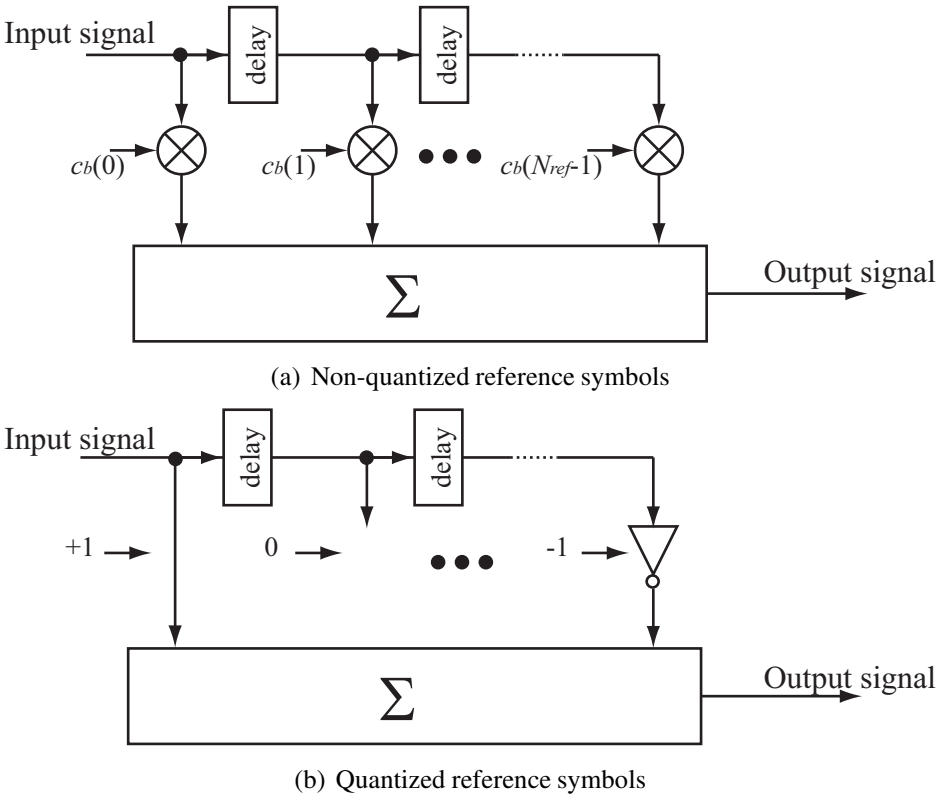

(a) Non-quantized reference symbols

(b) Quantized reference symbols

Figure 4.7: Structures of matched filters in cross-correlators.

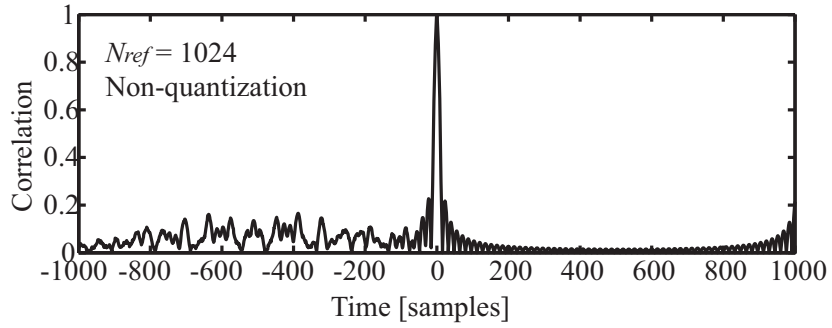

(a) Conventional full symbol

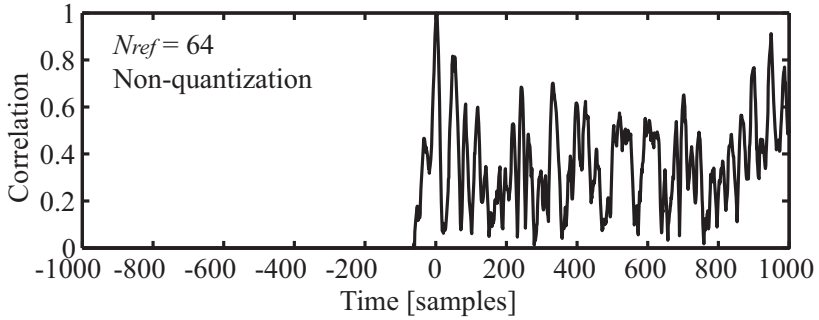

(b) Shortened and non-quantized symbol

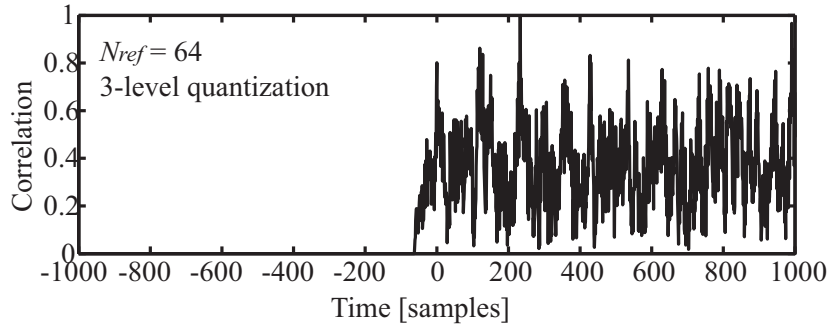

(c) Shortened and 3-level quantized symbol

Figure 4.8: Correlation characteristics of conventional and simplified symbols.

(for example, see Fig. 4.10). To mitigate the degradation, 2-step precedent path detection (2PPD) is introduced to CRTAC. Hereafter, the original precedent path detection is called as 1PPD.

Figure 4.9 illustrates the configuration of the PD estimator and timing synchronizer with 2PPD, and Fig. 4.10 illustrates the behavior of 2PPD. 2PPD employs a received signal power based threshold in addition to the maximum power path based one. First, AP computes the cross-correlations between $r(k)$ and $c'_b(k)$, $P_{p,b}(k)$, for $b = 0, \cdots, B-1$:

$$P_{p,b}(k) = \left| \sum_{m=0}^{N_{ref}-1} r(k+m)\, c'^{*}_{b}(m) \right|. \tag{4.8}$$

At the same time, AP also computes a received signal power $R(k)$:

$$R(k) = \sum_{m=0}^{N_f-1} |r(k+m)|^2 . \tag{4.9}$$

In 2PPD, a tentative detection with the received signal power based threshold $\beta R^{-1}(k)$ $(0 \le \beta \le 1)$ is performed on each SCB. The tentative detections acquire the timings $\tilde{k}_b$ for $b = 0, \cdots, B-1$:

$$\tilde{k}_b = \min \left\{ k \;\middle|\; \beta R^{-1}(k) \le P_{p,b}(k) \right\}. \tag{4.10}$$

After the detection, buffers store $P_{p,b}(k)$ from the time $\tilde{k}_b$ to $\tilde{k}_b + F$. Then, the second detection with the maximum power path based threshold $\alpha P_{p,max,b}$ decides the precedent path timings $k_{f,b}$ as follows:

$$k_{f,b} = \min \left\{ k \mid \alpha P_{p,max,b} \le P_{p,b}(k),\ \tilde{k}_b \le k \le \tilde{k}_b + F - 1 \right\}, \tag{4.11}$$

$$P_{p,max,b} = \max \left\{ P_{p,b}(k) \;\middle|\; \tilde{k}_b \le k \le \tilde{k}_b + F - 1 \right\}. \tag{4.12}$$

After the second detection, CRTAC estimates PD on each SBC $\tilde{\tau}_{d,b}$ and decides the FFT window timing k_{fft} with the same ways of (4.5) and (4.6), respectively. Figure 4.10 indicates that 2PPD could much accurately detect the precedent path timing compared with 1PPD.

4.5 Evaluation and Discussion

4.5.1 Simulation Scenario

The reverse link PER performance of PR-DSMA based OFDMA system is evaluated by computer simulation. Especially, PER of ACTS and MDS are evaluated.

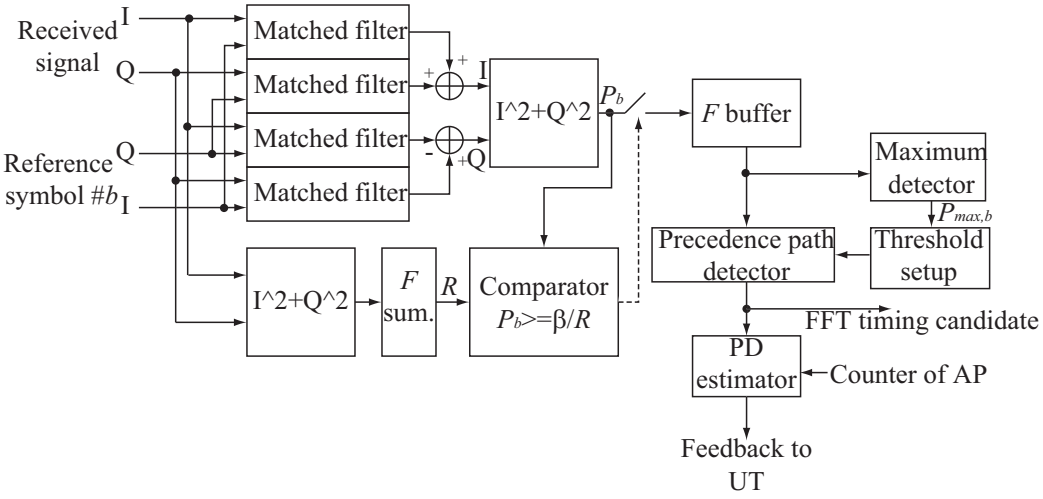

Figure 4.9: Configurations of PD estimator and timing synchronizer with 2PPD.

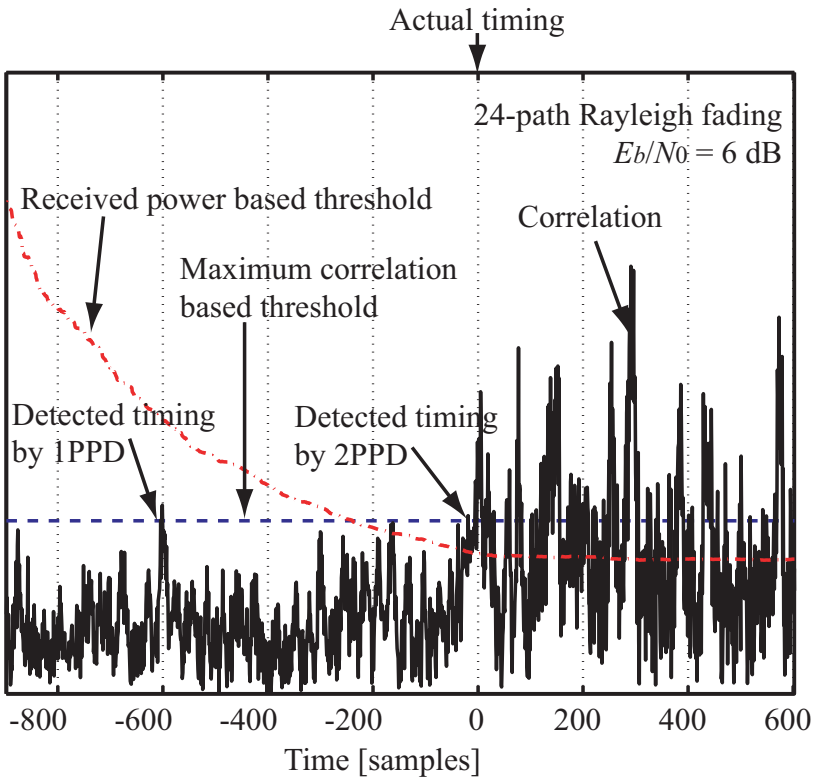

Figure 4.10: Behaveir of PD estimator with 2PPD.

Table 4.3 shows the major parameters used in the simulations. In the simulation, the OFDMA system is operating at 5 GHz of carrier frequency, that is, $f_C = 5$ GHz. The cell model is a single circular cell and no interference comes from adjacent cells. The cell radius R_c and antenna height of AP h_{ap} are 500 m and 40 m, respectively. B UTs exist uniformly in the cell. In addition, they move with 100 km/h of velocities toward uniform directions. This velocity corresponds 500 Hz of the maximum Doppler frequency f_D. Each UT just utilizes one SCB at the same time and no collision occurs in the simulation. The multi-path model is an exponential decaying 24-path Rayleigh fading with a delay spread $\sigma = 0.36\,\mu$sec. The round-trip PD of UT using the b-th SCB $\tau_{d,b}$ is given by:

$$\tau_{d,b} = 2\sqrt{d_b^2 + \left(h_{ap} - h_{ms}\right)^2}\Big/c, \tag{4.13}$$

where d_b is the distance between AP and UT using the b-th SCB, and c is the speed of light. From Table 4.3 and (4.13), the maximum difference of possible round-trip PD between UT under AP and that on the cell boundary achieves 3.1 μsec. QPSK modulation and half of coding rate are applied to ACTS. One ACTS includes 40 bytes of data in its data domain. On the other hand, QPSK and 16QAM modulation and half of coding rate are applied to MDS. One MDS includes 128 and 256 bytes of data with QPSK and 16QAM, respectively. In this chapter, 8 % of PER is defined as the required PER for the system. 2 of pilot symbols are commonly added at the head of packet. It is noted that the length of GI for ACTS is twice as that for MDS because TAC is not performed for the ACTS period.

4.5.2 Relationships between slot error rate, N_{ref}, and quantization schemes

Figure 4.11 shows the relationship between the MDS-PER performance and the length of simplified reference symbol when modulation is QPSK. Energy per bit to noise density ratio E_b/N_0 is set to 10 and 16 dB. 1PPD is used in this simulation. The parameter α is set to 0.6 for $N_{ref} = 1024$ and 0.4 for the other cases. The reception interval T_R is fixed to 2.5 msec, which is equivalent to one frame period of PR-DSMA proposed in Ref. [53]. In Fig. 4.11, N_{ref} is varied from 1024 to 16. Clearly, the PER performance with $N_{ref} = 1024$ is the best one because this case maintains the orthogonality among the pilot symbols and reference symbols. On the other hand, those with the other N_{ref} are degraded by the loss of orthogonality. However, it is observed that those with $N_{ref} = 256$, 128, and 64 are almost equiv-

Table 4.3: Major parameters in simulation scenario.

Total number of sub-carriers: K	768
Number of SCBs: B	12
Number of sub-carriers per SCB: N_{sc}	64 (= K/B)
Sub-carrier spacing: Δ_f	125 kHz
FEC scheme	Convolutional codes coding rate = 1/2 constraint length = 7
Sub-carrier modulation	QPSK, 16QAM
IFFT/FFT points: F	1024
Effective symbol length	1024
GI length: G	512 for ACTS 256 for MDS
Operating frequency: f_C	5 GHz
Cell model	Single circular cell
Cell radius: R_c	500 m
Number of UTs	12 (= B)
Antenna height of AP: h_{ap}	40 m
Antenna height of UT: h_{ms}	1 m
Maximum round-trip PD	3.1 μsec
Multi-path model	Exponential decaying 24-path Rayleigh fading
Maximum delaying	1.4375 μsec
Delay spread: σ	0.36 μsec
Maximum Doppler frequency: f_D	500 Hz (100 km/h at 5 GHz)

alent each other. Then, $N_{ref} = 32$ and 16 slightly degrade the PER performances again.

Figure 4.12 shows the relationship between the MDS-PER performance and the quantization scheme of simplified reference symbol when modulation is QPSK. In this figure, three quantization schemes, the non-, 2-level, and 3-level ones, are compared for $N_{ref} = 64$. 1PPD is also used in this simulation. The parameter α is set to 0.4. While the orthogonality is already lost by $N_{ref} = 64$, the PER differences among three quantization schemes are almost negligible. From these results, we choose the parameter $N_{ref} = 64$ and the 3-level quantization scheme in the following simulations.

4.5.3 Parameter Setting for Precedent Path Detection

Figures 4.13 and 4.15 show the ACTS-PER and MDS-PER performances versus the parameter α, respectively for $E_b/N_0 = 10$ dB. Similarly, Figs. 4.14 and 4.16 show those performances for $E_b/N_0 = 16$ dB. Modulation is QPSK for both the ACTS and MDS transmission. The reception interval T_R is fixed to 2.5 msec. In those figures, three types of PPDs are compared: (a) 1PPD with the full-size reference symbols, (b) 1PPD with the simplified reference symbols, and (c) 2PPD with the simplified symbols. In the case of (c), the parameter β is varied from 0.05 to 0.25.

In the case of ACTS, the PER performance with 1PPD and the full reference symbols are flat over when α is greater than 0.5. On the other hand, the PER performance with 1PPD the simplified symbols is sensitive to the variation of α. This sensitivity is occurred due to the loss of orthogonality. Moreover, the optimal value of α is different in each condition of E_b/N_0 in the case of the simplified symbols and 1PPD. This fact inherently leads to the difficulty on the determination of α. Meanwhile, the combination of the simplified symbols and 2PPD mitigates the sensitivity to α. The sensitivity to β appears but it is very small. For instance, the ACTS-PER performances are almost same when $\beta = 0.15$, 0.20, and 0.25. Moreover, the ACTS-PER performance of 2PPD with the optimal α approaches that of 1PPD and the full reference symbols. Consequently, the FFT timing is well-detected by 2PPD.

In the case of MDS, the PER performances employing the simplified reference symbols are inferior to that employing the full-size ones. These degradations mean that the estimated PDs given by (4.5) is inaccurate due to the loss of orthogonality. Especially 1PPD with the simplified symbols degrades the performance

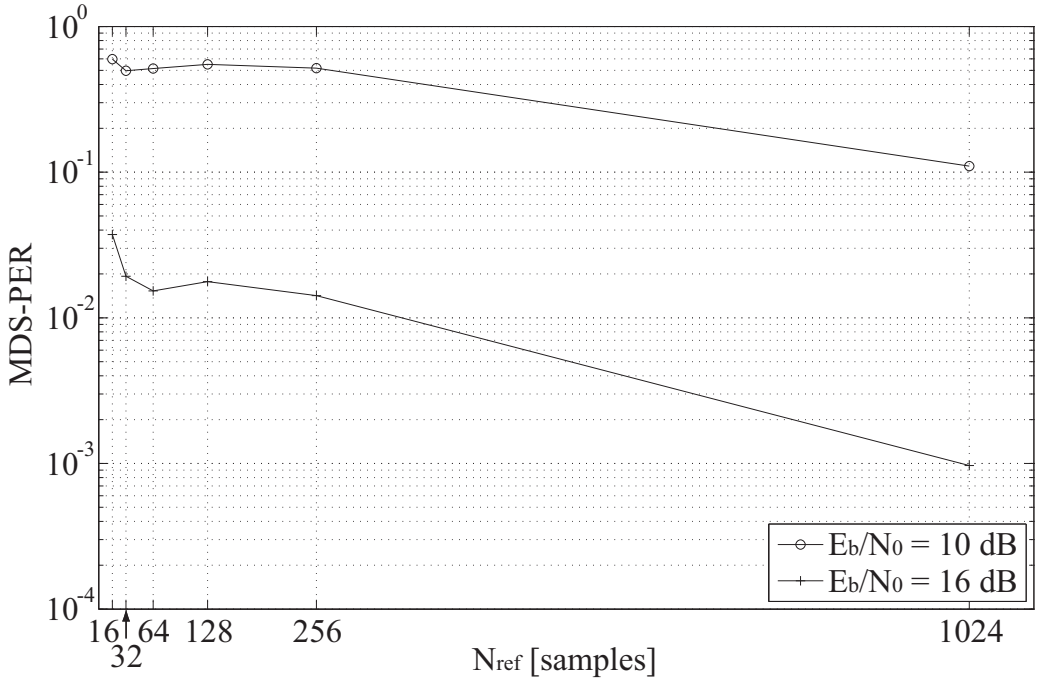

Figure 4.11: Relationship between MDS-PER performance and the length of shortened reference symbols (QPSK, 1PPD,, non-quantization, T_R = 2.5 msec and f_D = 500 Hz).

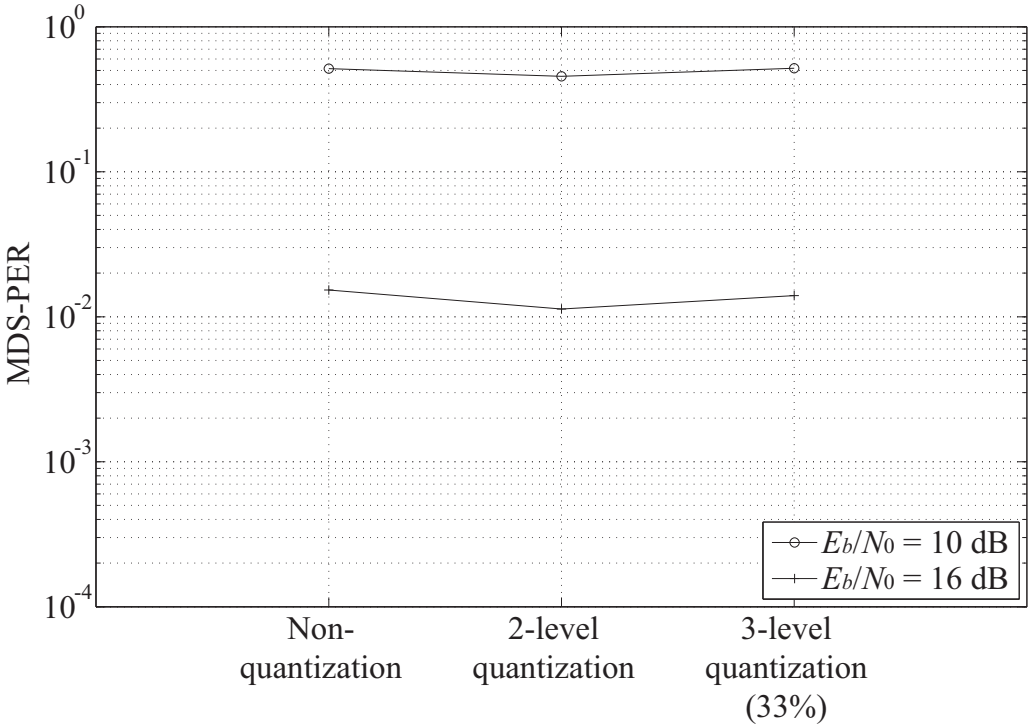

Figure 4.12: Relationship between MDS-PER performance and quantization schemes (QPSK, 1PPD,, N_{ref} = 64, T_R = 2.5 msec and f_D = 500 Hz).

drastically. On the other hand, 2PPD mitigates the loss of performance in comparison with 1PPD.

The following simulations choose the parameters α and β from the optimal ones in the case of $E_b/N_0 = 16$ dB. Then, α is set to 0.6 and 0.4 in 1PPD with the full-size reference symbols and simplified ones, respectively. Similarly, α and β are 0.5 and 0.20 in 2PPD with the simplified ones.

4.5.4 Packet Error Rate Performances in OFDMA reverse link

First, Fig. 4.17 plots the ACTS-PER performance. This figure also plots that performance with the ideal timing synchronization for reference. The PER performance of 1PPD with the full symbols and that of 2PPD with the simplified ones approach the PER performance of the ideal one. On the other hand, the PER performance of 1PPD with the simplified symbols is degraded at $E_b/N_0 < 12$ dB. This result means that 1PPD with the simplified ones is unstable for the fixed α.

Figs. 4.18 and 4.19 plots the MDS-PER performances when modulation are QPSK and 16QAM, respectively. The reception interval T_R is set to 2.5 msec. In Fig. 4.18, the PER performance without TAC cannot achieve the required PER because of MAI due to PDs. It means that TAC is necessary for OFDMA reverse link, or that the extended length of GI is necessary while it reduces the frame efficiency of OFDMA. On the other hand, the PER performance with Full-TAC approaches that with the ideal TAC. Thus, Full-TAC is very effective scheme to avoid MAI. The PER performances are degraded by using the simplified symbols. However, both of them achieve the required PER. For QPSK, 1PPD with the simplified reference symbols has 2.0 dB loss and 2 PPD with the simplified reference symbols has 1.3 dB loss at the required PER. The similarly trends appear in Fig. 4.19. However, 1PPD with the simplified reference symbols clearly degrades the PER performance compared to Fig. 4.18. For 16QAM, 1PPD with the simplified reference symbols has 8.8 dB loss and 2 PPD with the simplified reference symbols has 1.6 dB loss at the required PER. Full-TAC also has 0.4 dB loss compared to the ideal TAC at the required PER.

4.5.5 Impact of Reception Interval

Figure 4.20 shows the MDS-PER performance versus the reception interval T_R. Only the case of QPSK is simulated, and E_b/N_0 is fixed to 16 dB. The PER performances are flat over the period $T_R < 250$ msec for all PPD schemes. How-

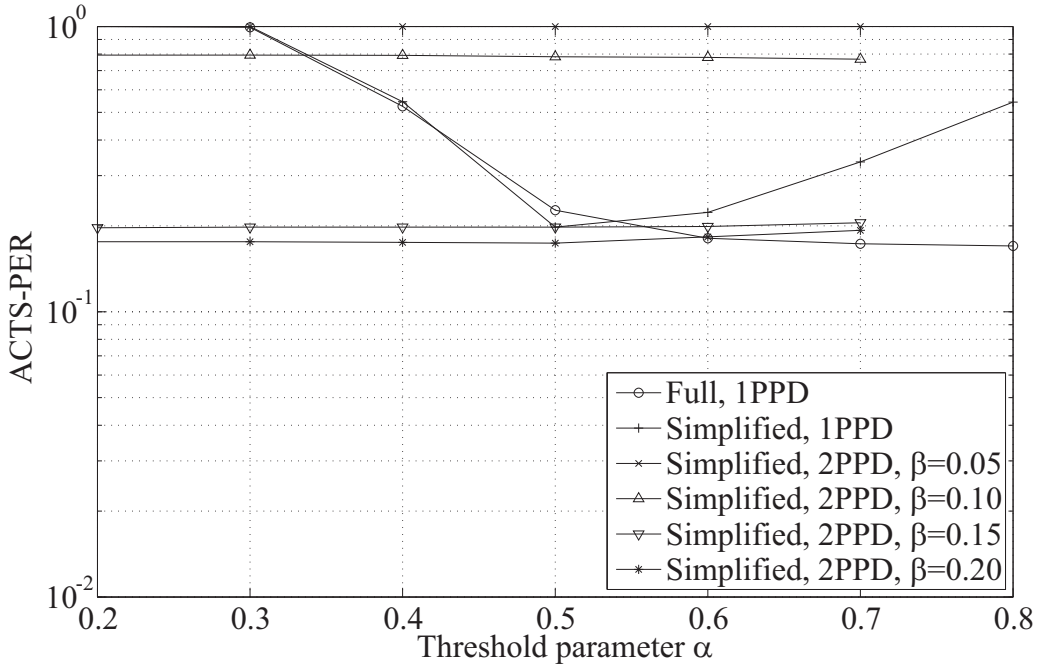

Figure 4.13: ACTS-PER performance versus α (E_b/N_0 = 10 dB, QPSK and f_D = 500 Hz).

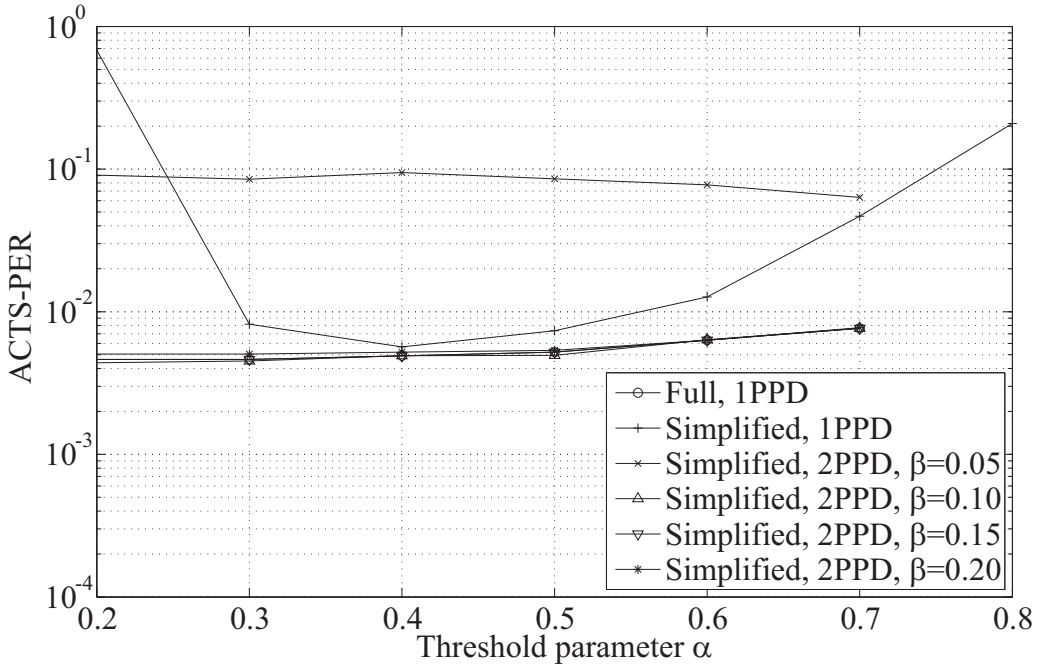

Figure 4.14: ACTS-PER performance versus α (E_b/N_0 = 16 dB, QPSK and f_D = 500 Hz).

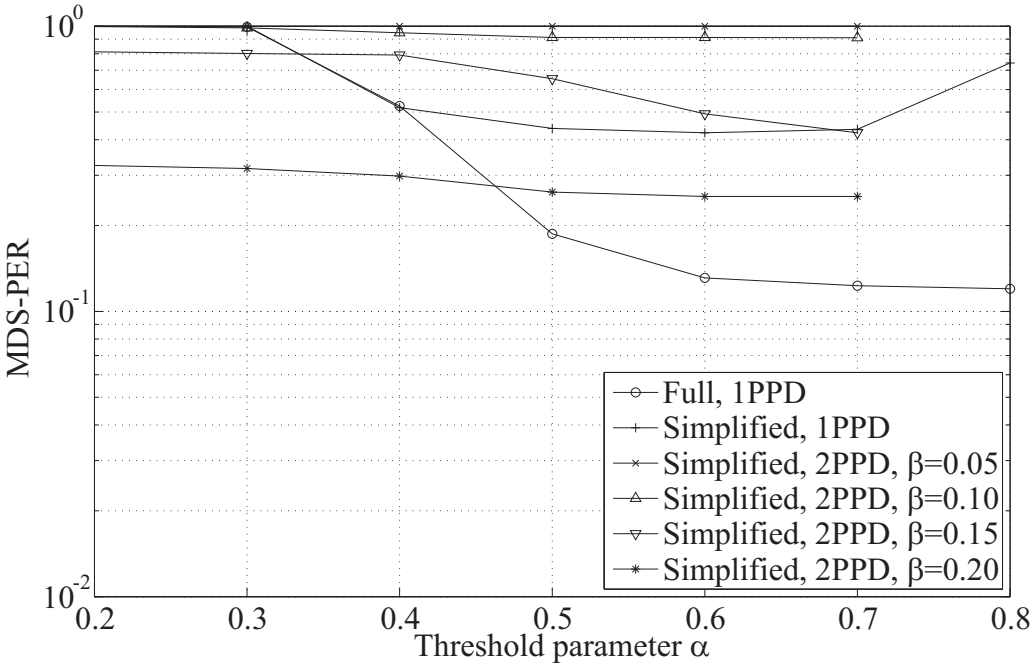

Figure 4.15: MDS-PER performance versus α (E_b/N_0 = 10 dB, QPSK, T_R = 2.5 msec and f_D = 500 Hz).

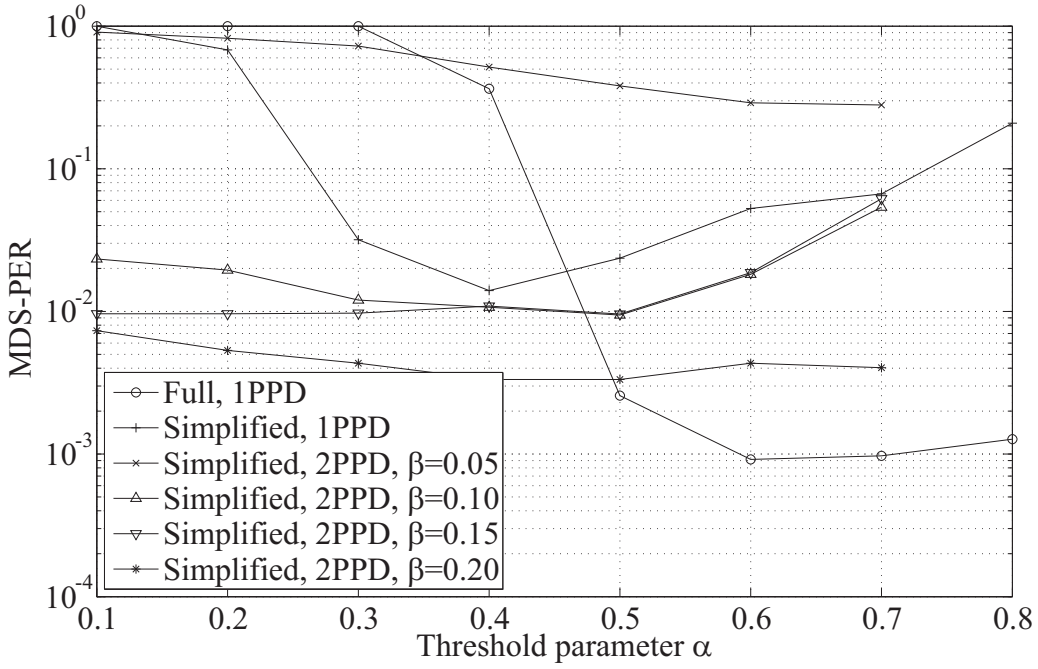

Figure 4.16: MDS-PER performance versus α ($E_b/N_0 = 16$ dB, QPSK, $T_R = 2.5$ msec and $f_D = 500$ Hz).

ever, the PER performances except for Full-TAC are degraded by the elapse when $T_R > 250$ msec. The PER performance with Full-TAC is also degraded when $T_R > 2500$ msec. From these results, MDSs must be assigned to UTs at least within 250 msec from the PD estimations, when CRTAC is employed in the proposed OFDMA system. This period is equivalent to the period of 100 frames in PR-DSMA.

4.5.6 Complexity Comparison of Precedent Path Detection

Table 4.4 lists the required numbers of multipliers, adders, inverters, and comparators for PPDs. This table compares the different three PPD schemes as well as Section 4.5: (a) 1PPD with the full-size reference symbols, (b) 1PPD with the simplified reference symbols, and (c) 2PPD with the simplified reference symbols. In Table 4.4, the following conditions are assumed: (i) the parallel B PPDs are embedded into AP ($B = 12$ in this chapter), (ii) one matched filter consists of N_{ref} multipliers (or $N_{ref}/3$ inverters for the use of the simplified symbols) and one adder, (iii) computing the correlations requires four matched filters because the input signals have complex values, and (iv) the comparators are employed in the detection with each threshold, as explained in (4.3), (4.10), and (4.11). From Table 4.4, it is confirmed that the simplified symbols drastically reduce the number of multipliers in the matched filters. Generally, digital multipliers make a volume of DSP devices larger and larger. Therefore, this reduction means that the matched filters with the simplified symbols can be embedded into the hardware devices much easily. In addition, this reduction brings the low cost of the hardware layout, since the number of available multipliers is generally limited in the hardware devices such as field programmable gate array. Moreover, it is also confirmed that 2PPD hardly brings any hardware cost compared to 1PPD. Thus, 2PPD can mitigate the error rate degradation of reverse link transmission without driving the cost for the hardware structure.

4.6 Conclusion

In this chapter, TAC and its complexity reduction schemes are proposed for the reverse link transmission of OFDMA. The purposes of TAC are (i) estimating PDs of UTs at AP, (ii) informing those estimates from AP to UTs and (iii) controlling UTs' transmit timings according to those informed estimates. Two complexity reduction schemes, which are simplified reference symbols and 2PPD, reduce and

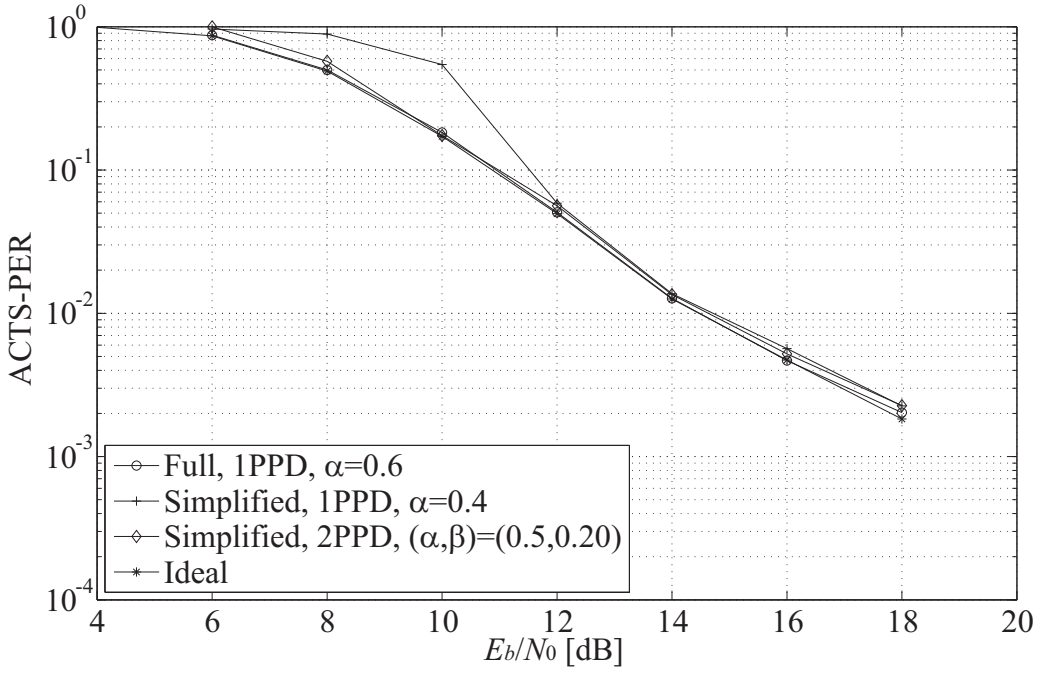

Figure 4.17: ACTS-PER performance (QPSK and f_D = 500 Hz).

Table 4.4: Operational structures of precedent path detections.

	(a)	(b)	(c)
PPD scheme	1PPD	1PPD	2PPD
Reference symbols	Full	3-level	3-level
N_{ref}	1024	64	64
#Multipliers	49118	36	38
#Adders	84	84	85
#Inverters	0	2048	2048
#Comparators	1	1	2

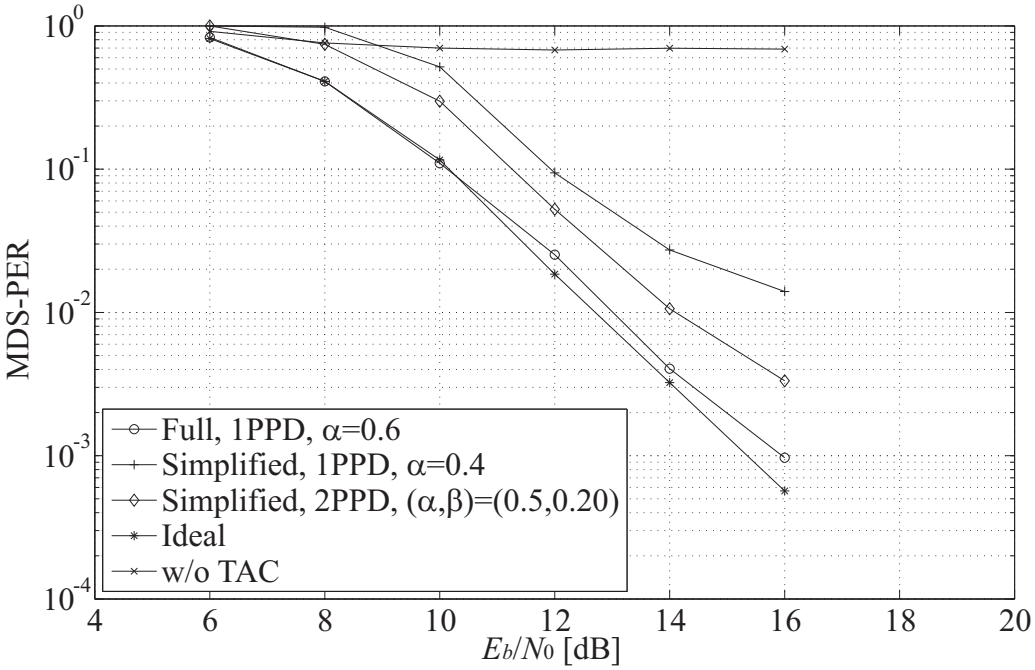

Figure 4.18: MDS-PER performance with TAC and CRTAC (QPSK, T_R = 2.5 msec and f_D = 500 Hz).

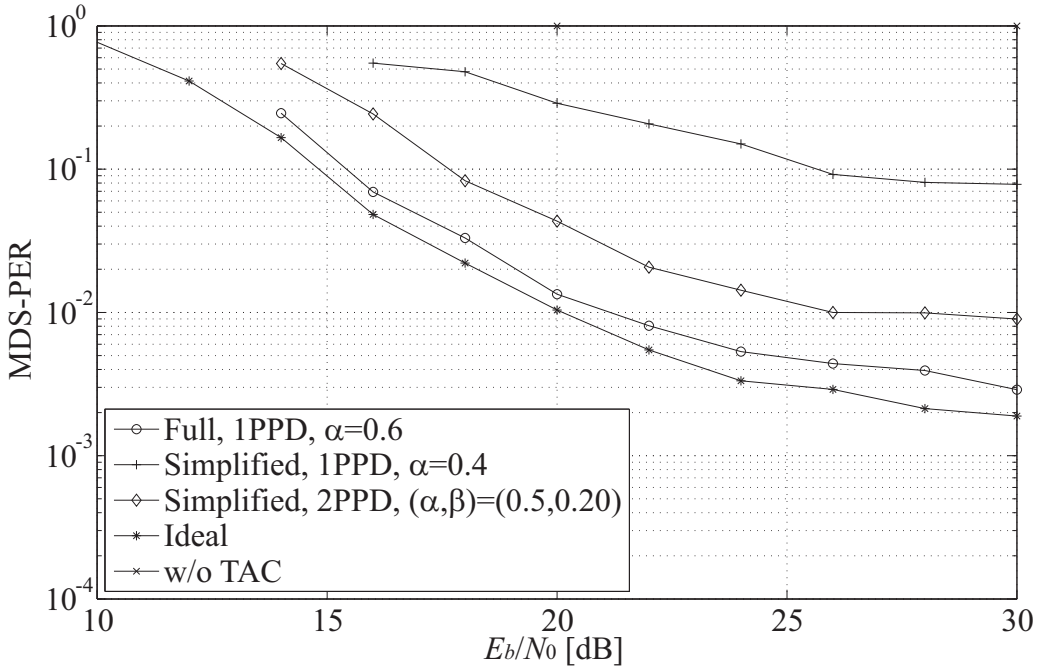

Figure 4.19: MDS-PER performances with TAC and CRTAC (16QAM, $T_R = 2.5$ msec and $f_D = 500$ Hz).

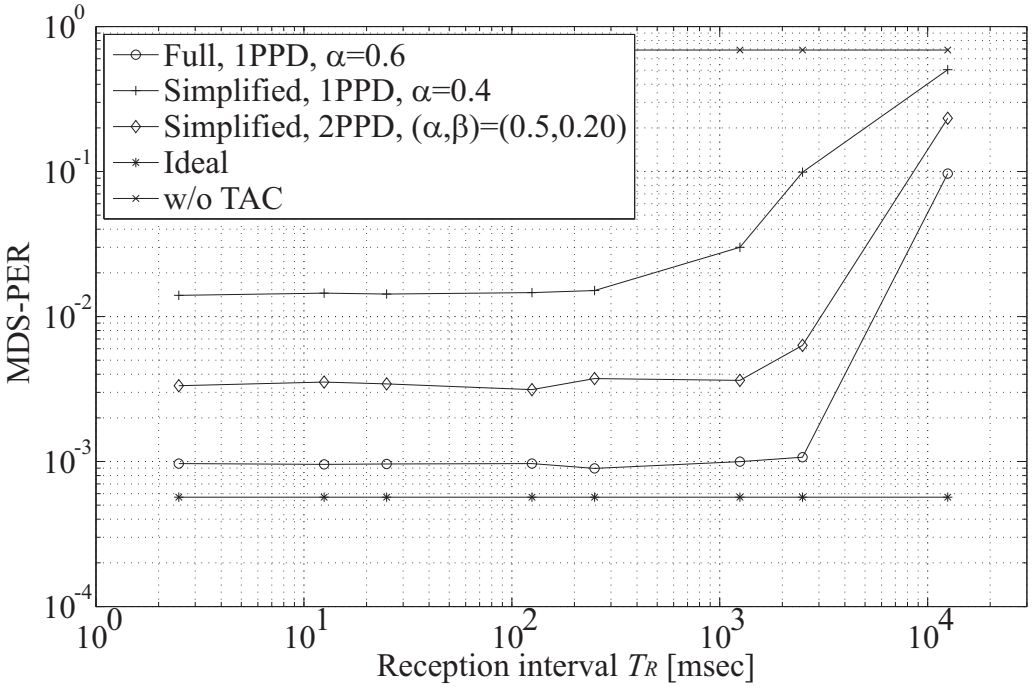

Figure 4.20: MDS-PER performance versus reception interval T_R (QPSK, E_b/N_0 = 16 dB and f_D = 500 Hz).

replace complex multiplications to simple inverters in the algorithm of TAC. Thus, the implementation cost of AP is reduced by these schemes. From the simulation results, it is observed that Full-TAC approaches the ideal performance of reverse link transmission in the proposed OFDMA system. Then, CRTAC also approaches the ideal one with about 1.6 dB loss. The study on complexity comparison indicates that CRTAC replaces almost of complex multiplications to inverters. Thus, both Full-TAC and CRTAC are effective techniques to avoid MAI and to improve the performance of reverse link transmission.

Chapter 5

Multi-Carrier Division Duplex: A New Duplex Scheme Based on Multi-Carrier Transmission

Summary

MCDD, a new duplex scheme based on the MC transmission technology, is proposed in this chapter. The basic concept of MCDD is to configure duplex channels by different sets of orthogonal sub-carriers. Each of these sets is called as sub-channel block (SCB) and is the unit of channel assignment. One of problems of MCDD is loss of orthogonality which causes inter-link interference (ILI) among SCBs. The proposed MCDD system exploits time-spreading to reduce the impact of ILI. In this chapter, the BER performance of MCDD in the presence of carrier frequency offset (CFO) is evaluated by computer simulation. When desired SCB ratio is half and spreading factor is 1, 0.2 dB of loss appears between the BER performances with 0 and 0.1 of normalized CFO (NCFO) at 10^{-5} of convolutional-coded BER. Moreover, ILI due to 0.5 of NCFO induces a BER floor. On the other hand, when the number of SCBs is 16 and spreading factor is equal to or greater than 8, time-spreading suppresses the impact of ILI. When desired SCB ratio is half, 0.6 dB of loss appears between the BER performances with 16 and 8 of spreading factors at 10^{-5} of coded BER.

5.1 Introduction

As mentioned in the previous chapters, the advantage of MC transmission is robustness against frequency-selective and multi-path fading channels by helps of narrowband sub-carriers and insertion of GI. In addition, flexible frequency resource management is also the advantage of MC transmission technology. The MC transmission can control frequency resource sub-carrier-by-sub-carrier. MC based adaptive modulation [171], [172] and multiple access [46] are the respective techniques of latter advantage.

Duplexing is the key factor of wireless communication systems as well as multiplexing and multiple access. Duplexing prepares forward and reverse link channels which user terminals (UTs) use to communicate each other. The existing wireless systems have adopted frequency division duplex (FDD) and time division duplex (TDD) as duplexing schemes [35]. Recently, hybrid FDD and TDD schemes were proposed for flexible wireless communication systems [178]–[180]. However, any new concept of duplexing itself is hardly treated in these days.

In this chapter, a new duplexing scheme based on the MC transmission, which is called MCDD, is proposed. MCDD employs flexibility of frequency resource management of MC transmission and extends it to duplexing. It prepares different sets of orthogonal sub-carriers as the duplex channels. By using these duplex channels, MCDD could control frequency resource more flexibly.

Recently, multiplexing and multiple access are combined by spread spectrum or MC technologies in wireless communication systems. Because MCDD itself is based on the MC technology, duplexing is also combined with multiplexing and multiple access in the MC based wireless systems.

A significant issue of MCDD is ILI due to the loss of orthogonality among the duplex channels [166], [167]. Conventional MC transmission also suffers from ICI due to the loss of ortohgonality among the sub-carriers [69]–[71], [79]–[90]. However, the impact of ILI is much greater than that of ICI in MCDD [166], [167]. To suppress the impact of ILI, time-spreading technique is also proposed for MCDD in this chapter. It is noted that the time-spreading technique reduces transmission data rate of MCDD. Thus, reuse of spreading codes is investigated to avoid the decrease of data rate while to suppress ILI.

5.2 Conventional Duplex Schemes

5.2.1 Frequency Division Duplex

FDD is the most popular duplex scheme in the current wireless access systems. Figure 5.1 illustrates an example of channel assignment of FDD. In the FDD systems, UT can easily separate desired and undesired signals by a band pass filter because the duplex channels consist of different frequency bands. Moreover, FDD requires no particular synchronization between the forward and reverse link channels. However, the capacity of FDD is almost fixed because the constant bandwidths are pre-assigned to forward and reverse links. In addition, UT cannot monitor the channel condition of reverse link by itself. So FDD requires a closed-loop control to adopt some adaptive processing based on the channel state information (CSI) such as pre-equalization [182] and adaptive modulation and coding [171], [172].

5.2.2 Time Division Duplex

TDD is another famous scheme to compose the duplex channels. Figure 5.2 illustrates an example of channel assignment of TDD. In the TDD systems, UTs share the same frequency band but use different time slots to receive the forward link signals and transmit the reverse link ones. The capacity of TDD is variable by changing the number of slots assigned to the forward and reverse links. Then, TDD is more suitable for the wireless systems with asymmetric traffics. Moreover, TDD can easily adopt the CSI based adaptive processing through an open-loop control because CSIs between the forward and reverse links has very high correlation and UT can monitor both the forward and reverse link channels by itself. However, TDD requires an accurate time synchronization to avoid interference between the forward and reverse links, or ILI in a sense.

5.3 Concept of Multi-Carrier Division Duplex

5.3.1 Features

Table 5.1 lists the features of FDD, TDD and MCDD. It seems that MCDD is a particular format of FDD with orthogonal sub-carriers. However, it also comprises the features of TDD by considering packet based communication. MCDD can control capacities of forward and reverse links by changing the number of

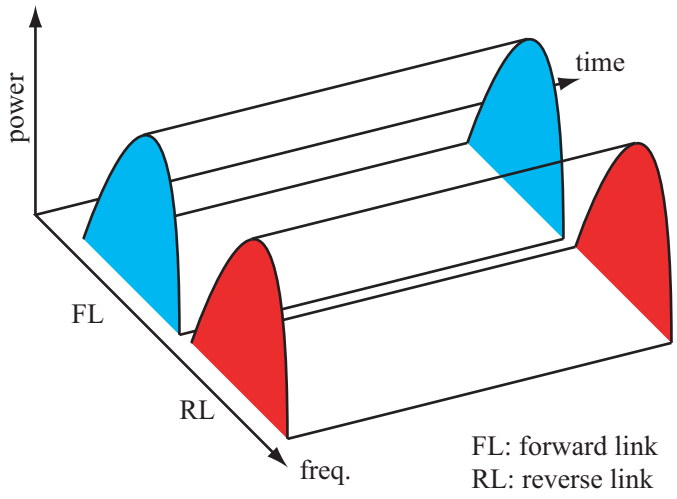

Figure 5.1: Channel allocation of FDD.

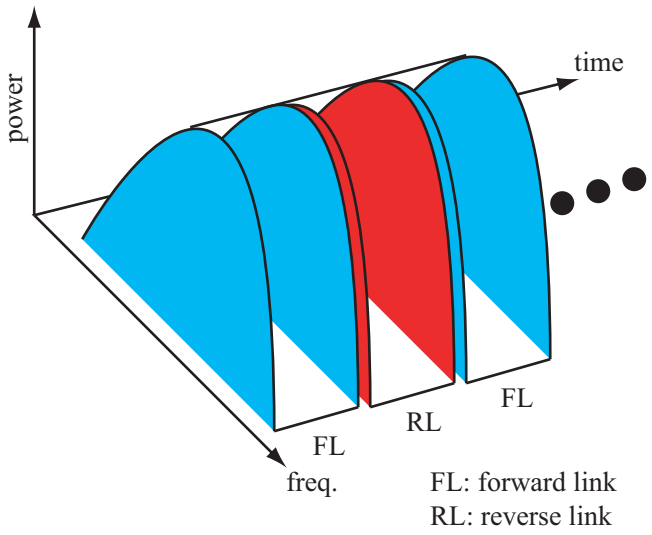

Figure 5.2: Channel allocation of TDD.

sub-carriers assigned to each duplex channel. Thus, it is very suitable for wireless systems with dynamic and asymmetric traffic. UT can monitor the channel conditions of both forward and reverse links by modifying pilot signal structures of MCDD. Therefore, the CSI based signal processing could be realized by an open-loop control in MCDD. Moreover, because it itself is based on the multi-carrier transmission, MCDD can be combined with multiplexing and multiple access. Therefore, the MCDD based systems could manage frequency resource more flexibly than conventional multi-carrier based systems.

5.3.2 Duplex Channel Planning

In this chapter, a concept of sub-channel block (SCB) is introduced to MCDD. Figure 5.3 illustrates the relationship of SCB and sub-carriers. SCB is defined by a set of orthogonal sub-carriers, and is the unit of duplex channel assignment to users. When K sub-carriers are available, MCDD prepares B SCBs, each of which consists of K/B sub-carriers. In addition, K_N null sub-carriers are allocated at both ends of each SCB. The purpose of these null sub-carriers is to moderate required performances of analog and radio frequency (RF) devices of MCDD receiver. The set of sub-carrier indices for the b-th SCB Λ_b is defined by

$$\Lambda_b = \{k \mid bK/B + K_N \leq k \leq (b+1)K/B - (K_N + 1)\}. \tag{5.1}$$

By this definition, the efficiency of sub-carrier use achieves $(K - 2BK_N)/K$.

5.3.3 Significant Issues

MCDD is sensitive to inter-link interference (ILI) which is caused by loss of orthogonality among SCBs [166], [167]. Thus, MCDD also requires precise time and frequency synchronization as well as conventional MC transmission. In addition, small coverage areas are desirable for MCDD from the point of time synchronization. From the point of UT, a transmitted signal loops back to UT itself as illustrated in Fig. 5.4. Therefore, a received signal contains desired signals transmitted from connecting UT and the loop signal. In general, the power of loop signal is much greater than that of desired signal. Therefore, the loop signal induces nonlinear characteristics of analog and RF devices in the UT receiver. To avoid such nonlinear characteristics, the MCDD terminal has to remove the loop signal at the front of receiver. For example, coupling reduction [183], a loop cancelling

Table 5.1: Features of FDD, TDD and MCDD.

	FDD	TDD	MCDD
Flexibility of capacity	Fixed	Flexible	Flexible
Synchronization	Not necessary	Time sync. is required	Time and freq. sync. is required
Immunity to multi-path fading	Robust	Guard time is required	Robust
Zone size	Any size is OK	Small size is preferable	Small size is preferable
Adaptive processing based on CSI	Complex	Easy	Easy

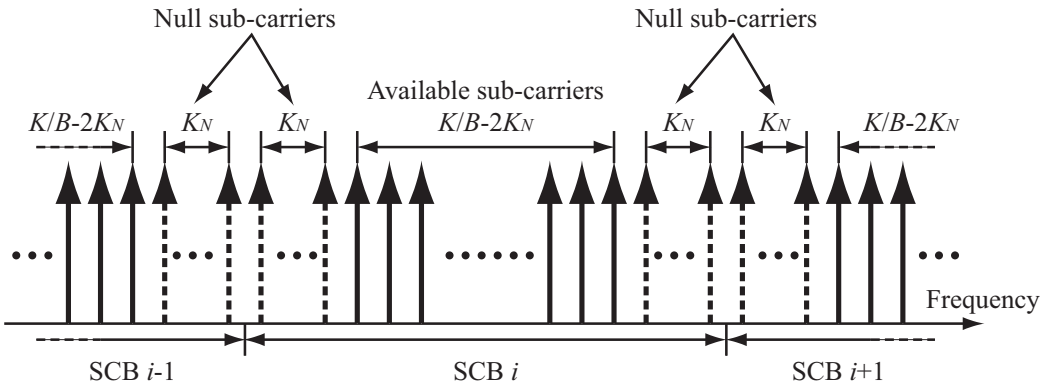

Figure 5.3: Introduction of sub-channel blocks to MCDD.

filter and negative phase signal combiner are solutions to overcome the loop signal. Analog and RF device technologies including the loop signal cancellation are most important issues to realize MCDD terminals.

5.4 Transmission Procedure

5.4.1 Configuration of Transmitter

Figure 5.5 illustrates the configuration of MCDD UT proposed in this chapter. The following explains the transmission procedure of UT using b-th SCB. Transmitted bit stream is encoded by an FEC scheme, and then converted to parallel streams corresponding to sub-carriers. Each bit stream is modulated onto phase shift keying (PSK) constellation. Let $S_b(d,k)$ be the d-th modulated symbols on the k-th sub-carrier. After modulation, the modulated symbols are spread by a spreading code assigned to each SCB. The spread symbol $\bar{S}_b(d,k)$ is expressed by

$$\bar{S}_b(d,k) = C_b\left(\mathrm{mod}\left(d, S_F\right)\right) S_b\left(\lfloor d/S_F \rfloor, k\right), \tag{5.2}$$

where $C_b(d)$ is the spreading code for b-th SCB, $\mathrm{mod}(a,b)$ is a residue of a/b and $\lfloor a \rfloor$ is the maximum integer equal to or less than a. Then, the spread symbols are converted to time-domain symbols by IFFT. The l-th sample of the d-th time-domain symbol $\bar{s}_b(d,l)$ $(l = 0, \cdots, G+F-1)$ is expressed by

$$\bar{s}_b(d,l) = \frac{1}{F} \sum_{k \in \Lambda_b} \bar{S}_b(d,k) e^{j2\pi(l-G)k/F}, \tag{5.3}$$

where F is the IFFT/FFT points and G is the length of GI. A transmitted packet $s_b(t)$ consists of $S_F P$ pilot and $S_F D$ data time-domain symbols. $s_b(t)$ is expressed by

$$s_b(t) = \sum_{d=0}^{S_F(P+D)-1} \sum_{l=0}^{G+F-1} \bar{s}_b(d,l)\delta(t - d(G+F-1) - l) \tag{5.4}$$

$$\delta(t) = \begin{cases} 1 & t = 0 \\ 0 & \text{otherwise} \end{cases}. \tag{5.5}$$

5.4.2 Spreading Code Assignment for Sub-Channel Blocks

The aim of applying time-spreading to MCDD is reducing the impact of ILI among SCBs. It is noted that the spreading factor should be as small as possible from the point of transmission efficiency. The impact of ILI from a certain

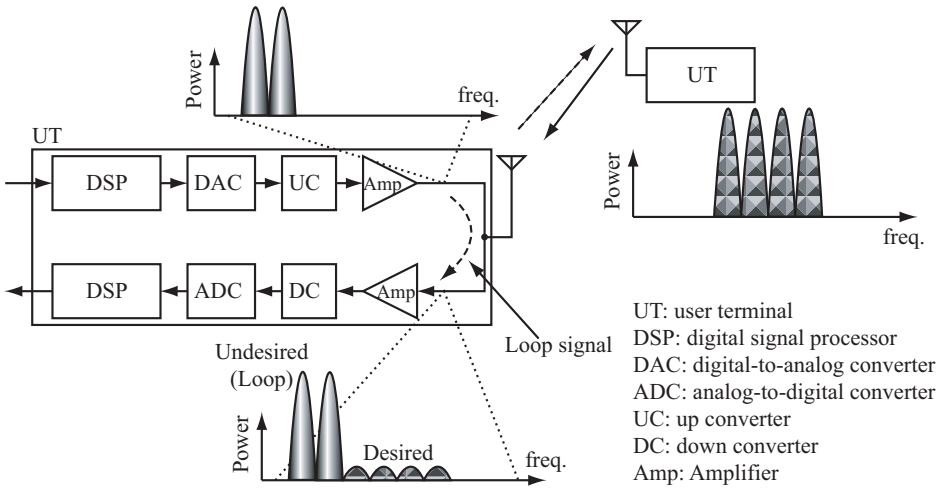

Figure 5.4: Example of loop signal in MCDD.

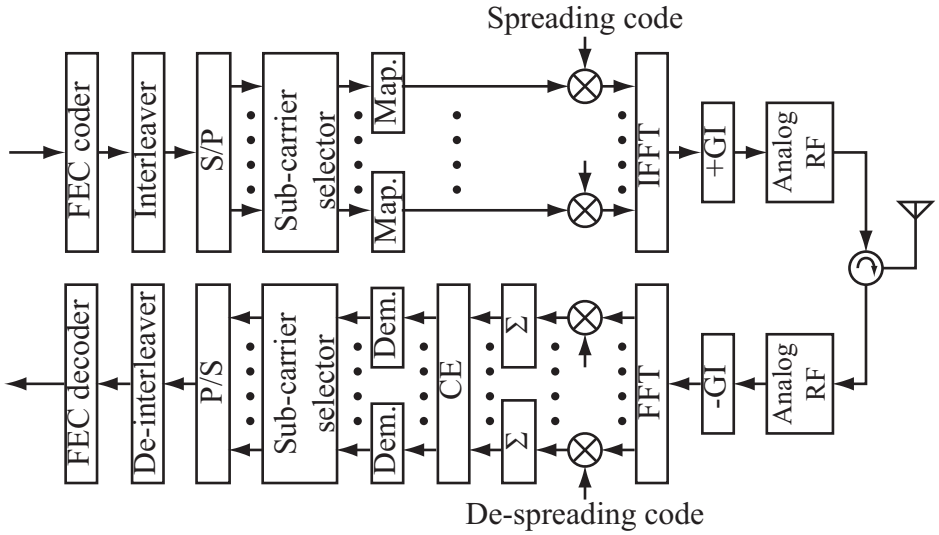

FEC: forward error correction, Map.: mapper, Dem.: de-mapper
S/P: serial-to-parallel converter, P/S: parallel-to-serial converter
DAC: digital-to-analog converter, ADC: analog-to-digital converter
CE: channel estimator, Σ: accumulator, RF: radio frequency

Figure 5.5: Configuration of MCDD transceiver.

SCB to the other SCB decreases according to frequency separation. Thus, reuse of spreading codes, that is, same codes used for different SCBs, could be possible in MCDD. This chapter investigates on the reuse of spreading codes. In this chapter, Walsh codes are used as the spreading codes. When the spreading factor is set to S_F, S_F codes can be obtained. Hereafter, the i-th spreading code of S_F ones is defined by $\bar{C}_i(d)$. By considering this definition and reuse of codes, the spreading code for the b-th SCB $C_b(d)$ (see (5.2)) is replaced by (5.6):

$$C_b(d) = \bar{C}_{\mathrm{mod}(b,S_F)}(d). \tag{5.6}$$

When S_F is 1, a certain SCB might suffer from ILI from all the other SCBs. However, MCDD with 1 of S_F can obtain the highest data rate. If ILI does not exist longer, it is very effective to use 1 of S_F. On the other hand, when S_F is greater than 1, the achievable data rate decreases to one S_F-th of that without spreading. Of course, the impact of ILI also decreases because of the help of spreading.

5.5 Receiption Procedure

5.5.1 Configuration of Receiver

The bottom of Fig. 5.5 illustrates a configuration of MCDD receiver proposed in this chapter. As above-mentioned, it is very important to reduce a loop signal which is transmitted from UT itself. For example, preparing a filter and adding a signal with inverse phase to the received signal at the front of receiver are solutions for reducing the loop signal. In this chapter, a multi-stage filter is used at the front of receiver to reduce the loop signal. Figure 5.6 illustrates the configuration of multi-stage filter. This filter has $\log_2(B)$ stages for MCDD system with B SCBs. In addition, the i-th stage consists of 2^{i-1} low pass filters (LPFs) and 2^{i-1} high pass filters (HPFs) [169]. Output of LPFs and HPFs at the final stage are signals of corresponding SCBs.

After passing through the multi-stage filter, the received signal is converted to digital baseband signal. In this chapter, it is assumed that carrier frequency offset (CFO) exist among the users. Then, the received and converted signal $r(t)$

is expressed by

$$r(t) = \sum_{b=0}^{B-1} r_b(t - \tau_{dly,b}) e^{j2\pi f_{o,b} t} + n(t) \tag{5.7}$$

$$r_b(t) = \sum_{t'=0}^{T_{ch,b}-1} h_b(t, t') s_b(t - t'), \tag{5.8}$$

where $f_{o,b}$ is the relative CFO of UT using the b-th SCB, $\tau_{dly,b}$ is the propagation delay (PD), $h_b(t, t')$ is the channel impulse response (CIR) at time t, $T_{ch,b}$ is the length of CIR and $n(t)$ is AWGN component with zero mean and σ_N^2 variance. This chapter assumes that UT receiving $r(t)$ also transmits its own signal on a certain SCB and that the length of GI is enough long to avoid ISI caused by CIR and PD.

GIs are removed from the received time-domain symbols, and then the time-domain symbols are converted to the frequency-domain sub-carrier symbols by FFT. By considering CFO, the received symbol on the k-th sub-carrier $\bar{R}(d, k)$ is expressed by

$$\begin{aligned}
\bar{R}(d,k) &= \sum_{l=G}^{G+F-1} r(d,l) e^{-j2\pi(l-G)k/F} \\
&= \sum_{b=0}^{B-1} \sum_{q=0}^{K-1} \left\{ \bar{H}_b(d,q) \bar{S}_b(d,q) \frac{\sin\left(\pi f_{o,b}/\Delta_f\right)}{F \sin\left(\pi\left(q - k + f_{o,b}/\Delta_f\right)/F\right)} \right. \\
&\quad \left. \cdot\, e^{j\pi f_{o,b}/\Delta_f (F-1)/F} \cdot e^{-j\pi(q-k)/F} \right\} + \bar{N}(d,k),
\end{aligned} \tag{5.9}$$

where $r(d, l)$ is the l-th sample of the d-th received time-domain symbol, $\bar{H}_b(d, k)$ is the overall channel frequency response (CFR) of the k-th sub-carreri which the signal on the b-th SCB suffers from and $\bar{N}(d, k)$ is the AWGN component. It is noted that $\bar{H}_b(d, k)$ includes the responses of wireless channel, multi-stage filter and the phase rotation due to PD. After FFT, the received symbols are de-spread by corresponding codes sub-carrier-by-sub-carrier. The received symbol after de-spreading $R_b(d, k)(b \in \Lambda_b)$ is expressed by

$$R_b(d,k) = \frac{1}{S_F} \sum_{q=0}^{S_F-1} C_b^*(q) \bar{R}(dS_F + q, k). \tag{5.10}$$

A channel estimator obtains estimates of CFR by using pilot symbols. The

estimates of CFR $\hat{H}_b(k)$ is expressed by

$$\begin{aligned}\hat{H}_b(k) &= \frac{1}{PS_F}\sum_{p=0}^{P-1} S_b^*(p,k)R_b(p,k) \\ &= H_b(k) + \Gamma_b(k) + N(k),\end{aligned} \tag{5.11}$$

where

$$H_b(k) = \frac{1}{PS_F}\sum_{p=0}^{P-1}\sum_{d=0}^{S_F-1}\bar{H}_b(pS_F+d,k), \tag{5.12}$$

$$\begin{aligned}\Gamma_b(k) = \frac{1}{PS_F}\sum_{b'=0,b'\neq b}^{B-1}\sum_{k'\notin\Lambda_b}\sum_{p=0}^{P-1}\Bigg[& S_b^*(p,k) \\ & \cdot\sum_{d=0}^{S_F-1}\Bigg\{C_b^*(d)C_{b'}(d)\bar{H}_{b'}(pS_F+d,k')S_{b'}(p,k') \\ & \cdot\frac{\sin\left(\pi f_{o,b'}/\Delta_f\right)}{F\sin\left(\pi\left(k'-k+f_{o,b'}/\Delta_f\right)/F\right)}e^{j\pi f_{o,b'}/\Delta_f(F-1)/F}\cdot e^{-j\pi(k'-k)/F}\Bigg\}\Bigg],\end{aligned} \tag{5.13}$$

$$N(k) = \frac{1}{PS_F}\sum_{p=0}^{P-1} S_b^*(p,k)\sum_{d=0}^{S_F-1} C_b^*(d)\bar{N}(pS_F+d,k). \tag{5.14}$$

In the right hand of (5.11), $H_b(k)$ indicates the actual CFR, $\Gamma_b(k)$ indicates ILI due to CFO and $N(k)$ is the AWGN component.

The received data symbols $R_b(d,k)$ are compensated by the estimates of CFR $\hat{H}_b(d,k)$ at de-mappers. The compensated symbols $\hat{S}_b(d,k)$ are expressed by

$$\hat{S}_b(d,k) = \frac{\hat{H}_b^*(k)}{\left|\hat{H}_b(k)\right|^2}R_b(d,k), \tag{5.15}$$

where the operator a^* means a complex conjugate of a. Assuming ideal channel estimation, that is, $\hat{H}_b(k) = H_b(k)$, (5.15) is replaced by

$$\begin{aligned}\hat{S}_b(d,k) &= \frac{\hat{H}_b^*(k)}{\left|\hat{H}_b(k)\right|^2}R_b(d,k) \\ &= S_b(d,k) + \Xi_b(d,k) + \hat{N}(d,k),\end{aligned} \tag{5.16}$$

where

$$\Xi_b(d,k) = \frac{\hat{H}_b^*(k)}{\left|\hat{H}_b(k)\right|^2} \sum_{b'=0,b'\neq b}^{B-1} \sum_{k'\notin\Lambda_b} \cdot \sum_{q=0}^{S_F-1} \left\{ C_b^*(q) C_{b'}(q) \bar{H}_{b'}(q,k') S_{b'}(q,k') \cdot \frac{\sin\left(\pi f_{o,b'}/\Delta_f\right)}{F\sin\left(\pi\left(k'-k+f_{o,b'}/\Delta_f\right)/F\right)} e^{j\pi f_{o,b'}/\Delta_f (F-1)/F} \cdot e^{-j\pi(k'-k)/F} \right\}, \tag{5.17}$$

$$\hat{N}(d,k) = \frac{\hat{H}_b^*(k)}{\left|\hat{H}_b(k)\right|^2} \sum_{q=0}^{S_F-1} C_b^*(q) \bar{N}(q,k). \tag{5.18}$$

In (5.16), $\Xi_b(d,k)$ is the ILI component which $S_b(d,k)$ suffers from. After compensation, the de-mappers generate bit-wise soft information from $\hat{S}_b(d,k)$ and feeds them to an FEC decoder. The FEC decoder recovers the transmitted bit stream by using the soft information.

5.6 Evaluation and Discussion

5.6.1 Major Parameters

The bit error rate (BER) performance of proposed MCDD is evaluated by computer simulation. Table 5.2 lists major parameters used in the simulation. In the simulation, all SCBs are randomly assigned to users. Synchronization is assumed to be ideal at the receiver side. The wireless channel is modeled as equal-level 6-path Rayleigh fading channel for both desired and undesired signals. The normalized delay spread σ/T_F is set to 0.05 for the desired signal and 0.003 for the undesired signal. The normalized maximum Doppler frequency f_D/Δ_f is fixed to 10^{-5}, which assumes a static environment, e.g. 0.5 km/h of velocity at 5 GHz of carrier frequency.

For the multi-stage filter at the front of receiver, Chebishev type-I LPF and HPF are designed by MATLAB function [170]. LPF at the i-th stage has $(2v-1)K/(2^i) - K_N$ of normalized pass frequency and HPF at the i-th stage has $(2v-1)K/(2^i) + K_N$ of that, where $v = 1, \cdots, 2^{i-1}$. The filter order is set to 15 and ripple at the passband is set to 1.5 dB. The number of resoluble bits of ADC is set to 10 and power amplifiers are assumed to be performed linearly in the simulation.

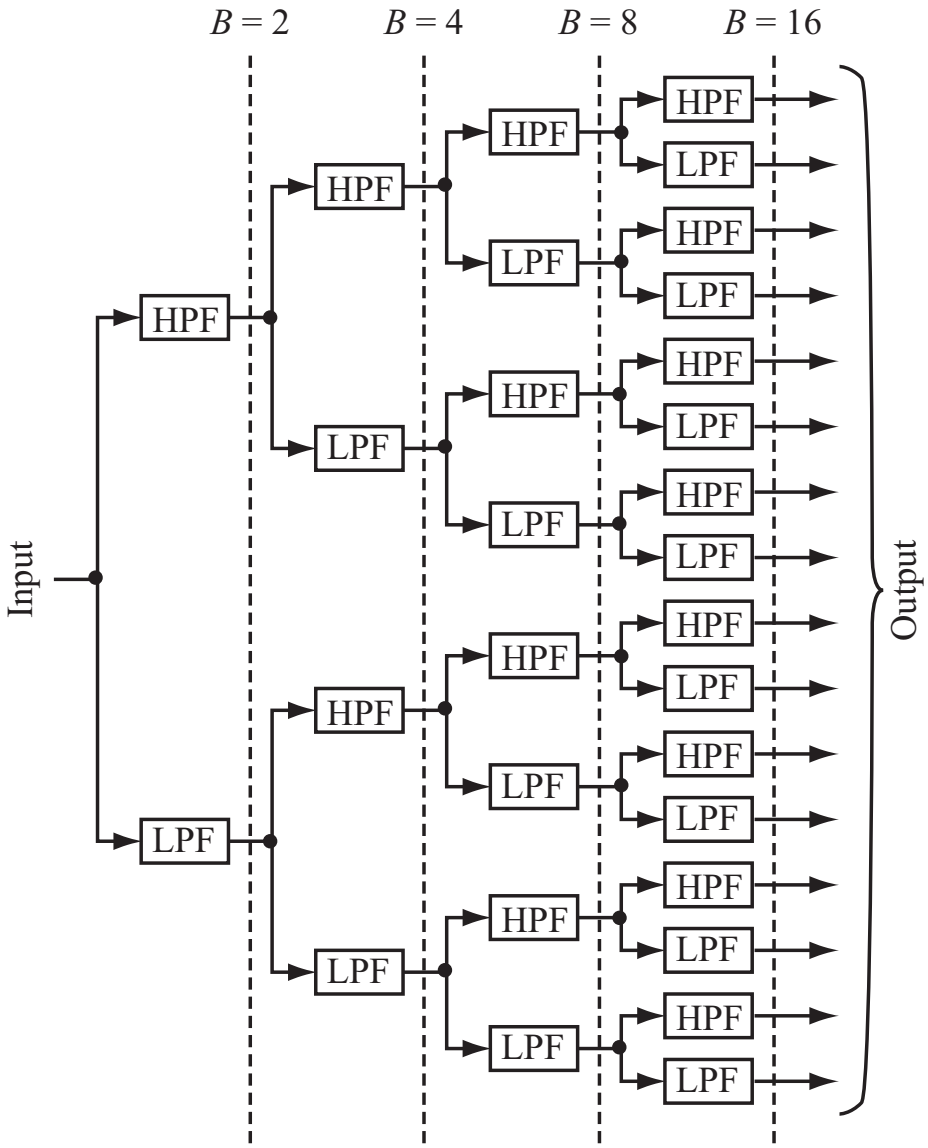

Figure 5.6: Configuration of multi-stage filter bank.

Table 5.2: Simulation parameters.

Parameter	Value
Number of sub-carriers: K	1024
Sub-carrier spacing: Δ_f	125 kHz
Number of SCBs: B	16
Number of null sub-carriers: K_N	4
Desired SCB ratio	$1/2$, $1/B$
Forward error correction	Convolutional coding (rate $R = 1/2$, constraint = 7)
Interleave scheme	Block interleave per OFDM symbol
Modulation	QPSK
IFFT/FFT points: F	1024(= K)
Effective symbol period: T_F	$1/\Delta_f$ sec
GI period: T_G	$(1/4)\,T_F$ sec
Number of data symbols: D	19
Number of pilot symbols: P	1
Spreading factor: S_F	1, 2, 4, 8, B
Synchronization	Perfect
Analog filter bank	Chebyshev type I
The order of LPF and HPF	15
Amplifier	Linear
Number of resoluble bits of ADC	10 bits
Normalized CFO (NCFO): f_o/Δ_f	0, 0.05, 0.1 or 0.5
Channel model	Equal level 6-path Rayleigh fading
Normalized delay spread of channel model: σ/T_F	0.05 (desired signal) 0.003 (undesired signal)
Normalized maximum Doppler frequency: f_D/Δ_f	10^{-5}
SIR before filtering	-60 dB

5.6.2 Signal-to-Interference Plus Noise Power Ratio Characteristics at Filter Output

This section evaluates signal-to-interference plus noise power ratio (SINR) after the filter. SINR is defined by

$$\mathrm{SINR} = 10\log\frac{\left\langle |r_D(t)|^2 \right\rangle / (B_D K/B)}{\left\langle |r_U(t)|^2 \right\rangle / (B_U K/B) + \sigma_N^2}, \tag{5.19}$$

where $r_D(t)$ is the desired signal, $r_U(t)$ is the loop signal, B_D is the number of SCBs assigned for $r_D(t)$, B_U is the number of SCBs assigned for $r_U(t)$ (thus, B_D+$B_U = B$) and the operator $\langle\cdot\rangle$ means average. In the simulation, signal-to-interference ratio (SIR) before the filter is set to -60 dB, which assumes wireless communication in several tens meters of coverage. It is noted that the definition of SINR in (5.19) is not equivalent to that of SINR per sub-carrier.

Figure 5.7 plots SINR of filter output versus the number of null sub-carriers K_N when the desired SCB ratio is $1/2$. In this simulation, CFO normalized by sub-carrier spacing (NCFO) is varied from 0 to 0.5, and signal-to-noise ratio (SNR) is fixed to 20 dB. SINR of filter output should be greater than 0 dB to avoid unwanted quantization noise at ADC which follows the filter. From Fig. 5.7, it is confirmed that more than 3 null sub-carriers are required to obtain 0 dB of SINR after filtering. Moreover, it is observed that SINR is saturated by more than 4 null sub-carriers. The characteristic of SINR is insensitive to CFO. Figure 5.8 plots SINR of filter output versus the number of null sub-carriers K_N when the desired SCB ratio is $1/B$. This figure shows the similar characteristic of SINR to Fig. 5.7. From this fact, the impact of desired SCB ratio is small for the characteristic of SINR. In the following sections, 4 of K_N is used for simulation to obtain as large SINR as possible.

5.6.3 Bit Error Rate Performance with 1 of Spreading Factor in the Presence of Carrier Frequency Offset

Figure 5.9 plots the BER performances with $1/2$ of desired SCB ratio and 1 of spreading factor. NCFO is varied from 0 to 0.5 in this simulation. Figure 5.9 plots both uncoded and convolutional-coded BER performances. In addition, this figure plots the theoretical and uncoded BER performance in a flat Rayleigh fading channel [35] for reference. In this chapter, target packet error rate (PER) is defined as 8×10^{-2}. From Table 5.2, bit amount per packet per SCB is 133 bytes. Thus,

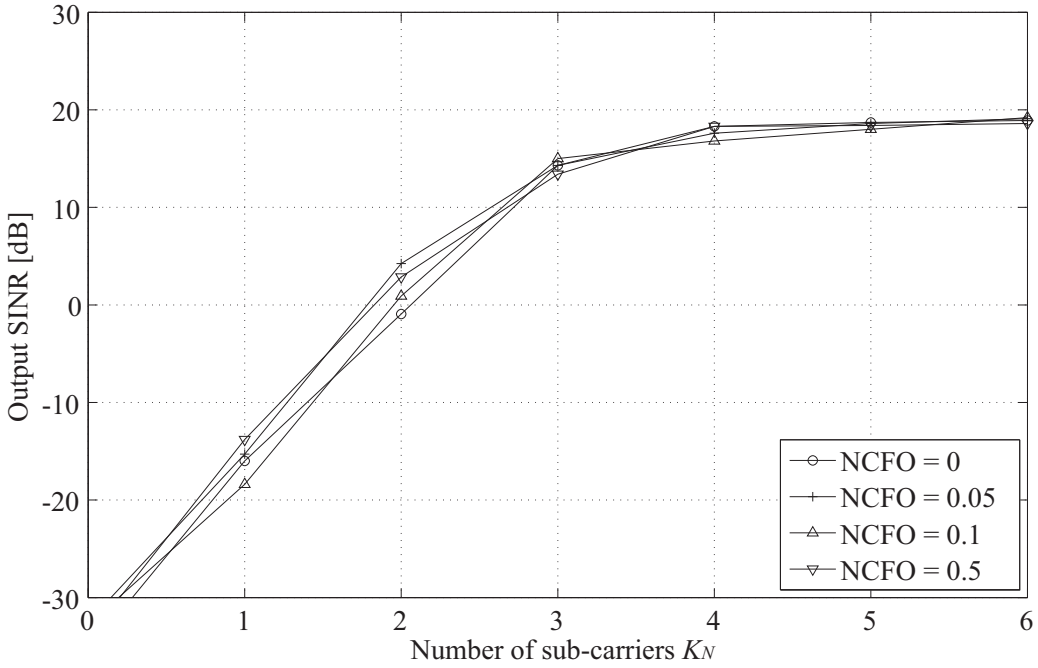

Figure 5.7: SINR of filter output versus the number of null sub-carriers when desired SCB ratio is $1/2$ and SNR = 20 dB.

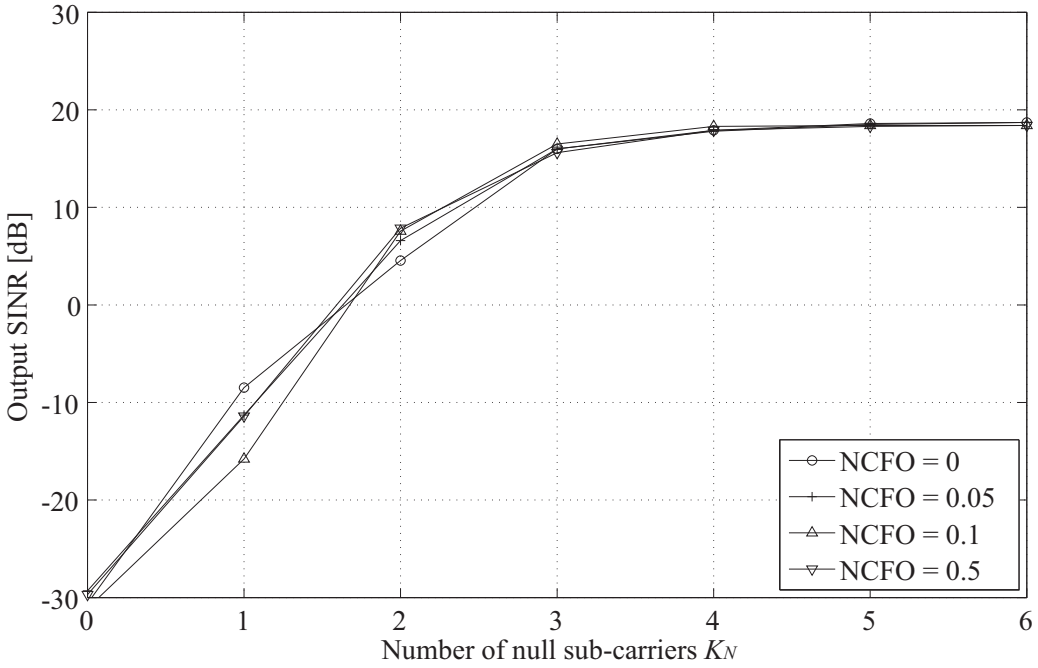

Figure 5.8: SINR of filter output versus the number of null sub-carriers when desired SCB ratio is $1/B$ and SNR = 20 dB.

BER required to obtain the target PER should be 10^{-5} after FEC decoding. Figure 5.9 shows that the uncoded BER performances are almost same except for that with 0.5 of NCFO. When NCFO is 0.5, BER is degraded by ILI. It is noted that there is 4.0 dB loss between the BER performance without CFO and the theoretical BER. This loss includes power loss due to pilot symbol insertion, that due to GI insertion and performance loss due to imperfect channel estimation. Figure 5.9 shows that there is 0.2 dB difference between the coded BER performances with 0.1 and 0.05 of NCFO at the required BER. This figure also shows that the impact of ILI caused by 0.5 of NCFO cannot be reduced even by using convolutional codes, and BER floor appears by ILI.

Figure 5.10 plots the BER performances with $1/B$ of desired SCB ratio and 1 of spreading factor. This figure shows the similar trend to Fig. 5.9. However, degradation due to 0.1 of NCFO becomes larger than that in Fig. 5.9. The degradation at the required BER is 0.6 dB when NCFO is 0.1. This fact means that the impact of ILI increases when the desired SCB is small. Nevertheless, according to the parameters listed in Table 5.2, BER floor disappears up to 0.1 of NCFO when the spreading factor is 1.

5.6.4 Impact of Spreading Factor to Bit Error Rate Performance in the Presence of Carrier Frequency Offset

Figure 5.11 plots the BER performances of MCDD with $1/2$ of desired SCB ratio in the presence of 0.5 of NCFO. In this simulation, the spreading factor is set to 1, 2, 4, 8 and 16 (= B). This figure shows that, when the spreading factor is equal to or less than 4, the degradation due to ILI still remains in the BER performance. It means that the impact of ILI coming from 5-SCB separation is not negligible in the MCDD system with the parameters listed in Table 5.2. On the other hand, when the spreading factor is equal to or greater than 8, the BER performance is improved drastically by the time-spreading technique. The time-spreading with 8 of spreading factor improves 7.7 dB at the required BER from that with 4 of spreading factor. Moreover, Fig. 5.11 also indicates that there is only 0.6 dB difference between the BER performance with 8 and 16 of spreading factors at the required BER. It means that the impact of ILI coming from 9-SCB separation is almost negligible in this MCDD system.

Figure 5.12 plots the BER performances of MCDD with $1/B$ of desired SCB ratio and 0.5 of NCFO. This figure shows that the impact of ILI becomes greater than that observed in Fig. 5.11. Then, the difference between the BER perfor-

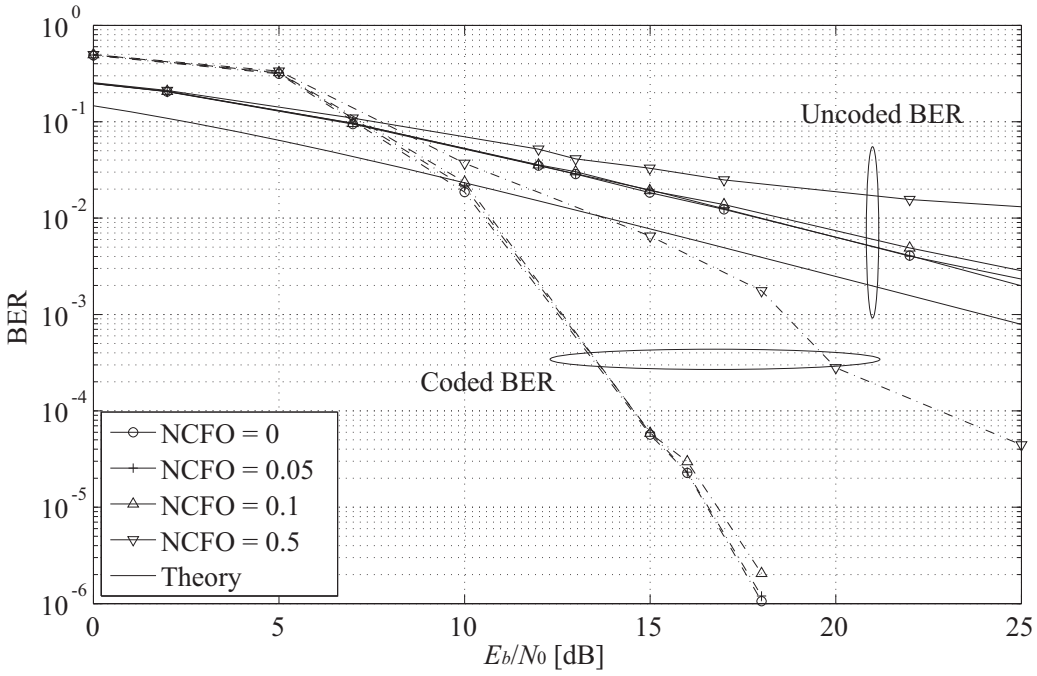

Figure 5.9: BER performance when desired SCB ratio is 1/2 and spreading factor is 1.

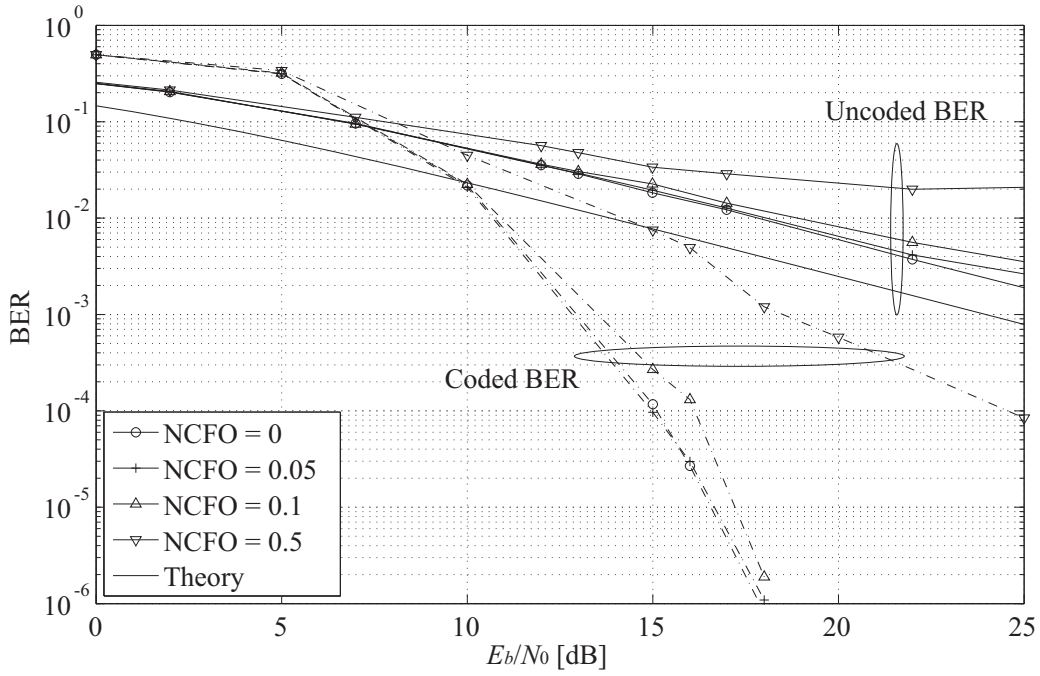

Figure 5.10: BER performance when desired SCB ratio is $1/B$ and spreading factor is 1.

mances with 8 and 16 of spreading factors increases to 1.0 dB at the required BER. However, the MCDD system achieves the required BER even when the spreading factor is 8. It means that the impact of ILI coming from 9-SCB separation is still very small when the desired SCB ratio is $1/B$.

5.7 Conclusion

In this chapter, a new duplex scheme based on the multi-carrier transmission, MCDD, is proposed. The concept of MCDD is configuring the duplex channels by different sets of sub-carriers. The proposed MCDD introduces the unit of SCB which frequency resource is assigned to users according to. Moreover, MCDD also introduces the time-spreading technique to reduce the impact of ILI among SCBs. In this chapter, the BER performance of MCDD system with 1024 sub-carriers and 16 SCBs in the presence of CFO among the users is evaluated by the computer simulation. The simulation results indicate that, when the NCFO is equal to or less than 0.1, the impact of ILI is almost negligible, and then time-spreading is not necessary. When the spreading factor 1 and the desired SCB ratio is $1/2$, there is 0.2 dB loss between BER performances with 0 and 0.1 of NCFO at 10^{-5} of BER after FEC decoding. When the spreading factor 1 and the desired SCB ratio is $1/16$, there is 0.6 dB loss between BER performances with 0 and 0.1 of NCFO at 10^{-5} of BER after FEC decoding. On the other hand, when NCFO is 0.5, BER floor appears because of ILI, and this ILI is irreducible even when FEC scheme is used. From the point of time-spreading, 8 of spreading factor reduces the impact of ILI for MCDD with 16 SCB even when NCFO is up to 0.5. When the desired SCB ratio is $1/2$, there is 0.6 dB loss between BER performances with 8 and 16 of spreading factors at 10^{-5} of BER after FEC decoding. When the desired SCB ratio is $1/16$, there is 1.0 dB loss between BER performances with 8 and 16 of spreading factors at 10^{-5} of BER after FEC decoding.

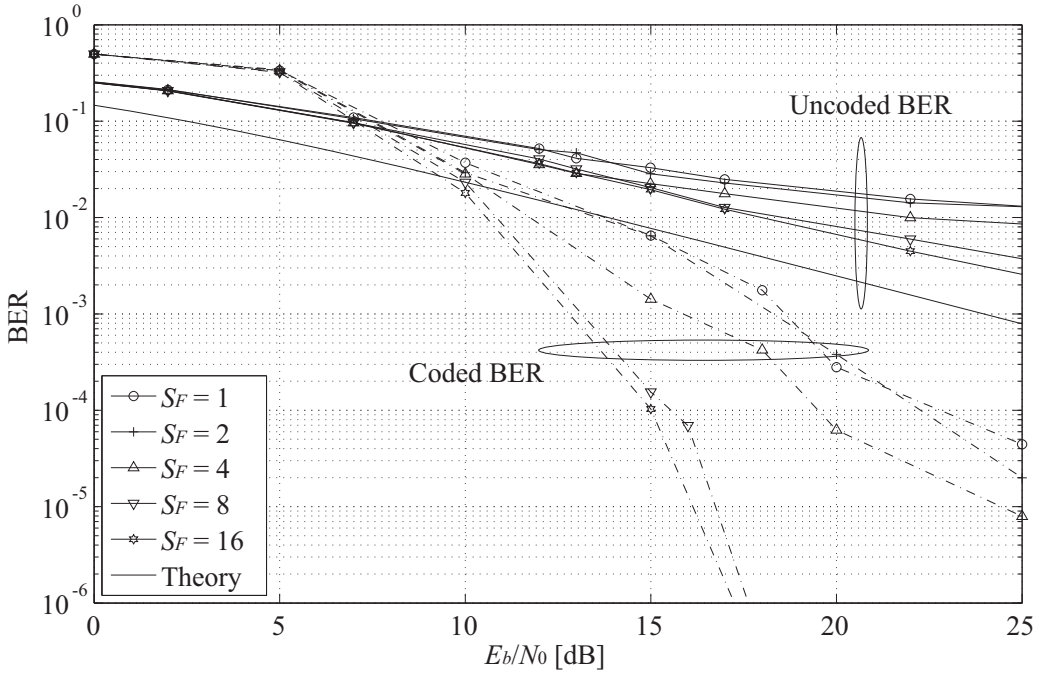

Figure 5.11: Impact of spreading factor to BER performance when desired SCB ratio is 1/2 and NCFO is 0.5.

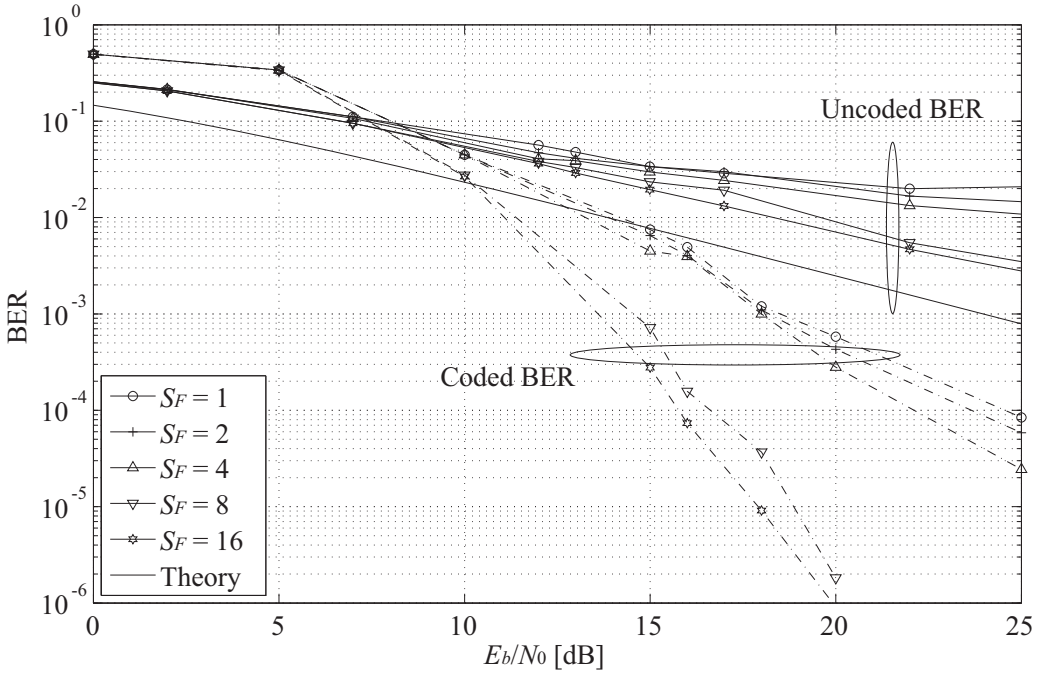

Figure 5.12: Impact of spreading factor to BER performance when desired SCB ratio is $1/B$ and NCFO is 0.5.

Chapter 6

Analyses of Technical and Strategic Solutions for Standardization Activity for Millimeter-Wave Wireless Personal Area Network Systems

Summary

In this chapter, recent issues and solutions related to wireless system standardization are analyzed. Recently, several major promotion groups get into a tangle in the standardization activities. Such standoff would delay the status of standardization activities, and then they would prevent the open of new market. In addition, such delays uselessly waste development costs and human resources. In this chapter, two examples of standoff in IEEE802.11n and IEEE802.15.3a are first introduced. Then, a latest standardization activity of IEEE802.15.3c Task Group (TG3c), which aims at the establishing millimeter-wave based wireless personal area network (WPAN) systems, is introduced. There were two major concepts of system, SC and MC based systems, in the TG3c activity. Then, a technical solution, "Common Mode," was proposed for bridging between the SC and MC. Finally, Common Mode helped to bring the SC and MC based systems to a single system specification. Through the analysis of TG3c activity, what is important for succeeding at the establishment of wireless system standard is addressed.

6.1 Introduction to IEEE802.15.3c Task Group

As mentioned in the previous chapters, the high-speed wireless access systems are strongly desired over the world. However, the micro-wave spectral band has already been occupied by the existing wireless system, such as cellular phone, WLAN, broadcasting systems and so on. Thus, it is very difficult to assign an enough broad bandwidth to a new system in the micro-wave spectrum. A way to solve this problem is exploring undeveloped spectral bands. Currently, millimeter-wave band has been interesting for realizing high-speed wireless access systems. A certain millimeter-wave band is unlicensed one, and thus it is possible to decrease the development costs. The propagation characteristics of millimeter-wave are close to those of light-wave, for example, the path loss by atmosphere is dominant and the directivity is very strong. Because of the propagation characteristics, the millimeter-wave band is not suitable for large coverage systems like the cellular systems but suitable for small coverage systems.

The TG3c was launched in May 2004 [184]. Since then, TG3c has been discussing on and building the standard of 60 GHz millimeter-wave based WPAN systems [25], [26]. This WPAN system covers short range communication up to 10 meters because of the strong directivity of millimeter-wave. In return for such a short range, this system aims at providing high speed data throughput over several Gbps at the medium access control layer level. The system requirements of IEEE802.15.3c have focused on two types of main usage models (UMs): one is file transferring model, so-called UM5, and another is video streaming model, so-called UM1 [27]. UM5 assumes communication between a kiosk file server and portable terminals. On the other hand, UM1 assumes video streaming between a video set-top box and display in-home facility.

In July 2007, TG3c approved and released call for proposals (CFP), whose due was May 2007. Sixteen proposers submitted their system proposals in May 2007. Through merges and down-selections, they were going forward the unification. Then, single unified proposal was finally approved by TG3c in November 2007. It was done for only a half year. It can be seen that the down-selection process of TG3c is much smoother than those of IEEE802.11n and IEEE802.15.3a.

6.2 Strategy for Two-Party Standoff

6.2.1 Two-Party Standoff

Recently, several, or two, major promotion groups get into a tangle in the standardization activities as illustrated in Fig. 6.1. Such standoff would delay the status of standardization activities, and then they would prevent the open of new market. In addition, such delays uselessly waste development costs and human resources. Thus, all the proposers, supporters and attendees should consider avoiding the fruitless standoff.

6.2.2 Examples in IEEE802.15.3a and IEEE802.11n

So far, two major examples of standoff can be found in the recent standardization activities. One is IEEE802.11n [185], and another is IEEE802.15.3a [186]. The IEEE802.11n Task Group has compiled WLAN systems with enhanced throughput. The concept of MIMO has been common in IEEE802.11n for a long time. However, there were a lot of minute differences among the proposers. At the time, two industrial groups, TGn Sync [187] and WWiSE [188], competed to get the majority in the task group. Although now single proposal was approved by the task group, the current draft version includes many options related to MIMO, it means And as of November 2007, the final draft of IEEE802.11n has not been compiled yet since September 2003.

The IEEE802.15.3a Task Group aimed at establishing UWB based high-speed WPAN systems. The other two major groups also competed in the task group. One group promoted an OFDM based UWB system [189], and another promoted a direct-spreading based UWB one. Unfortunately, they gave up to unify single proposal, and IEEE802.15.3a Task Group broke up in January 2006 [190], [191]. They wasted almost four years for the discussions.

6.2.3 Common Mode Concept in IEEE802.15.3c

6.2.3.1 Single-Carrier and OFDM Groups

As above-mentioned, TG3c has focused on UM5 and UM1 as the usage model. In the UM5 situation, the user himself adjusts the antenna direction of his terminal onto the file server, and thus line-of-sight (LOS) condition can be kept easily. On the other hand, the main situation of UM1 is in-home facility, and then it might be

difficult to keep LOS condition in this situation. It means that non LOS (NLOS) conditions should be considered in UM1.

It is well-known that the SC transmission is superior to the MC transmission from the points of simplicity, nonlinearity immunity and power consumption. Therefore, SC based air interface is the better choice for UM5 taking the advantages of SC into account [34]. Meanwhile, the MC transmission is generally suitable for the NLOS environments with the ISI channels. From such situations, it was expected before CFP that two major groups, the SC and MC (OFDM) ones, might compete in TG3c.

6.2.3.2 Common Mode

Consortium of Millimeter-Wave Practical Applications (CoMPA), an industrial-government-academic complex from Japan, has been working actively in TG3c since TG3c launching. The members of CoMPA are listed in Table A.1 of Appendix A.6. CoMPA has proposed "Common Mode" to avoid the fruitless stand-off and to unify SC and OFDM into single WPAN system. Common Mode is a signal mode which both the SC and OFDM terminals can transmit and receive. It will be used for association, connection set-up, acknowledgement and so on among the terminals.

The Common Mode signal is formed by Golay binary and complementary codes (see Appendix A.7). The baseband modulated symbols are repeated by Golay codes at the transmitter side. Then, the received signal is correlated by the identical codes and rake-combined at the receiver side. Because Golay codes are also used for the CoMPA's common preamble design, both SC and OFDM terminals will have the Golay correlator. Thus, they can decode the Common Mode signals.

6.2.3.3 Technical Impact

It can be seen that Common Mode is a bridge between SC and OFDM as illustrated in Fig. 6.2. In the other words, SC and OFDM can share the same frequency channel via Common Mode and TDMA time assignment. Moreover, SC/OFDM dual-mode piconet coordinators (PNCs) can translate the data signals between the SC and OFDM terminals. In this case, the customers could care nothing for the types of WPAN systems.

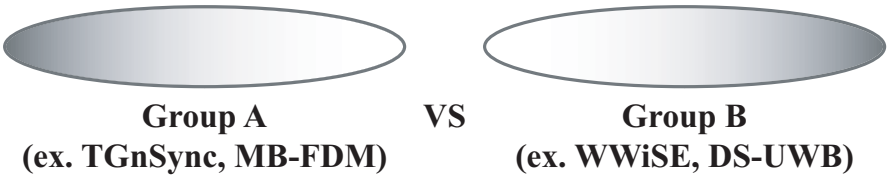

Figure 6.1: Two-party standoff.

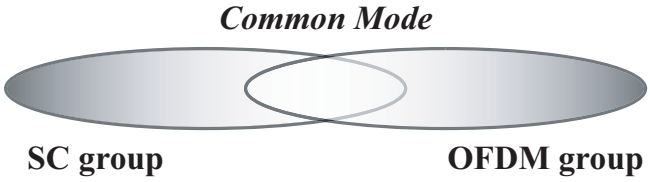

Figure 6.2: Common Mode concept in IEEE802.15.3c.

6.2.3.4 Political Impact

The Common Mode concept is not only a bridge between SC and OFDM but also that between the proposers. CoMPA consistently promoted the implementation of Common Mode to the WPAN system. It was important for CoMPA to make the others understand the concept. Moreover, resentment should be avoided during negotiations. Actually, CoMPA was careful of the merges and negotiations while it was the largest group in TG3c. They must have talked over the other proposers with the Common Mode concept, and never killed them.

6.3 Analysis of Contirubutions to IEEE802.15.3c

In this section, the trends of contributions for TG3c are analyzed. The following results count the amounts of contributions and their presenters from May 2004 to November 2007, that is, from the launch of TG3c to the approval of single proposal. The contribution materials can be obtained from the IEEE802.15 document server [195]. Totally 211 contributions including the system proposals can be seen at the server.

Figure 6.3 shows the percentage of presenters' affiliations in TG3c. Each first author 's affiliations in the latest revision are counted in this figure. This result proves that CoMPA has most contributed to TG3c. The amount of CoMPA's con-

tributions is triple of that of the second contributor. Figure 6.4 shows the annual variation of contribution amounts from 2004 to 2007. This figure focuses on the top seven affiliations appearing at Fig. 6.3. CoMPA had worked hard especially in 2006. In that year, several important topics, 60 GHz WPAN usage models, channel models and system evaluation methodologies, were compiled for the TG3c system requirement and CFP. Actually, CoMPA was involved with all those important topics [197]–[199]. These results indicate that CoMPA aimed at deeply analyzing the millimeter-wave principle and phenomenon, and keeping on the top of standardization activity. Those activities could help them develop the conceptual and logical WPAN system.

Figure 6.5 shows the percentage of affiliations' nationalities. There were many US contributors in the IEEE standardization. Not only the major companies such as Intel, Motorola and IBM but also venture companies such as Tensorcom, NewLANs, Astrin Radio and Decawave can be found in the contributors list. The amount of Japanese contributors is the second-large number. In contrast to the US, no venture company contributed to TG3c. The situation of Korea was similar to Japan. It is noted that there were some academic contributors, Tohoku University, National Taiwan University, Korea University and Yuan-ze University, collaborating with the industrial companies. It means that the circles of industry and academic have spread in the recent development.

6.4 Analysis of Down Selection

In this section, the TG3c down-selection is analyzed. The down-selection had been done from May to November 2007. It is noted that the proposers were often merged toward single proposal. Table 6.1 lists the initial proposers in May 2007. As expected, there were two major groups, SC and OFDM ones. However, key points are that CoMPA members proposed multiple WPAN systems and that the CoMPA members proposed both the SC and OFDM based WPAN systems. In addition, they also proposed the Common Mode concept. Most likely CoMPA aimed at smoothly negotiating and merging proposers from both the SC and OFDM sides at the first time. Table 6.2 lists the surviving proposers at the end of July 2007 meeting. At that time, some of SC proposers, IBM, NewLANs, IMEC, Motorola and Phiar, were merged into the CoMPA's SC proposal. While, an OFDM one, the France Telecom and IHP collaboration, was merged into Tensorcom's OFDM proposal. Similarly, CoMPA's SC and Tensorcom's OFDM proposals remained at

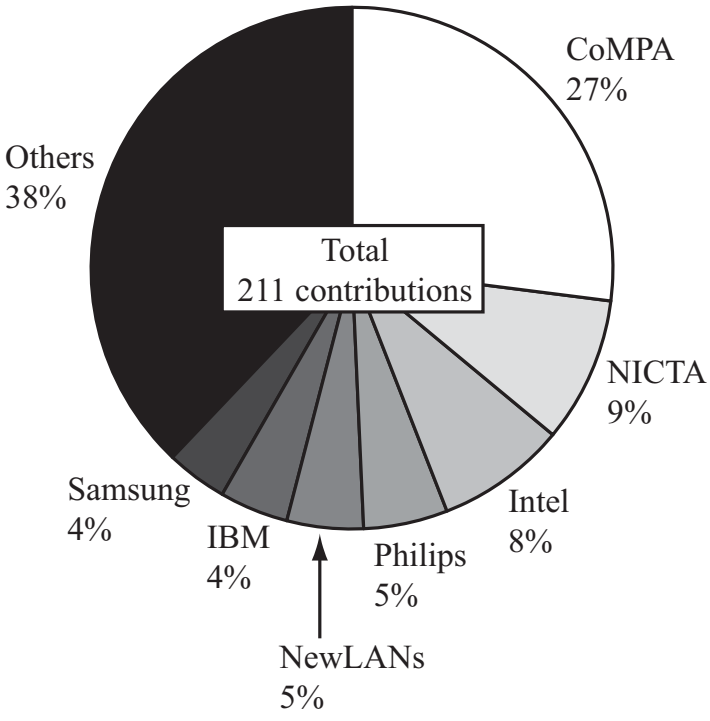

Figure 6.3: Major affiliations presenting their contributions in IEEE802.15.3c.

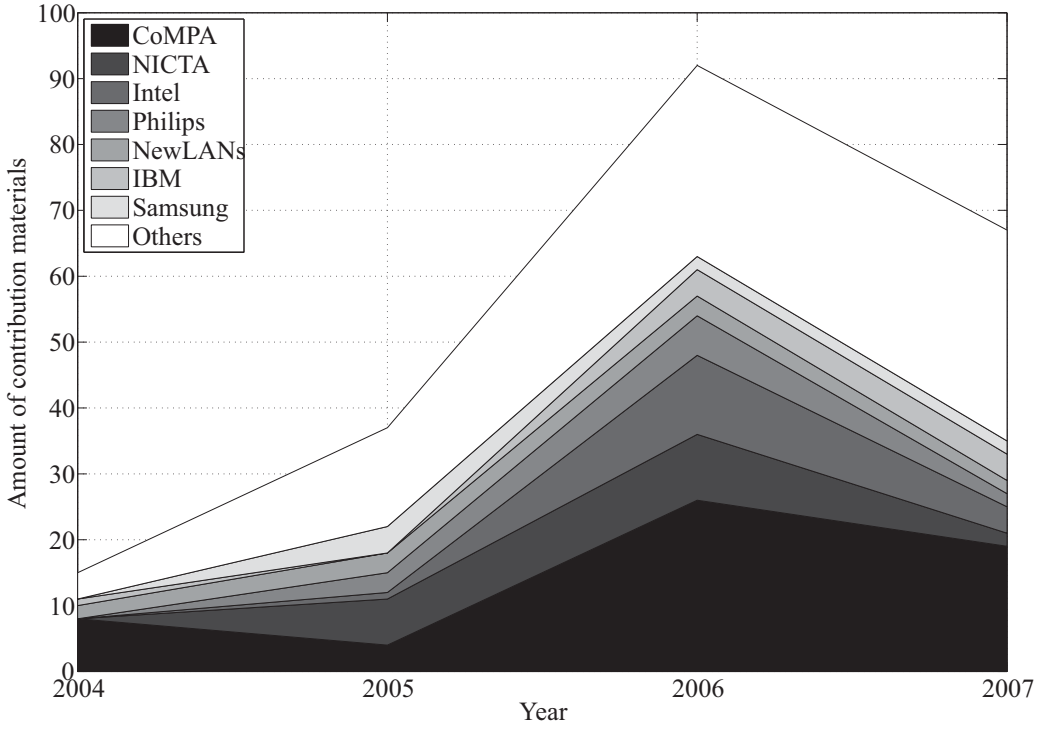

Figure 6.4: Annual variation of contribution amounts in IEEE802.15.3c.

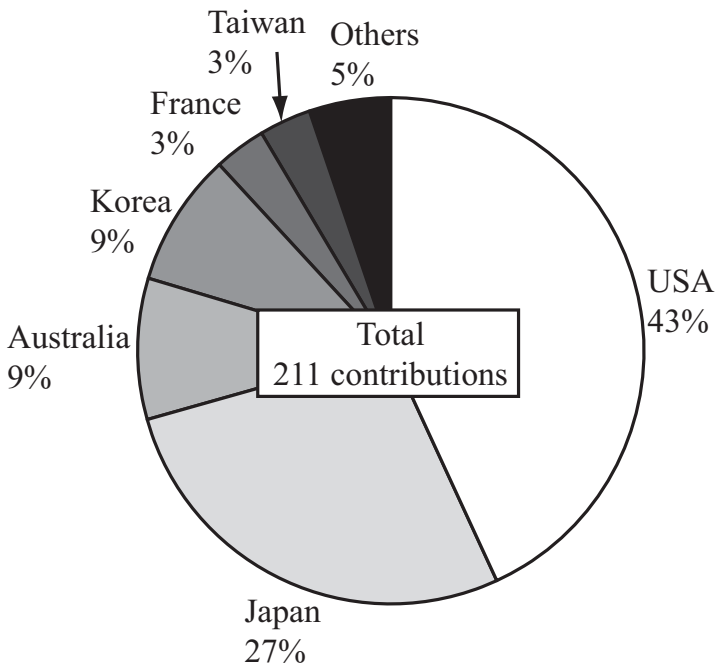

Figure 6.5: Major nationalities of affiliations presenting their contributions in IEEE802.15.3c.

the end of September 2007 meeting like listed in Table 6.3. Because Tensorcom, Inc. is a member of CoMPA and both the proposals included the Common Mode concept, it was natural for them to be merged into single SC/OFDM proposal. Finally, they were merged and unified in November 2007 meeting. Remember that there was no voting to choose the single proposal.

Reviewing the TG3c down-selection makes it clear that strategic concept and proposal can decrease the risk of standoff which will occur in the standardization activities.

6.5 Conclusion

In this chapter, the recent issue of two-party standoff and solutions related to the standardization are analyzed. Reviewing the TG3c movement indicates some important solutions for the standardization activities. First, technical efforts and contributions could make it clear what the systems really require to be operated in certain environments. Second, strategic and logical concepts of systems could reduce the risks of standoff and speed up the processes. Actually, it can be seen that CoMPA has completed to unify the SC and OFDM based systems into the single one within a half year.

At February 2008 present, TG3c has moved toward the approval of baseline document. It is very important to observe how TG3c finalizes the millimeter-wave WPAN standard. The continuous observation could help all the engineers earn the success and business behind it.

Table 6.1: Initial proposers in May 2007.

No.	Proposers' affiliation	Major features	# sildes
1	Astrin Radio	SC	10
2	CoMPA	SC-FDE, Common Mode, MAC enhancement	116
3	France Telecom, IHP	OFDM, binary&tone interleaving	52
4	IBM	MSK	22
5	IMEC	SC-FDE	61
6	Motorola, Phiar	ASK	40
7	NewLANs	Bipolar coding	27
8	NICTA	OFDM	16
9	Philips, Korea Univ., ETRI, GEDC	SC-FDE, beam-forming, channel bonding	82
10	Tensorcom	SC&OFDM, Common Mode	77
11	Samsung	UEP	12
12	SiBEAM, LG, Samsung, Toshiba, NEC, Sony, Matsushita	OFDM, UEP	37
13	Panasonic	OOK, multi-beacon	47
14	Tohoku Univ., Mitsubishi	Binding SC, MAC enhancement	12
15	National Taiwan Univ., CSIST, Yuan-ze Univ.	MC-CDMA	19
16	Decawave	8QAM, Ternary sequences	46

Table 6.2: Merged proposers at the end of meeting in July 2007.

No.	Proposers' affiliation
2	CoMPA, IBM, NewLANs, IMEC, Motorola, Phiar
9	Philips, Korea Univ., ETRI, GEDC
10	Tensorcom, France Telecom, IHP
11	Samsung
12	SiBEAM, LG, Samsung, Toshiba, NEC, Sony, Matsushita
13	Panasonic
14	Tohoku Univ., Mitsubishi
15	National Taiwan Univ., CSIST, Yuan-ze Univ.

Table 6.3: Merged proposers at the end of meeting in September 2007.

No.	Proposers' affiliation
2	CoMPA, IBM, NewLANs, IMEC, Motorola, Phiar, Philips, Korea Univ., ETRI, GEDC, Samsung, Panasonic, Tohoku Univ., Mitsubishi, National Taiwan Univ., CSIST, Yuan-ze Univ.
10	Tensorcom, France Telecom, IHP, SiBEAM, LG, Samsung, Toshiba, NEC, Sony, Matsushita, Intel

Table 6.4: Single merged proposer at the end of meeting in November 2007.

No.	Proposers' affiliation
2	CoMPA, Tensorcom, IBM, NewLANs, IMEC, Motorola, Phiar, Philips, Korea Univ., ETRI, GEDC, Samsung, Panasonic, Tohoku Univ., Mitsubishi, National Taiwan Univ., CSIST, Yuan-ze Univ., France Telecom, IHP, SiBEAM, LG

Chapter 7

Conclusion

This dissertation comprises the proposals and evaluation of wireless communication technologies based on the MC transmission. All the proposed technologies are the important factors of wireless communication systems from the points of multiplexing, multiple access and duplexing. Moreover, this dissertation also investigates the IEEE802.15.3c standardization activities which unified the SC and MC transmission techniques into single millimeter-wave WPAN system. It is important to analyze what occurs in the task group for the future standardization activities. The following paragraphs conclude the remarkable outcomes of this dissertation.

In Chapter 2, the basis of MC transmission techniques and its related issues are introduced. Moreover, the comparison of the features of SC and MC transmission techniques, and that of the features of OFCDM and OFDMA are addressed. The major features of MC techniques are high spectral efficiency, robustness against ISI channels, and flexibility of spectral resource management. In addition, the advantage of OFDMA is the multi-user diversity, which is most effective under the frequency-selective fading condition. It would be clear from this chapter why OFDMA and MC techniques are focused on in this dissertation.

In Chapter 3, the new signal detection and channel estimation algorithms are proposed for MIMO-OFDM systems in fast time-varying fading environments. These proposed algorithms are called as Multi-QRD-GD and SUCE, respectively. Both the proposed algorithms reduce not only computational complexity but also latency of signal processing. In the mobile fading environments, reducing the latency is very important to avoid channel estimation errors. The computer simulation clarifies the BER performance of MIMO-OFDM with the proposed algorithms. SUCE outperforms the conventional MMSE CE in the mobile fading envi-

ronments. SUCE achieves 10^{-5} of BER without any error floor when the Doppler frequency is up to 500 Hz, though MMSE CE shows the error floor. Moreover, SUCE also achieves 10^{-5} of BER even when the Doppler frequencies are 800 and 1000 Hz which indicate 160 and 200 km/h of terminal velocities in 5 GHz wireless systems, respectively. Multi-QRD-GD also outperforms the conventional MLD and QRM-MLD in the mobile fading environments. The combination of Multi-QRD-GD and SUCE has 2.8 dB of gain compared to that of QRM-MLD and SUCE at 10^{-5} of BER when modulation is QPSK and the Doppler frequency is 800 Hz. Moreover, both the proposed Multi-QRD-GD and SUCE reduces the computational complexity. The combination of them requires 54.8 and 0.4 % multiplications of MLD when modulation are QPSK and 16QAM, respectively. Thus, MIMO-OFDM employing Multi-QRD-GD and SUCE is a promising solution for enhancing the data rate and transmission performance in the mobile fading environments. For the further work, the improvement of CE is necessary to combat much higher Doppler frequency towards the higher level modulation. Moreover, the detection algorithm which is free from the antenna configurations is desirable.

In Chapter 4, the new TAC algorithm is proposed for the reverse link transmission of OFDMA. The reverse link transmission is very sensitive to MAI due to PDs among UTs accessing to AP. The proposed TAC algorithm suppresses the impact of MAI by (i) estimating PDs at PA, (ii) informing UTs of the estimated PDs, and (iii) controlling the transmit timing of UTs according to the informed PDs. TAC does not require any extended length of GI longer. Moreover, CR-TAC with two complexity reduction techniques; simplified reference symbol and 2PPD, is also proposed for OFDMA in Chapter 4. The computer simulation clarifies that the PER performance of Full-TAC approaches that with ideal control of transmit timing. On the other hand, the PER performance of CRTAC also approaches that of ideal control while it induces about 1.6 dB loss. CRTAC can replace the complex multiplications of Full-TAC to the simple inverters. Thus, CRTAC is suitable for implementation of AP with less hardware cost.

In Chapter 5, the new duplex scheme based on the multi-carrier transmission technology, that is, MCDD is proposed. MCDD prepares the multiple duplex channels which consist of the different sets of sub-carriers each other. MCDD can change the capacities of duplex channels and then it is suitable for wireless systems with asymmetric traffic. The concept of SCB is also introduced to MCDD. This concept considers the simplification of RF and analog devices in MCDD UTs. Moreover, the time-spreading technique with the reuse of spreading codes is proposed to mitigate the impact of ILI, which is caused by the loss of orthog-

onality among the duplex channels. The computer simulation evaluates the BER performance of MCDD in the presence of ILI due to CFO. MCDD is tolerable up to 0.1 of NCFO even when no spreading is used for it. If MCDD system has any control scheme to compensate CFO on ahead, the time-spreading technique is unnecessary. Because the time-spreading decreases the data rate of MCDD while it also reduces the impact of ILI, the spreading factor should be small as possible. On the other hand, when NCFO is 0.5, the time-spreading technique is necessary for MCDD without any CFO control scheme. Nevertheless, only 8 of spreading factor is required for the MCDD system with 16 SCBs. It means that the fully orthogonality is not mandatory for MCDD to mitigate ILI because the impact of ILI depends on the frequency separation of SCBs. The concept of MCDD could be smoothly combined with the MC based multiplexing and multiple access technologies. Thus, the frequency resource management could be more flexible through multiplexing, multiple access and duplexing.

In Chapter 6, the important activities of standardization is analyzed through the case study of IEEE802.15 TG3c history. Before the analyses, two examples of standardization standoff, IEEE802.11n and IEEE802.15.3a, are introduced. The standoff wastes work time, develop cost and human resource. Thus, such fruitless standoff should be avoided there. In TG3c, the strategic concept, Common Mode, has been proposed to realize SC and OFDM coexistence in the WPAN systems and to speed up the process of standardization. The analyses indicate that technical efforts and contributions could make it clear what the systems really require to be operated in certain environments, and that strategic and logical concepts of systems could reduce the risks of standoff and speed up the processes. It is desirable to analyze the other status of standardization, not only good cases but also bad ones for future success.

Techniques of adaptive frequency, time and space resource allocation and PHY-MAC cross layer collaboration are very important for the future MC transmission techniques toward more flexible and efficient wireless systems. The techniques proposed in this dissertation could bring the flexibility to the MC transmission techniques and they could help developing such systems.

Appendix

A.1 Derivation of ICI Term

The ICI term in (3.1) is derived through focusing on the l-th transmitter and the m-th receiver antennas. It is assumed that GI is enough long to avoid ISI. The OFDM symbol received at the m-th antenna in the time-domain $y_m(t,\tau)(\tau = 0, \cdots, G + F - 1)$ is expressed by:

$$y_m(t,\tau) = \sum_{p=0}^{P_M-1} \eta_{p,m,l}(t,\tau_{p,m,l}) x_l(t,\tau-\tau_{p,m,l}) + w_m(t,\tau), \tag{A.1}$$

where $x_l(t,\tau)$ is the τ-th sample in the t-th OFDM symbol transmitted from the l-th antenna:

$$x_l(t,\tau) = \frac{1}{F}\sum_{k=0}^{F-1} s_l(t,k) e^{j2\pi(\tau-G)k/F}, \tag{A.2}$$

$\eta_{p,m,l}(t,\tau_{p,m,l})$ is the channel impulse response (CIR) with the delay time $\tau_{p,m,l}$, P_M is the number of paths composing the multi-path channel, $w_m(t,\tau)$ is AWGN, F is the FFT points and G is the GI points. The symbol on the k-th sub-carrier output

from FFT $r_m(t,k)$ is expressed as follows:

$$\begin{aligned}
r_m(t,k) &= \sum_{\tau=G}^{G+F-1} y_m(t,\tau)e^{-j2\pi(\tau-G)k/F} \\
&= \frac{1}{F}\sum_{k=0}^{K-1}\sum_{\tau=G}^{G+F-1}\sum_{p=0}^{P_M-1}\eta_{p,m,l}(t,\tau)e^{j2\pi(-\tau_{p,m,l}-G)k/F}s_l(t,k) \\
&\quad + \sum_{\tau=G}^{G+F-1} w_m(t,\tau)e^{-j2\pi(\tau-G)k/F} \\
&= \left\{\frac{1}{F}\sum_{\tau=G}^{G+F-1}\sum_{p=0}^{P_M-1}\eta_{p,m,l}(t,\tau)e^{j2\pi(-\tau_{p,m,l}-G)k/F}\right\}s_l(t,k) \\
&\quad + \sum_{\substack{k'=0\\k'\neq k}}^{K-1}\left\{\frac{1}{F}\sum_{\tau=G}^{G+F-1}\sum_{p=0}^{P_M-1}\eta_{p,m,l}(t,\tau)e^{j2\pi(-\tau_{p,m,l}-G)k'/F}\right\}s_l(t,k') \\
&\quad + n_m(t,k) \\
&= h_{m,l}(t,k)s_l(t,k) + \sum_{\substack{k'=0\\k'\neq k}}^{K-1} h_{C,m,l}(t,k')s_l(t,k') + n_m(t,k),
\end{aligned} \tag{A.3}$$

where

$$h_{m,l}(t,k) = \frac{1}{F}\sum_{\tau=G}^{G+F-1}\sum_{p=0}^{P_M-1}\eta_{p,m,l}(t,\tau)e^{j2\pi(-\tau_{p,m,l}-G)k/F}, \tag{A.4}$$

$$h_{C,m,l}(t,k') = \frac{1}{F}\sum_{\tau=G}^{G+F-1}\sum_{p=0}^{P_M-1}\eta_{p,m,l}(t,\tau)e^{j2\pi(-\tau_{p,m,l}-G)k'/F}, \tag{A.5}$$

$$n_m(t,k) = \sum_{\tau=G}^{G+F-1} w_m(t,\tau)e^{-j2\pi(\tau-G)k/F}. \tag{A.6}$$

According to (3.1) and (A.3), $h_{C,m,l}(t,k)$ lies on the m-th row and the l-th column element in the matrix $\boldsymbol{H}_C(t,k)$.

A.2 Output of Sub-Space Projector

For instance, when L is four and G_r is two, the output of the sub-space projector $\boldsymbol{z}(t,k)$ is expressed as follow:

$$\begin{aligned}\boldsymbol{z}(t,k) &= [z_{\lceil L/G_r\rceil+1,1}(t,k)\ \cdots\ z_{L,1}(t,k) \\ &\qquad z_{\lceil L/G_r\rceil+1,2}(t,k)\ \cdots\ z_{L,2}(t,k)]^T \\ &= \boldsymbol{Q}^H(t,k)\boldsymbol{r}(t,k),\end{aligned} \tag{A.7}$$

where

$$\begin{aligned}\boldsymbol{Q}(t,k) = \Big[&\boldsymbol{q}_{\lceil L/G_r\rceil+1,1}(t,k)\ \cdots\ \boldsymbol{q}_{L,1}(t,k) \\ &\boldsymbol{q}_{\lceil L/G_r\rceil+1,2}(t,k)\ \cdots\ \boldsymbol{q}_{L,2}(t,k)\Big]\end{aligned} \tag{A.8}$$

and $\boldsymbol{q}_{l,g}(t,k)$ is the l-th column vector of $\boldsymbol{Q}_g(t,k)$. Although the original way generating $z_{l,g}(t,k)$ from the sub-space projector requires $4G_rL^2KD$ multiplications, the way modified by (A.7) requires $4L^2KD$ ones.

A.3 Carrier Interferometory Pilot Assisted Channel Estimation

Carrier interferometory pilot assisted CE exploits the delay-time-domain. Here introduces this CE scheme with $\lceil L/2\rceil$ pilot OFDM symbols for the initial CE. The t-th pilot OFDM symbol is used for estimating $\boldsymbol{h}_{2t-1}(0,k)$ and $\boldsymbol{h}_{2t}(0,k)$.

Let $s_{CE}(t,k)$ be known QPSK symbols in the frequency-domain. Before IFFT, the known pilot symbols are linearly rotated as follows:

$$s'_{l,CE}(t,k) = \begin{cases} s_{CE}(t,k)e^{-j2\pi k(1+2\mathrm{mod}(l,2))G/F} & l = 2t-1, 2t \\ 0 & \text{otherwise} \end{cases}, \tag{A.9}$$

where $\mathrm{mod}(a,b)$ is a resudue of a/b. We assume a condition that $4G \le F$ in this paper. Pilot OFDM symbols are generated by IFFT:

$$x_{l,CE}(t,\tau) = \frac{1}{F}\sum_{k=0}^{F-1} s'_{l,CE}(t,k)e^{j2\pi k(\tau-G)/F}. \tag{A.10}$$

After passing through a MIMO channel, received pilot OFDM symbols are converted to the frequency-domain symbols by FFT in a receiver side:

$$r_{m,CE}(t,k) = \sum_{\tau=G}^{G+F-1} y_{m,CE}(t,k)e^{-j2\pi k(\tau-G)/F}. \tag{A.11}$$

The output of FFT is divided by the known symbol and again converted to the time-domain symbol by IFFT as follows:

$$r'_{m,CE}(t,k) = \frac{s^*_{CE}(t,k)}{|s_{CE}(t,k)|^2} r_{m,CE}(t,k), \tag{A.12}$$

$$\hat{\eta}_{m,CE}(t,\tau) = r'_{m,CE}(t,k) e^{j2\pi k\tau/F}. \tag{A.13}$$

To isolate tentative CIRs related to the $(2t-1)$-th and $2t$-th transmitter antennas, delay-time windows are applied to the output of IFFT, that is:

$$\hat{\eta}_{m,l,CE}(t,\tau) = \begin{cases} \hat{\eta}_{m,CE}(t,\tau) & l = 2t-1, 2t \text{ and} \\ & \frac{F}{2}\mathrm{mod}\,(l,2) \le \tau \le \frac{F}{2}\,(1+\mathrm{mod}\,(l,2)) - 1 \\ 0 & \text{otherwise} \end{cases} \tag{A.14}$$

Then, FFT is again performed for $\hat{\eta}_{m,l,CE}(t,\tau)$. After that, an initial channel estimate $\hat{h}_{m,l}(0,k)$ is obtained by reverse linear rotation:

$$\hat{h}_{m,l}(0,k) = \frac{1}{F}\sum_{\tau=0}^{F-1} \hat{\eta}_{m,l,CE}(t,\tau) e^{j2\pi k\{\tau+(1+2\mathrm{mod}(l,2))G\}/F}, \quad l = 2t-1, 2t. \tag{A.15}$$

A.4 Simplified Minimum Mean Square Error Based Channel Estimation

In MMSE CE, CFR $\tilde{h}_{m,l}(t,k)$ is temporarily estimated as follow:

$$h'_{m,l}(t,k) = \hat{h}_{m,l}(t,k) + \frac{\mu_0}{P}\left(r_m(t,k) - \sum_{q=1}^{L} \hat{h}_{m,q}(t,k)\hat{s}_q(t,k)\right)\hat{s}^*_l(t,k), \tag{A.16}$$

where P is an average transmit symbol power and μ_0 is a forgetting factor ($0 \le \mu_0 \le 1$). Reference [137] mentioned that MMSE CE represented by (A.16) is equivalent to the scheme proposed in Ref. [136] when μ_0 is one. The temporal estimates of CFR $h'_{m,l}(t,k)$ are converted to those of CIR $\hat{\eta}_{m,l}(t,\tau)$ by IFFT:

$$\hat{\eta}_{m,l}(t,\tau) = \frac{1}{F}\sum_{k=0}^{F-1} h'_{m,l}(t,k) e^{j2\pi k\tau/F}. \tag{A.17}$$

To mitigate the noise effect, CIRs exceeding the channel length $\tau_{\max}$ are replaced by zeros:

$$\bar{\eta}_{m,l}(t,\tau) = \begin{cases} \hat{\eta}_{m,l}(t,\tau) & \tau \le \tau_{\max} \\ 0 & \text{otherwise} \end{cases}. \tag{A.18}$$

After that, CFR $\hat{h}_{m,l}(t+1,k)$ is finally estimated by FFT:

$$\hat{h}_{m,l}(t+1,k) = \sum_{\tau=0}^{F-1} \bar{\eta}_{m,l}(t,\tau) e^{-j2\pi k\tau/F}. \tag{A.19}$$

A.5 Maximum Likelihood Detection

MLD searches possible transmitted symbols minimizing a metric. Let $\check{s}_l(t,k)$ and $\check{\boldsymbol{s}}(t,k)$ be the candidates of transmitted symbol and transmitted symbol vector, respectively. MLD computes squared Euclidean norms between the received symbol vector and all the candidate vectors as the metrics $\mu(t,k)$:

$$\mu(t,k) = \left\| \boldsymbol{r}(t,k) - \hat{\boldsymbol{H}}(0,k)\check{\boldsymbol{s}}(t,k) \right\|^2. \tag{A.20}$$

The operator $\|\boldsymbol{a}\|$ means norm of a vector $\boldsymbol{a}$. MLD generates log-likelihood ratio (LLR) for the i-th bit of $s_l(t,k)$ [119]:

$$\begin{aligned} \hat{b}_{l,i}(t,k) &= \log \frac{p\left(b_{l,i}(t,k)=1 \mid \boldsymbol{s}(t,k)\right)}{p\left(b_{l,i}(t,k)=0 \mid \boldsymbol{s}(t,k)\right)} \\ &= \log \frac{\sum_{\check{\boldsymbol{s}}(t,k):b_{l,i}(t,k)=1} e^{-\mu_{l,i,1}(t,k)+\sum \log p(\check{s}_l(t,k))}}{\sum_{\check{\boldsymbol{s}}(t,k):b_{l,i}(t,k)=0} e^{-\mu_{l,i,0}(t,k)+\sum \log p(\check{s}_l(t,k))}}. \end{aligned} \tag{A.21}$$

In (A.21), $p\,(a)$ is a posterior probability of a.

A.6 Members of CoMPA

Table A.1: Members list of CoMPA (November 2007).

NICT, Tensorcom, Sony Corporation, Matsushita Electric Industry Co. Ltd.,
NTT Corporation, Tohoku University, Fujitsu Limited,
Mitsubishi Electric Corporation, Oki Electric Industry Co. Ltd.,
Maspro Denkoh Corporation, ATR, NEC Corporation,
KYOCERA Corporation, Tokyo Institute of Technology,
Eudyna Devices Inc., Japan Radio Co. Ltd., EMMEX Inc.,
TAIYO YUDEN Co. Ltd., RICOH Co. Ltd.,
Toyo System Engineering Co. Ltd.

A.7 Golay Codes

A.7.1 Property

Reference [192] proposed pairs of complementary sequences. These pairs of sequences have an attractive property that the sum of their autocorrelation has a unique peak and no side-lobe. We call these pairs of sequences "Golay codes" in this paper.

Let $a_N(i)$ and $b_N(i)$ for $i = 0, \cdots, N-1$ be a pair of Golay codes with $N = 2^M$ of length. Golay codes are defined by the following autocorrelation property:

$$R_a(i) + R_b(i) = 2N\delta(i), \tag{A.22}$$

where

$$R_a(i) = \sum_{k=0}^{N-i-1} a_N(k)a_N^*(k+i), \tag{A.23}$$

and

$$R_b(i) = \sum_{k=0}^{N-i-1} b_N(k)b_N^*(k+i). \tag{A.24}$$

The operator a^* indicates conjugation of a.

Golay codes with N of length are generated by delay and weight vectors with M of length and a recursive algorithm [193], [194]. Binary Golay codes are generated when the delay vector $\boldsymbol{D} = [D_0 \cdots D_{M-1}]$ is chosen as any permutation of $\left[2^0 \ \cdots 2^{M-1}\right]$ and the weight vector $\boldsymbol{W} = [W_0 \cdots W_{M-1}]$ has ± 1 of elements. The recursive algorithm for generating Golay codes is described as follows:

$$a_{N,(0)}(i) = \delta(i), \tag{A.25}$$
$$b_{N,(0)}(i) = \delta(i), \tag{A.26}$$
$$a_{N,(m)}(i) = W_{m-1}a_{N,(m-1)}(i) + b_{N,(m-1)}(i - D_{m-1}), \tag{A.27}$$
$$b_{N,(m)}(i) = W_{m-1}a_{N,(m-1)}(i) - b_{N,(m-1)}(i - D_{m-1}), \tag{A.28}$$
$$a_N(i) = a_{N,(M)}(i), \tag{A.29}$$
$$b_N(i) = b_{N,(M)}(i). \tag{A.30}$$

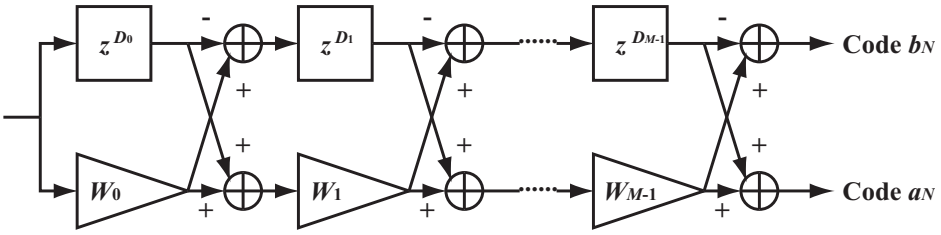

Figure A.1: Golay code generator.

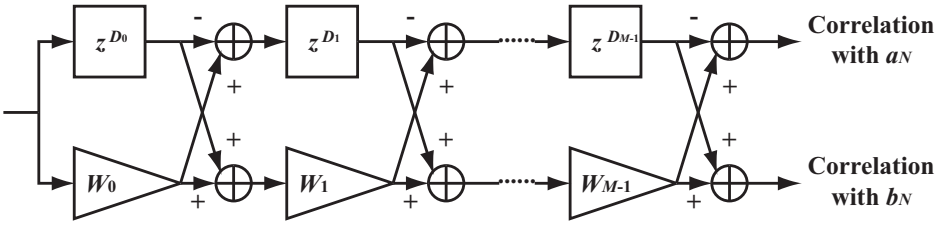

Figure A.2: Golay correlator.

A.7.2 Code Generator and Correlator

Golay codes enable their code generator and correlator to be very simple [193], [194]. Figures A.1 and A.2 illustrate the configurations of Glay code generator and correlator, respectively. These configurations are derived from the recursive algorithm (A.25) to (A.30). Both the generator and correlator consists of M delay circuits, M inverters and $2M$ adders for binary Golay codes with 2^M of length. Moreover, they can generate and calculate the output corresponding to the pair of Golay codes at the same time.

Bibliography

[1] Ministry of Internal Affairs and Communications website, http://www.soumu.go.jp/menu_02/ict/u-japan_en/index.html

[2] The Third Generation Partnership Project website, http://www.3gpp.org/

[3] The Third Generation Partnership Project 2 website, http://www.3gpp2.org/

[4] UMTS-TDD Alliance website, http://www.umtstdd.org/

[5] The Third Generation Partnership Project, "HSPA evolution (FDD)," 3GPP TR 25.999, V2.3.0, Sept. 2007.

[6] R. van Nee, G. Awater, M. Morikura, H. Takanashi, M. Webster and K. Halford, "New high-rate wireless LAN standards," IEEE Commun. Mag., vol.37, no.12, pp.82–88, Dec. 1999.

[7] M. Morikura and H. Matsue, "Trends of IEEE 802.11 based wireless LAN," IEICE Trans. Commun. (Japanese Edition), vol.J84-B, no.11, pp.1918–1927, Nov. 2001. (written in Japanese)

[8] IEEE Std 802.11a-1999, "Wireless LAN medium access control (MAC) and physical layer (PHY) specifications: High-speed physical layer in the 5 GHz band," Sept. 1999.

[9] IEEE Std 802.11g-2003, "Wireless LAN medium access control (MAC) and physical layer (PHY) specifications: Amendment 4: further higher data rate extension in the 2.4 GHz band," June 2003.

[10] N. Ohkubo, Y. Kishiyama, K. Higuchi, H. Atarashi and M. Sawahashi, "Investigations on optimum sub-carrier spacing for OFDM radio access in evolved UTRA downlink," IEICE Technical Report, RCS2005-69, pp.31–36, Aug. 2005. (written in Japanese)

[11] T. Ihara, H. Atarashi, A. Morimoto, Y. Kishiyama, K. Higuchi and M. Sawahashi, "Investigations on optimum cyclic prefix length in unicast channel for OFDM radio access in evolved UTRA downlink," IEICE Technical Report, RCS2005-70, pp.37–42, Aug. 2005. (written in Japanese)

[12] A. Morimoto, Y. Kishiyama, K. Higuchi, H. Atarashi and M. Sawahashi, "Investigations on optimum cyclic prefix length in multicast/broadcast channel for OFDM radio access in evolved UTRA downlink," IEICE Technical Report, RCS2005-71, pp.43–48, Aug. 2005. (written in Japanese)

[13] Y. Kishiyama, K. Higushi, H. Atarashi and M. Sawahashi, "Investigations on optimum radio parameter set for OFDM radio access in evolved UTRA downlink," IEICE Technical Report, RCS2005-72, pp.49–54, Aug. 2005. (written in Japanese)

[14] The Third Generation Partnership Project, "Feasibility study for evolved universal terrestrial radio access (UTRA) and universal terrestrial radio access network (UTRAN)," 3GPP TR 25.912, V7.2.0, June 2007.

[15] L. Franca-Neto, R. Eline and B. Bisla, "WiMAX," Intel Technology Journal, vol.8, no.3, Aug. 2004.

[16] Y. Yamao, N. Umeda, T. Otsu and N. Nakajima, "Fourth generation mobile communications system—Issues regarding radio system technologies—," IEICE Trans. Commun. (Japanese Edition), vol.J83-B, no.10, pp.1364–1373, Oct. 2000. (written in Japanese)

[17] B. Evans and K. Baughan, "Visions of 4G," IEE Electronics & Communication Engineering Journal, vol.12, no.6, pp.293–303, Dec. 2000.

[18] S. Ohmori, Y. Yamao and N. Nakajima, "The future generations of mobile communications based on broadband access technologies," IEEE Commun. Mag., vol.38, no.12, pp.134–142, Dec. 2000.

[19] W. Mohr, "European and international research activities towards systems beyond third generation mobile communications," IEICE Trans. Fundamentals, vol.E86-A, no.7, pp.1566–1575, July 2003.

[20] Y. Kishiyama, N. Maeda, K. Higuchi, H. Atarashi and M. Sawahashi, "Field experiments on throughput performance above 100 Mbps in forward

link for VSF-OFCDM broadband wireless access," IEICE Trans. Commun., vol.E88-B, no.2, pp.604–614, Feb. 2005.

[21] Y. Goto, T. Kawamura, H. Atarashi and M. Sawahashi, "Variable spreading and chip repetition factors (VSCRF)-CDMA in reverse link for broadband packet wireless access," IEICE Trans. Commun., vol.E88-B, no.2, pp.509–519, Feb. 2005.

[22] T. Fujii and N. Nakajima, "Radio channel assignment system for cellular mobile communications," IEICE Trans. Commun. (Japanese Edition), vol.J84-B, no.5, pp.872–882, May 2001. (written in Japanese)

[23] H. Takagi, H. Yoshino, N. Matoba and M. Azuma, "Methodology for calculation of spectrum requirements for the next generation mobile communication systems," IEICE Trans. Commun. (Japanese Edition), vol.J89-B, no.2, pp.135–142, Feb. 2006. (written in Japanese)

[24] ITU-R WRC website, http://www.itu.int/ITU-R/go/wrc/en/

[25] A. Seyedi, "TG3c system requirements," IEEE P802.15 Working Group for Wireless Personal Area Networks, IEEE802.15-07-0583-00-003c, Jan. 2007.

[26] A. Seyedi, "TG3c selection criteria," IEEE P802.15 Working Group for Wireless Personal Area Networks, IEEE802.15-05-0493-26-003c, Jan. 2007.

[27] A. Sadri, "Summary of the usage models for 802.15.3c," IEEE P802.15 Working Group for Wireless Personal Area Networks, IEEE802.15-06-0369-09-003c, Nov. 2006.

[28] J. Ruiz and S. Shimamoto, "Statistical modeling of intra-body propagation channel," Proc. IEEE WCNC 2007, pp.2063–2068, March 2007.

[29] T. Kobayashi and S. Kouya, "Overview of research and development in ultra wideband wireless systems," IEICE Trans. Fundamentals, vol.J86-A, no.12, pp.1264–1273, Dec. 2003. (written in Japanese)

[30] R. Kohno, "Collaboration among industry, academia and government for R&D of ultra wideband wireless technologies and contribution in standardization in wireless PAN," IEICE Trans. Fundamentals, vol.J86-A, no.12, pp.1274–1283, Dec. 2003. (written in Japanese)

[31] Y. Shoji, M. Nagatsuka, K. Hamaguchi and H. Ogawa, "60 GHz band 64QAM/OFDM terrestrial digital broadcasting signal transmission by using millimeter-wave self-heterodyne system," IEEE Trans. Broadcasting, vol.47, no.3, pp.218–227, Sept. 2001.

[32] Y. Shoji and H. Ogawa, "Simple millimeter-wave quasi-maximal-ratio-combining antenna diversity system based on millimeter-wave self-heterodyne transmission technique," IEICE Trans. Commun., vol.E87-B, no.8, pp.2203–2211, Aug. 2004.

[33] Y. Shoji, C. Choi and H. Ogawa, "70-GHz-band OFDM transceivers based on self-heterodyne scheme for millimeter-wave wireless personal area network," IEEE Trans. Microwave Theory and Techniques, vol.54, no.10, pp.3664–3674, Oct. 2006.

[34] R. Funada, H. Harada, Y. Shoji, R. Kimura, Y. Nishiguchi, M. Lei, C. Choi, F. Kojima, C. Pyo, Z. Lan, I. Lakkis, M. Umehira and S. Kato, "A design of single carrier based PHY for IEEE 802.15.3c standard," Proc. IEEE PIMRC 2007, Sept. 2007.

[35] S. Sampei, Applications of Digital Wireless Technologies to Global Wireless Communication Systems, Prentice-Hall, 1997.

[36] A. Duel-Hallen and C. Heegard, "Delayed decision-feedback sequence estimation," IEEE Trans. Commun., vol.37, no.5, pp.428–436, May 1989.

[37] H. Sawaguchi and W. Sakurai, "Performance evaluation and error propagation analysis of decision-feedback equalization with maximum-likelihood detector," IEICE Trans. Electron., vol.E78-C, no.11, pp.1575–1581, Nov. 1995.

[38] N. Maeda, S. Sampei and N. Morinaga, "Performance of a complexity reduced decision feedback equalizer using a delayed wave canceller with an adaptive transmission control scheme," IEICE Trans. Commun. (Japanese Edition), vol.J82-B, no.10, pp.1888–1897, Oct. 1999. (written in Japanese)

[39] K. Hayashi and S. Hara, "A spatio-temporal equalization method with cascade configuration of an adaptive antenna array and a decision feedback equalizer," IEICE Trans. Commun. (Japanese Edition), vol.J85-B, no.6, pp.900–909, June 2002. (written in Japanese)

[40] H. Kubo, K. Tanada, A. Iwase, S. Hayaashi and K. Murakami, "A single carrier modulation scheme in the presence of highly time dispersive intersymbol interference," IEICE Trans. Commun. (Japanese Edition), vol.J85-B, no.11, pp.1913–1923, Nov. 2002. (written in Japanese)

[41] H. Sari, G. Karam and I. Jeanclaude, "Frequency-domain equalization of mobile radio and terrestrial broadcast channels," Proc. IEEE GLOBECOM 1994, vol.1, pp.1–5, Nov. 1994.

[42] D. Falconer, S. Ariyavisitakul, A. Benyamin-Seeyar and B. Eidson, "Frequency domain equalization for single-carrier broadband wireless systems," IEEE Commun. Mag., vol.40, no.4, pp.58–66, April 2002.

[43] S. Hara, and R. Prasad, "Overview of multicarrier CDMA," IEEE Commun. Mag., vol.35, no.12, pp.126–133, Dec. 1997.

[44] R. van Nee, and R. Prasad, OFDM for Wireless Multimedia Communications, Artech House, 1999.

[45] H. Liu and G. Li, OFDM-Based Broadband Wireless Networks, John Wiley & Sons, Inc., 2005.

[46] I. Koffman, and V. Roman, "Broadband wireless access solutions based on OFDM access in IEEE 802.16," IEEE Commun. Mag., vol.40, pp.96-103, April 2002.

[47] H. Sari, G. Karam, and I. Jeanclaude, "Transmission techniques for digital terrestrial TV broadcasting," IEEE Commun. Mag., vol.33, no.2, pp.100–109, Feb. 1995.

[48] S. Abeta, H. Atarashi, M. Sawahashi, and F. Adachi, "Performance of coherent multi-carrier/DS-CDMA and MC-CDMA for broadband packet wireless access," IEICE Trans. Commun., vol.E84-B, no.3, pp.406–414, March 2004.

[49] H. Atarashi, N. Maeda, S. Abeta and M. Sawahashi, "Broadband packet wireless access based on VSF-OFCDM and MC/DS-CDMA," Proc. IEEE PIMRC 2002, vol.3, pp.992–997, Sept. 2002.

[50] H. Atarashi, S. Abeta, and M. Sawahashi, "Variable spreading factor-orthogonal frequency and code division multiplexing (VSF-OFCDM) for broadband packet wireless access," IEICE Trans. Commun., vol.E86-B, no.1, pp.291–299, Jan. 2003.

[51] A. Sumasu, T. Nihei, K. Kitagawa, M. Uesugi and O. Kato, "An OFDM-CDMA system using combination of time and frequency domain spreading," IEICE Technical Report, RCS2000-3, pp.13–18, April 2000. (written in Japanese)

[52] N. Maeda, Y. Kishiyama, H. Atarashi and M. Sawahashi, "Variable spreading factor-OFCDM with two dimensional spreading that prioritizes time domain spreading for forward link broadband wireless access," Proc. IEEE VTC 2003-Spring, vol.1, pp.127–132, April 2003.

[53] H. Harada, C.J. Ahn, S. Takahashi, Y. Kamio, and S. Sampei, "Dynamic parameter controlled orthogonal frequency and time division multiple access," Proc. IEEE PIMRC 2004, vol.4, pp.2648–2652, Sept. 2004.

[54] R. Bohnke, M. Suzuki and K. Sakoda, "Spectral efficient modulation schemes in a SFH-TDMA orthogonal frequency division multiplexing (OFDM) wireless communication system to support advanced services," Proc. IEEE VTC 1998, vol.3, pp.2202–2206, May 1998.

[55] M. Suzuki, R. Bohnke and K. Sakoda, "Band division mltiple access (BDMA) system: a novel approach for next generation mobile telecommunication system, based on OFDM and SHF-TDMA," Proc. IEEE VTC 1998, vol.2, pp.1326–1330, May 1998.

[56] T. Kunihiro, T. Yamaura, M. Suzuki and E. Fujita, "BDMA testbed —configuration and performance results—," Proc. IEEE VTC 1999, vol.3, pp.1836–1840, May 1999.

[57] T. Fujii, N. Izuka, H. Masui and A. Nagate, "SCS-MC-CDMA system with best effort cell structure," Proc. IEEE ICC 2005, vol.4, pp.2213–2217, May 2005.

[58] J. van de Beek, O. Edfors, M. Sandell, S. Wilson and P. Borjesson, "On channel estimation in OFDM systems," Proc. IEEE VTC 1995, vol.2, pp.815–819, July 1995.

[59] O. Edfors, M. Sandell, J. van de Beek, S. Wilson and P. Borjesson, "OFDM channel estimation by singular value decomposition," IEEE Trans. Commun., vol.46, no.7, pp.931–939, July 1998.

[60] T. Onizawa, M. Mizoguchi and M. Morikura, "A novel channel estimation scheme employing adaptive selection of frequency-domain filters for OFDM systems," IEICE Trans. Commun., vol.E82-B, no.12, pp.1923–1931, Dec. 1999.

[61] H. Harada, T. Yamamura and M. Fujise, "A new estimation scheme of propagation characteristics using pilot-data-inserted OFDM signals for high-mobility OFDM transmission scheme," IEICE Trans. Commun., vol.E85-B, no.5, pp.882–894, May 2002.

[62] K. Fukawa, H. Suzuki and T. Usami, "OFDM channel estimation with RLS algorithm for different pilot schemes in mobile radio transmission," IEICE Trans. Commun., vol.E86-B, no.1, pp.266–274, Jan. 2003.

[63] W. Lee, "On channel estimation for OFDM systems in multipath environments with relatively large delay spread," Proc. IEEE VTC 2003-Spring, vol.2, 1303–1307, April 2003.

[64] R. Ku, S. Takaoka and F. Adachi, "Bit error rate analysis of OFDM with pilot-assisted channel estimation," IEICE Trans. Commun., vol.E90-B, no.7, pp.1725–1733, July 2007.

[65] H. Harada and Y. Kamio, "A feasibility study of the 16QAM-OFDM transmission scheme for multimedia mobile access communication systems," IEICE Trans. Commun., vol.E84-B, no.8, pp.2207–2218, Aug. 2001.

[66] H. Futaki and T. Ohtsuki, "Low-density parity-check (LDPC) coded OFDM systems," Proc. IEEE VTC 2001-Fall, vol.1, pp.82–86, Oct. 2001.

[67] F. Tosato and P. Bisaglia, "Simplified soft-output demapper for binary interleaved COFDM with application to HIPERLAN/2," Proc. IEEE ICC 2002, vol.2, pp.664–668, April 2002.

[68] D. Abematsu, T. Ohtsuki, S. Jarot and T. Kaneko, "Performance evaluation of LDPC coded high data rate multiband OFDM systems," IEICE Technical Report, RCS2005-129, pp.31–36, Jan. 2006.

[69] J. van de Beek, M. Sandell and P. Borjesson, "ML estimation of time and frequency offset in OFDM systems," IEEE Trans. Signal Process., vol.45, no.7, pp.1800–1805, July 1997.

[70] T. Schmidl and D. Cox, "Robust frequency and timing synchronization for OFDM," IEEE Trans. Commun., vol.45, no.12, pp.1613–1621, Dec. 1997.

[71] T. Onizawa, M. Mizoguchi, M. Morikura, and T. Tanaka, "A fast synchronization scheme of OFDM signals for high-rate wireless LAN," IEICE Trans. Commun., vol.E82-B, pp.455–463, Feb. 1999.

[72] H. Minn, M. Zeng and V. Bhargava, "On timing offset estimation for OFDM systems," IEEE Commun. Lett., vol.4, no.7, pp.242–244, July 2000.

[73] A. Taira, F. Ishizu and M. Miyake, "A timing synchronization scheme for OFDM in frequency selective fading environment," IEICE Trans. Commun. (Japanese Edition), vol.J84-B, pp.1255–1264, July 2001. (written in Japanese)

[74] E. Larsson, G. Liu, J. Li and G. Giannakis, "Joint symbol timing and channel estimation for OFDM based WLANs," IEEE Commun. Lett., vol.5, no.8, pp.325–327, Aug. 2001.

[75] N. Chen, M. Tanaka and R. Heaton, "OFDM timing synchronization under multi-path channels," Proc. IEEE VTC 2003-Spring, vol.1, pp.378–382, April 2003.

[76] R. Kimura, R. Funada, H. Harada, S. Shinoda and M. Fujise, "A new simple timing synchronization method by subtraction process for OFDM packet transmission systems," Proc. IEEE PIMRC 2003, vol.1, pp.526–530, Sept. 2003.

[77] Y. Mostofi and D. Cox, "Timing synchronization in high mobility OFDM systems," Proc. IEEE ICC 2005, vol.4, pp.2402–2406, June 2004.

[78] R. Kimura, R. Funada, H. Harada, M. Sawada and S. Shinoda, "A timing synchronization method with low-volume DSP for OFDM packet transmission systems," IEICE Trans. Fundamentals, vol.E88-A, no.7, pp.1912–1920, July 2005.

[79] P. Moose, "A technique for orthogonal frequency division multiplexing frequency offset correction," IEEE Trans. Commun., vol.42, pp.2908–2914, Oct. 1994.

[80] T. Pollet, M. van Bladel and M. Moeneclaey, "BER sensitivity of OFDM systems to carrier frequency offset and Wiener phase noise," IEEE Trans. Commun., vol.43, no.2/3/4, pp.191–193, Feb./March/April 1995.

[81] U. Lambrette, M. Speth and H. Meyr, "OFDM burst frequency synchronization by single carrier training data," IEEE Commun. Lett., vol.1, no.2, pp.46–48, March 1997.

[82] H. Aoki, M. Konishi, F. Sasamori and F. Takahata, "An initial acquisition scheme of carrier frequency in OFDM system," IEICE Trans. Commun. (Japanese Edition), vol.J82-B, no.9, pp.1709–1721, Sept. 1999. (written in Japanese)

[83] M. Konishi, T. Hosokawa, T. Maeda and F. Takahata, "A frame timing and carrier frequency synchronization scheme for OFDM using frequency shifted signal," IEICE Trans. Commun. (Japanese Edition), vol.J84-B, no.1, pp.61–70, Jan. 2001. (written in Japanese)

[84] J. Li, G. Liu and G. Giannakis, "Carrier frequency offset estimation for OFDM-based WLANs," IEEE Signal Process. Lett., vol.8, no.3, pp.80–82, March 2001.

[85] Y. Zhao and S. Haggman, "Sensitivity to Doppler shift and carrier frequency errors in OFDM systems —the consequences and solutions," Proc. IEEE VTC 1996, vol.3, pp.1564–1568, May 1996.

[86] G. Malmgren, "Impact of carrier frequency offset, Doppler spread and time synchronization errors in OFDM based single frequency networks," Proc. IEEE GLOBECOM 1996, vol.1, pp.729–733, Nov. 1996.

[87] P. Robertoson and S. Kaiser, "The effects of Doppler spreads in OFDM(A) mobile radio systems," Proc. IEEE VTC 1999-Fall, vol.1, pp.329–333, Sept. 1999.

[88] Y. Li and L. Cimini, "Interchannel interference of OFDM in mobile radio channels," Proc. IEEE GLOBECOM 2000, vol.2, pp.706–710, Nov. 2000.

[89] Y. Li and L. Cimini, "Bounds on the interchannel interference of OFDM in time-varying impairments," IEEE Trans. Commun., vol.49, no.3, pp.401–404, March 2001.

[90] Y. Mostofi and D. Cox, "ICI mitigation for pilot-aided OFDM mobile systems," IEEE Trans. Wireless Commun., vol.4, no.2, pp.765–774, March 2005.

[91] R. van Nee, "OFDM codes for peak-to-average power reduction and error correction," Proc. IEEE GLOBECOM 1996, vol.1, pp.740–744, Nov. 1996.

[92] S. Li and L. Cimini, "Effects of clipping and filtering on the performance of OFDM," Proc. IEEE VTC 1997, vol.2, pp.1634–1638, May 1997.

[93] J. Davis and J. Jedweb, "Peak-to-mean power control in OFDM, Golay complementary sequences, and Reed-Muller codes," IEEE Trans. Info. Theory, vol.45, no.7, pp.2397–2415, Nov. 1999.

[94] S. Deng and M. Lin, "OFDM PAPR reduction using clipping with distortion control," Proc. IEEE ICC 2005, vol.4, pp.2563–2567, May 2005.

[95] Z. Fedra, R. Marsalek and V. Sebesta, "Interleaving optimization in OFDM PAPR reduction," Proc. International Conference on Radioelektronika 2007, April 2007.

[96] C. Choi, Y. Shoji, H. Harada, R. Funada, S. Kato, K. Maruhashi, I. Toyoda and K. Takahashi, "RF impairment models for 60-GHz band SYS/PHY simulation," IEEE P802.15 Working Group for Wireless Personal Area Networks, IEEE802.15-06-477-01-003c, Nov. 2006.

[97] T. Ohgane, T. Nishimura and Y. Ogawa, "Applications of space division multiplexing and those performance in a MIMO channel," IEICE Trans. Commun., vol.E88-B, no.5, pp.1843–1851, May 2005.

[98] M. Jankiraman, Space-Time Codes and MIMO Systems, Artech House, 2004.

[99] V. Lay and Y. Kwok, Channel Adaptive Technologies and Cross Layer Designs for Wireless Systems with Multiple Antennas, John Wiley & Sons, Inc., 2006.

[100] G. Foschini and M. Gans, "On limits of wireless communications in a fading environment when using multiple antennas," Wireless Personal Communcations, vol.6, no.3, pp.311–335, March 1998.

[101] P. Vandenameele, L.V.D. Porre, M.G.E. Engels, B. Gyselinckx, and H.J.D. Man, "A combined OFDM/SDMA approach," IEEE J. Sel. Areas Commun., vol.18, no.11, pp.2312–2321, Nov. 2000.

[102] The third generation partnership project, "Spatial channel model for multiinput multioutput (MIMO) simulations," ETSI TR 125 996, V6.1.0, Sept. 2003.

[103] H. Yang, "A road to future broadband wireless access: MIMO-OFDM-based air interface," IEEE Commun. Mag., vol.43, no.1, pp.53–60, Jan. 2005.

[104] S. Nanda, R. Walton, J. Ketchum, M. Wallace and S. Howard, "A high-performance MIMO OFDM Wireless LAN," IEEE Commun. Mag., vol.43, no.2, pp.101–109, Feb. 2005.

[105] K. Higuchi, H. Kawai, N. Maeda, H. Taoka and M. Sawahashi, "Experiments on real-time 1-Gb/s packet transmission using MLD-based signal detection in MIMO-OFDM broadband radio access," IEEE J. Sel. Areas Commun., vol.24, no.6, pp.1141–1153, June 2006.

[106] G.D. Golden, C.J. Foschini, R.A. Valenzuela, and P.W. Wolniansky, "Detection algorithm and initial laboratory results using V-BLAST space-time communication architecture," Electron. Lett., vol.35, no.1, pp.14–16, Jan. 1999.

[107] A. van Zelst, R. van Nee, and G.A. Awater, "Space division multiplexing (SDM) for OFDM systems," Proc. IEEE VTC 2000-Spring, vol.2, pp.1070–1074, May 2000.

[108] T. Koike, D. Nishikawa and S. Yoshida, "Simplified maximum-likelihood detection scheme employing metric segmentation and norm constraint," IEICE Technical Report, RCS2004-291, pp.7–12, Jan. 2005. (written in Japanese)

[109] Y. Seki, T. Koike, H. Murata, S. Yoshida and K. Araki, "FPGA implementation and performance evaluation of real-time MIMO-MLD using simplified metrics," IEICE Technical Report, RCS2004-292, pp.13–18, Jan. 2005. (written in Japanese)

[110] X. Li, H. Huang, A. Lozano and G. Foschini, "Reduced-complexity detection algorithms for systems using multi-element arrays," Proc. IEEE GLOBECOM 2000, vol.2, pp.1072–1076, Dec. 2000.

[111] T. Aoki, H. Matsuoka and H. Shoki, "Novel reduced complexity algorithm based on group detection in multiple antenna systems," Proc. IEEE PIMRC 2004, vol.2, pp.1444–1448, Sept. 2004.

[112] T. Aoki, Y. Tanabe, H. Matsuoka and H. Shoki, "Reduced complexity max-log-MAP sphere decoder using group detection in MIMO-OFDM systems," IEICE Trans. Commun., vol.E88-B, no.11, pp.4220–4228, Nov. 2005.

[113] Y. Teng, K. Naito, K. Mori and H. Kobayashi, "Complexity reduced maximum likelihood detection for SDM-OFDM system," IEICE Trans. Commun., vol.E89-B, no.7, pp.2084–2087, July 2006.

[114] G. Awater, A. van Zelst and R. van Nee, "Reduced complexity space division multiplexing receivers," Proc. IEEE VTC 2000-Spring, vol.1, pp.11-15, Sept. 2000.

[115] K. Kim and J. Yue, "Joint channel estimation and data detection algorithms for MIMO-OFDM systems," Proc. Thirty-Sixth Asilomar Conference on Signals, Systems and Computers, pp.1857–1861, Nov. 2002.

[116] H. Kawai, K. Higuchi, N. Maeda, M. Sawahashi, T. Ito, Y. Kakura, A. Ushirokawa and H. Seki, "Likelihood function for QRM-MLD suitable for soft-decision turbo decoding and its performance for OFCDM MIMO multiplexing in multipath fading channel," IEICE Trans. Commun., vol.E88-B, no.1, pp.47–57, Jan. 2005.

[117] E. Viterbo and J. Boutros, "A universal lattice code decoder for fading channels," IEEE Trans. Info. Theory, vol.45, no.5, pp.1639–1642, July 1999.

[118] B. Hochwald and S. Brink, "Achieving near-capacity on a multiple-antenna channel," IEICE Trans. Commun., vol.51, no.3, pp.389–399, March 2003.

[119] H. Vikalo, B. Hassibi and T. Kailath, "Iterative decoding for MIMO channels via modified sphere decoding," IEEE Trans. Wireless Commun., vol.3, no.6, pp.2299–2311, Nov. 2004.

[120] M. Yee, "Max-log-MAP sphere decoder," Proc. IEEE ICASSP 2005, vol.3, pp.1013–1016, March 2005.

[121] T. Cui and C. Tellambura, "Approximate ML detection for MIMO systems using multistage sphere decoding," IEEE Signal Processing Lett., vol.12, no.3, pp.222–225, March 2005.

[122] V. Pammer, Y. Delignon, W. Sawaya and D. Boulinguez, "A low complexity suboptimal MIMO receiver: the combined ZF-MLD algorithm," Proc. IEEE PIMRC 2003, vol.3, pp.2271–2275, Sept. 2003.

[123] T. Fujita, A. Ohta, T. Onizawa and T. Sugiyama, "Reduced-complexity signal detection scheme employing ZF and K-best algorithms for OFDM/SDM," IEICE Trans. Commun., vol.E88-B, no.1, pp.66–75, Jan. 2005

[124] R. Kimura, R. Funada, H. Harada and S. Shimamoto, "Multiple-QR-decomposition assisted group detection for reduced-complexity-and-latency MIMO-OFDM receivers," Proc. IEEE PIMRC 2006, Sept. 2006.

[125] R. Funada, H. Harada, Y. Kamio, S. Shinoda, and M. Fujise, "A high-mobility packet transmission scheme based on conventional standardized OFDM formats," Proc. IEEE VTC 2002-Fall, vol.1, pp.204–208, Sept. 2002.

[126] R. Funada, H. Harada and S. Shinoda, "Performance improvement of decision-directed OFDM channel estimation in a fast fading environment," IEICE Trans. Fundamentals, vol.E87-A, no.8, pp.1994–2001, Aug. 2004.

[127] T. Tsutsumi, T. Nishimura, T. Ohgane and Y. Ogawa, "An impact of channel state information error on SDM applications," IEICE Trans. Commun. (Japanese Edition), vol.J87-B, no.9, pp.1496–1504, Sept. 2004. (written in Japanese)

[128] H. Kawai, N. Maeda, K. Higuchi and M. Sawahashi, "Effect of multi-slot and sub-carrier averaging channel estimation filter in QRM-MLD for MIMO multiplexing using OFDM," IEICE Technical Report, RCS2004-68, pp.73–78, May 2004. (written in Japanese)

[129] K. Adachi, R. Esmailzadeh, M. Nakagawa, H. Kawai and K. Higuchi, "Accurate channel estimation method using decision feedback data symbols af-

ter soft-decision turbo decoding in QRM-MLD for OFDM MIMO multiplexing," Proc. WPMC 2005, pp.716–720, Sept. 2005.

[130] M. Munster and L. Hanzo, "Parallel-interference-cancellation-assisted decision-directed channel estimation for OFDM systems using multiple transmit antennas," IEEE Trans. Wireless Commun., vol.4, no.5, pp.2148–2162, Sept. 2005.

[131] Y. Asai, W. Jiang, T. Onizawa and S. Aikawa, "Experimental studies on simplified decision-feedback channel tracking scheme for MIMO-OFDM systems," IEICE Technical Report, RCS2006-135, pp.13–18, Oct. 2006. (written in Japanese)

[132] Y. Asai, W. Jiang, T. Onizawa, A. Ohta and S. Aikawa, "A simplified and feasible decision-feedback channel tracking scheme for MIMO-OFDM systems," IEICE Trans. Commun., vol.E90-B, no.5, pp.1052–1060, May 2007.

[133] K. Yokomakura, S. Sampei, H. Harada and N. Morinaga, "A carrier interferometry based channel estimation technique for MIMO-OFDM/TDMA systems," IEICE Trans. Commun., vol.E90-B, no.5, pp.1181–1192, May 2007.

[134] Y. Li, L. Cimini and N. Sollenberger, "Robust channel estimation for OFDM systems with rapid dispersive fading channels," IEEE Trans. Commun., vol.46, no.7, pp.902–915, July 1998.

[135] Y. Li, N. Seshadri and S. Ariyavisitakul, "Channel estimation for OFDM systems with transmitter diversity in mobile wireless channels," IEEE J. Sel. Areas Commun., vol.17, no.3, pp.461–471, March 1999.

[136] Y. Li, "Simplified channel estimation for OFDM systems with multiple transmit antennas," IEEE Trans. Wireless Commun., vol.1, no.1, pp.67–75, Jan. 2002.

[137] A. Benjebbour, Y. Seki and S. Yoshida, "Simplified channel tracking for MIMO-OFDM systems," IEICE Trans. Commun., vol.E86-B, no.10, pp.3013–3022, Oct. 2003.

[138] A. Stamoulis, S.N. Diggavi and N. Al-Dhahir, "Intercarrier interference in MIMO OFDM," IEEE Trans. Signal Process., vol.50, no.10, pp.2451–2464, Oct. 2002.

[139] A. Taira, Y. Hara, F. Ishizu and K. Murakami, "A performance of channel estimation schemes for multi-carrier systems," IEICE Trans. Commun. (Japanese Edition), vol.J88-B, no.4, pp.751–761, April 2005. (written in Japanese)

[140] A.M. Tonello, N. Laurenti, and S. Pupolin, "Analysis of the uplink of an asynchronous multi-user DMT OFDMA system impaired by time offsets, frequency offsets, and multi-path fading," Proc. IEEE VTC 2000-Fall, vol.3, pp.1094–1099, Sept. 2000.

[141] J.J. van de Beek, P.O. Borjesson, M.L. Boucheret, D. Landstrom, J.M. Arenas, P. Odling, C. Ostberg, M. Wahlqvist, and S.K. Wilson, "A time and frequency synchronization scheme for multiuser OFDM," IEEE J. Sel. Areas Commun., vol.17, pp.1900–1914, Nov. 1999.

[142] S. Barbarossa, M. Pompili, and B. Giannakis, "Channel-independent synchronization of orthogonal frequency division multiple access systems," IEEE J. Sel. Areas Commun., vol.20, pp.474–486, Feb. 2002.

[143] M. Morelli, "Timing and frequency synchronization for the uplink of an OFDMA system," IEEE Trans. Commun., vol.52, pp.296–306, Feb. 2004.

[144] M. Park, K. Ko, H. Yoo, and D. Hong, "Performance analysis of OFDMA uplink systems with symbol timing misalignment," IEEE Commun. Lett., vol.7, pp.376–378, Aug. 2003.

[145] R. Kimura, R. Funada, H. Harada and S. Shinoda, "A new timing synchronization method for uplink DPC-OF/TDMA," IEICE Technical Report, RCS2004-31, pp.43–48, April 2004.

[146] R. Kimura, R. Funada, H. Harada and S. Shinoda, "A study on time alignment control for uplink dynamic parameter controlled OF/TDMA," 2004 IEICE Society Conference, B-5-44, Sept. 2004.

[147] R. Kimura, R. Funada, H. Harada, and S. Shinoda, "Perfomance evaluation of time alignment control under high-mobility environment for dynamic parameter controlled OF/TDMA," IEICE Trans. Commun., vol.E88-B, pp.541–551, Feb. 2005.

[148] R. Kimura, R. Funada, H. Harada, and S. Shinoda, "A complexity reduction scheme of time alignment control for uplink dynamic parameter controlled OF/TDMA," Proc. WPMC 2004, vol.2, pp.21–25, Sept. 2004.

[149] R. Kimura, R. Funada, H. Harada and S. Shinoda, "A study on complexity reduction scheme for time alignment control in uplink dynamic parameter controlled OF/TDMA," IEICE Technical Report, RCS2004-439, pp.43–48, Nov. 2004.

[150] H. Harada, "100 Mbps and beyond point-to-multipoint ultra high-speed radio access system —concept and fundamental experimental results—," Proc. IEEE VTC 2003-Fall, vol.3, pp.1874–1879, Oct. 2004.

[151] H. Harada, R. Matsumiya, and H. Gomi, "A point-to-multipoint wireless access protocol for dynamic parameter controlled OF/TDMA," Proc. WPMC 2004, vol.3, pp.387–391, Sept. 2004.

[152] H. Gomi, H. Harada and S. Shinoda, "Performance evaluation of dynamic parameter controlled OF/TDMA based on PR-DSMA," Proc. IEEE PIMRC 2005, vol.3, pp.1920–1924, Sept. 2005.

[153] T. Nakanishi, S. Sampei, H. Harada, and N. Morinaga, "An OFDM based adaptive modulation scheme employing variable coding rate in dynamic parameter controlled OF/TDMA systems," Proc. WPMC 2004, vol.3, pp.34–38, Sept. 2004.

[154] M. Koshimizu, R. Funada, H. Harada and S. Shirai, "A study on interference estimation method for adaptive modulation of downlink DPC-OF/TDMA," IEICE Technical Report, RCS2004-85, pp.55–60, June 2004. (written in Japanese)

[155] H. Harada, R. Funada, R. Kimura and S. Sampei, "Laboratory experiments on dynamic parameter controlled OF/TDMA system," IEICE Technical Report, RCS2006-151, pp.107-112, Oct. 2006. (written in Japanese)

[156] Y. Sun, and L. Tong, "Channel equalization for wireless OFDM systems with ICI and ISI," Proc. IEEE ICC '99, vol.1, pp.182–186, June 1999.

[157] S. Suyama, Y. Hara, H. Suzuki, Y. Kamio, and K. Fukawa, "A maximum likelihood OFDM receiver with smoothed FFT-window for large multipath

delay difference over the guard interval," Proc. IEEE VTC 2002-Spring, vol.3, pp.1247–1251, May 2002.

[158] S. Sangsathit, S. Suyama, K. Fukawa and H. Suzuki, "An OFDM adaptive equalizer with FFT over several symbol interval," IEICE Technical Report, RCS2002-270, pp.103–108, Jan. 2003.

[159] S. Suyama, H. Suzuki and K. Fukawa, "An OFDM turbo equalizer for multipath environments with the delay difference greater than guard interval," IEICE Technical Report, RCS2002-271, pp.109–114, Jan. 2003. (written in Japanese)

[160] L. Yang and S. Cheng, "Interference cancellation with DFE in frequency domain for OFDM systems with insufficient CP," IEICE Trans. Commun., vol.E88-B, no.12, pp.4616–4624, Dec. 2005.

[161] N. Suzuki, H. Uehara, and M. Yokoyama, "A new OFDM demodulation method with variable-length effective symbol and ICI canceller," IEICE Trans. Fundamentals, vol.E85-A, pp.2859–2867, Dec. 2002.

[162] T. Matsuda, S. Hara and N. Morinaga, "Application of multirate filter bank to group demodulation of frequency-multiplexed TDMA signals," IEICE Trans. Commun. (Japanese Edition), vol.J83-B, pp.1217–1225, Sept. 2000. (written in Japanese)

[163] S.L. Goff, A. Glavieux, and C. Berrou, "Turbo-codes and high spectral efficiency modulation," Proc. IEEE ICC '94, vol.2, pp.645–649, May 1994.

[164] P. Robertson, E. Villebrun, and P. Hoeher, "Comparison of optimal and sub-optimal MAP decoding algorithm operating in the log domain," Proc. IEEE ICC '95, vol.2, pp.1009–1013, June 1995.

[165] Xilinx, Inc. website, http://www.xilinx.com/products/tables/fpga.htm

[166] R. Kimura and S. Shimamoto, "A multi-carrier based approach to wireless duplex: orthogonal frequency division duplex (OFDD)," Proc. IEEE ISWCS 2006, Sept. 2006.

[167] R. Kimura and S. Shimamoto, "An orthogonal frequency division duplex (OFDD) system using an analog filter bank," Proc. IEEE WCNC 2007, pp.2275–2280, March 2007.

[168] R. Kimura, R. Funada, H. Harada and S. Shimamoto, "A highly mobile SDM-OFDM system using reduced-complexity-and-latency processing," Proc. IEEE PIMRC 2007, Sept. 2007.

[169] S. Winder, Analog and Digital Filter Design, Second Edition, Newnes, 2002.

[170] The Mathworks, Inc. website, http://www.mathworks.com/

[171] T. Yoshiki, S. Sampei and N. Morinaga, "High bit rate transmission scheme with a multilevel transmit power control for the OFDM based adaptive modulation systems," Proc. IEEE VTC 2001-Spring, vol.1, pp.727–731, May 2001.

[172] T. Nakanishi, S. Sampei, H. Harada and N. Morinaga, "An OFDM based adaptive modulation scheme employing variable coding rate," IEICE Trans. Commun., vol.E88-B, no.2, pp.526–534, Feb. 2005.

[173] C. Wong, R. Cheng, K. Letaief and R. Murch, "Multiuser subcarrier allocation for OFDM transmission using adaptive modulation," Proc. IEEE VTC 1999-Spring, vol.1, pp.479–483, May 1999.

[174] J. Fu and Y. Karasawa, "Fundamental analysis on throughput characteristics of orthogonal frequency division multiple access (OFDMA) in multipath propagationenvironments," IEICE Trans. Commun. (Japanese Edition), vol.J85-B, no.11, pp.1884–1894, Nov. 2002.

[175] L. Wang and Z. Niu, "An efficient rate and power allocation algorithm for multiuser OFDM systems," IEICE Trans. Commun., vol.E88-B, no.12, pp.4686–4689, Dec. 2005.

[176] R. Mino, S. Tsumura, Y. Hara and S. Hara, "A study on sub-carrier assignment method for multi-user OFDMA system," 2005 IEICE General Conference, B-5-31, March 2005. (written in Japanese)

[177] M. Furudate, T. Yamamoto, H. Ishikawa and T. Suzuki, "Throughput performance evaluation of OFDMA with sub-carrier adaptive control," 2005 IEICE General Conference, B-5-39, March 2005.

[178] K. Koumadi and Y. Han, "TDD time slot allocation and interference analysis for HDD sellular systems," Proc. APCC 2006, Aug. 2006.

[179] H. Yomo and R. Reynisson, "A power control method for channel non-reciprocity compensation in hybrid duplexing," Proc. IEEE PIMRC 2006, Sept. 2006.

[180] S. Shin, M. Kim, H. Yu, Y. Kang, N. Kim and O. Shin, "Advanced hybrid OFDM system with multi-layer TDD architecture," Proc. IEEE VTC 2007-Spring, pp.2712–2716, April 2007.

[181] S. Yun, S. Park, Y. Lee, D. Park, Y. Kim, K. Kim and C. Kang, "Hybrid division duplex system for next-generation cellular services," IEEE Trans. Veh. Technol., vol.56, no.5, pp.3040–3059, Sept. 2007.

[182] D. Mottier and D. Castelain, "SINR-based channel pre-equalization for uplink multi-carrier CDMA systems," Proc. IEEE PIMRC 2002, vol.4, pp.1488–1492, Sept. 2002.

[183] H. Suzuki, K. Itoh, Y. Ebine and M. Sato, "A booster configuration with adaptive reduction of transmitter-receiver antenna coupling for pager systems," Proc. IEEE VTC 1999-Fall, vol.3, pp.1516–1520, Sept. 1999.

[184] IEEE802.15.3c Task Group website, http://www.ieee802.org/15/pub/TG3c.html

[185] IEEE802.11 Working Group website, http://www.ieee802.org/11/

[186] IEEE802.15.3a Task Group website, http://www.ieee802.org/15/pub/TG3a.html

[187] TGn Sync website, http://www.tgnsync.org/

[188] WWiSE website, http://www.wwise.org/

[189] WiMedia Alliance website, http://www.wimedia.org/

[190] J. Lansford, "Mid-week Update for 802.15 WG Meeting," IEEE P802.15 Working Group for Wireless Personal Area Networks, IEEE802.15-06-0050-00-003a, Jan. 2006.

[191] M. McInnis, "Waikoloa TG3a interlim meeting minutes," IEEE P802.15 Working Group for Wireless Personal Area Networks, IEEE802.15-06-0057-00-003a, Jan. 2006.

[192] M. Golay, "Complementary series," IRE Trans. Inf. Theory, vol.IT-11, pp.82–87, April 1961.

[193] S. Budisin, "Efficient pulse compressor for Golay complementary sequences," Electronics Letters, vol.27, no.3, pp.219–220, Jan. 1991.

[194] B. Popovic, "Efficient Golay correlator," Electronics Letters, vol.35, no.17, pp.1427–1428, Aug. 1999.

[195] IEEE802.15 Working Group document server, https://mentor.ieee.org/802.15/documents/

[196] S. Kato, Y. Shoji, H. Harada, M. Ando, H. Ikeda, Y. Oishi, K. Kawasaki, K. Takahashi, I. Toyoda, H. Nakase and K. Maruhashi, "Research and standardization activity for IEEE802.15.3c mmW WPAN —(1) overview —," IEICE Technical Report, RCS2006-278, pp.175–178, March 2007.

[197] Y. Shoji, C. Choi, S. Kato, I. Toyoda, K. Kawasaki, Y. Oishi, K. Takahashi and H. Nakase, "Research and standardization activity for IEEE802.15.3c mmW WPAN —(2) target applications and usage model —," IEICE Technical Report, RCS2006-279, pp.179–182, March 2007.

[198] H. Sawada, K. Sato, T. Shoji, C. Choi, R. Funada, H. Harada, S. Kato and M. Umehira, "Research and standardization activity for IEEE802.15.3c mmW WPAN —(3) channel model —," IEICE Technical Report, RCS2006-280, pp.183–186, March 2007. (written in Japanese)

[199] H. Harada, R. Funada, M. Lei, C. Choi, Y. Nishiguchi, Y. Shoji, S. Kato, M. Takeda, I. Toyoda, K. Takahashi, K. Kawasaki, S. Kitazawa and H. Nakase, "Research and standardization activity for IEEE802.15.3c mmW WPAN —(4) design of PHY layer and evaluation method —," IEICE Technical Report, RCS2006-281, pp.187–190, March 2007. (written in Japanese)

[200] F. Kojima, Z. Lan, C. Pyo, S. Kato, H. Nakase, Y. Nagai, T. Yamauchi, T. Maeda, H. Ikeda and Y. Oishi, "Research and standardization activity for IEEE802.15.3c mmW WPAN —(5) study on essential items for 15.3cMAC —," IEICE Technical Report, RCS2006-282, pp.191–194, March 2007. (written in Japanese)

[201] I. Toyoda, M. Ando, K. Iigusa, K. Sawada, K. Maruhashi, N. Orihashi, T. Seki, S. Nishi, S. Kitazawa, A. Miura, Y. Fujita, H. Uchimura, T. Yoneyama, J. Hirokawa, Y. Hirachi, T. Hirano and J. Takada, "Research and standardization activity for IEEE802.15.3c mmW WPAN —(6) anntena

—,” IEICE Technical Report, RCS2006-283, pp.195–198, March 2007. (written in Japanese)

[202] C. Choi, Y. Shoji, H. Harada, K. Sawada, S. Kato, K. Maruhashi, I. Toyoda, K. Takahashi, Y. Aoki, K. Igarashi, T. Yoneyama, K. Nishikawa, M. Yamauchi, H. Nakase, “Research and standardization activity for IEEE802.15.3c mmW WPAN —(7) millimeter-wave RF front-ends for IEEE802.15.3c —,” IEICE Technical Report, RCS2006-284, pp.199–202, March 2007.

Research Achievements

Journal Papers

1. Ryota Kimura, Ryuhei Funada, Hiroshi Harada and Shoji Shinoda, "Performance evaluation of time alignment control under high-mobility environment for dynamic parameter controlled OF/TDMA," IEICE Trans. Commun., vol.E88-B, no.2, pp.541–551, Feb. 2005.

2. Ryota Kimura, Ryuhei Funada, Hiroshi Harada, Manabu Sawada and Shoji Shinoda, "A timing synchronization method with low-volume DSP for OFDM packet transmission systems," IEICE Trans. Fundamentals, vol.E88-A, no.7, pp.1912–1920, July 2005.

3. Ryota Kimura, Ryuhei Funada, Hiroshi Harada and Shigeru Shimamoto, "A complexity-reduced time alignment control in uplink dynamic parameter controlled OF/TDMA," IEICE Trans. Commun., vol.E89-B, no.8, pp.2196–2207, Aug. 2006.

International Conference Papers

1. Ryota Kimura, Ryuhei Funada, Hiroshi Harada, Shoji Shinoda and Masayuki Fujise, "A new simple timing synchronization method by subtraction process for OFDM packet transmission systems," Proc. IEEE Personal, Indoor and Mobile Radio Communications (PIMRC) 2003, vol.1, pp.526–530, Sept. 2003.

2. Ryota Kimura, Ryuhei Funada, Hiroshi Harada and Shoji Shinoda, "A novel time alignment control for uplink dynamic parameter controlled OF/TDMA," Proc. IEEE Personal, Indoor and Mobile Radio Communications (PIMRC) 2004, vol.4, pp.2337–2341, Sept. 2004.

3. Ryota Kimura, Ryuhei Funada, Hiroshi Harada and Shoji Shinoda, “A complexity reduction scheme of time alignment control for uplink dynamic parameter controlled OF/TDMA,” Proc. Wireless Personal Multimedia Communications (WPMC) 2004, vol.2, pp.21–25, Sept. 2004.

4. Ryota Kimura, Ryuhei Funada, Hiroshi Harada and Shigeru Shimamoto, “A complexity-reduced time alignment control with a 2-step precedence path detection in uplink dynamic parameter controlled OF/TDMA,” Proc. International Symposium on Wireless Personal Multimedia Communications (WPMC) 2005, pp.1122–1126, Sept. 2005.

5. Ryota Kimura and Shigeru Shimamoto, “A multi-carrier based approach to wireless duplex: orthogonal frequency division duplex (OFDD),” Proc. IEEE International Symposium on Wireless Communication Systems (ISWCS) 2006, Sept. 2006.

6. Ryota Kimura, Ryuhei Funada, Hiroshi Harada and Shigeru Shimamoto, “Multiple-QR-decomposition assisted group detection for reduced-complexity-and-latency MIMO-OFDM receivers,” Proc. IEEE International Symposium on Personal, Indoor and Mobile Radio Communications (PIMRC) 2006, Sept. 2006.

7. Ryota Kimura and Shigeru Shimamoto, “An orthogonal frequency division duplex (OFDD) system using an analog filter bank,” Proc. IEEE Wireless Communications and Networking Conference (WCNC) 2007, pp.2275–2280, March 2007.

8. Ryota Kimura, Ryuhei Funada, Hiroshi Harada and Shigeru Shimamoto, “A highly mobile SDM-OFDM system using reduced-complexity-and-latency processing,” Proc. IEEE International Symposium on Personal, Indoor and Mobile Radio Communications (PIMRC) 2007, Sept. 2007.

9. Ryuhei Funada, Hiroshi Harada, Yozo Shoji, Ryota Kimura, Yoshinori Nishiguchi, Ming Lei, Chang-Soon Choi, Fumihide Kojima, Chang-Woo Pyo, Zhou Lan, Ismail Lakkis, Masahiro Umehira and Shuzo Kato, “A design of single carrier based PHY for IEEE 802.15.3c standard,” Proc. IEEE International Symposium on Personal, Indoor and Mobile Radio Communications (PIMRC) 2007, Sept. 2007.

10. Ryota Kimura and Shigeru Shimamoto, “Multi-carrier division duplex towards flexible wireless networks,” Proc. IEEE Consumer Communications and Networking conference (CCNC) 2008, Jan. 2008.

Domestic and Japanese Conference Papers

1. Ryota Kimura, Ryuhei Funada, Hiroshi Harada, Shoji Shinoda and Masayuki Fujise, “A study on quantization error of high-mobility OFDM wireless transmission scheme,” 2003 IEICE General Conference, B-5-66, March 2003. (written in Japanese)

2. Ryota Kimura, Ryuhei Funada, Hiroshi Harada and Shoji Shinoda, “A study on timing synchronization method of uplink DPC-OF/TDMA,” 2004 IEICE General Conference, B-5-68, March 2004. (written in Japanese)

3. Ryota Kimura, Ryuhei Funada, Hiroshi Harada and Shoji Shinoda, “A new timing synchronization method for uplink DPC-OF/TDMA,” IEICE Technical Report, RCS2004-31, pp.43–48, April 2004. (written in Japanese)

4. Ryota Kimura, Ryuhei Funada, Hiroshi Harada and Shoji Shinoda, “A study on time alignment control for uplink dynamic parameter controlled OF/TDMA,” 2004 IEICE Society Conference, B-5-44, Sept. 2004. (written in Japanese)

5. Ryota Kimura, Ryuhei Funada, Hiroshi Harada and Shoji Shinoda, “A study on complexity reduction scheme for time alignment control in uplink dynamic parameter controlled OF/TDMA,” IEICE Technical Report, RCS2004-439, pp.43–48, Nov. 2004. (written in Japanese)

6. Ryota Kimura, Ryuhei Funada, Hiroshi Harada and Shoji Shinoda, “A sequentially updated channel estimation method for MIMO-OFDM systems in fast time-variant fading conditions,” 2005 IEICE General Conference, B-5-87, March 2005. (written in Japanese)

7. Ryota Kimura, Ryuhei Funada, Hiroshi Harada and Shigeru Shimamoto, “A sequentially-updated channel estimation combined with multi-QRD signal detection for SDM-OFDM in a fast-variant fading condition,” IEICE Technical Report, RCS2005-113, pp.37–42, Nov. 2005. (written in Japanese)

8. Ryota Kimura and Shigeru Shimamoto, “A proposal of a multi-carrier based duplex scheme; orthogonal frequency division duplex (OFDD),” 2006 IEICE General Conference, B-5-6, March 2006. (written in Japanese)

9. Ryota Kimura and Shigeru Shimamoto, “BER evaluation of orthogonal frequency division duplex wireless communication under the presence of interlink interference,” IEICE Technical Report, RCS2006-26, pp.49–54, May 2006. (written in Japanese)

10. Ryota Kimura, Ryuhei Funada, Hiroshi Harada and Shigeru Shimamoto, “A multi-QR-decomposition assisted group detection algorithm for MIMO-OFDM,” IEICE Technical Report, RCS2006-124, pp.115–120, Aug. 2006. (written in Japanese)

11. Masahiko Kamiyama, Ryota Kimura, Ryuhei Funada, Hiroshi Harada and Hiroshi Shirai, “Maximum likelihood estimation for frame control message slots in downlink one-cell reuse DPC-OF/TDMA system,” 2006 IEICE Society Conference, B-5-10, Sept. 2006. (written in Japanese)

12. Hiroshi Harada, Ryuhei Funada, Ryota Kimura and Seiichi Sampei, “Laboratory experiments on dynamic parameter controlled OF/TDMA system,” IEICE Technical Report, RCS2006-151, pp.107–112, Oct. 2006. (written in Japanese)

13. Masahiko Kamiyama, Ryuhei Funada, Ryota Kimura, Hiroshi Harada and Hiroshi Shirai, “Maximum likelihood estimation combined with sequentially-updated channel estimation for frame control message slots in downlink single frequency reuse DPC-OF/TDMA system,” IEICE Technical Report, RCS2006-183, pp.49–54, Jan. 2007. (written in Japanese)

14. Ryota Kimura and Shigeru Shimamoto, “Loop signal reduction by an analog filter bank for orthogonal frequency division duplex (OFDD),” 2007 IEICE General Conference, B-5-82, March 2007. (written in Japanese)

15. Toru Inoue, Ryota Kimura, Ryuhei Funada, Hiroshi Harada and Hiroshi Shirai, “Optimization of interleave for convolutional-encoded QAM orthogonal frequency division multiple access schemes,” 2007 IEICE Society Conference, B-5-18, Sept. 2007. (written in Japanese)

Standardization Activities

1. Hiroshi Harada, et al., "CoMPA PHY proposal," IEEE P802.15 Working Group for Wireless Personal Area Networks, IEEE802.15-07-0693-03-003c, May 2007.

2. Hiroshi Harada, et al., "Unified and flexible millimeter wave WPAN systems supported by common mode," IEEE P802.15 Working Group for Wireless Personal Area Networks, IEEE802.15-07-0761-15-003c, Nov. 2007.

3. Hiroshi Harada, et al., "Merged proposal: new PHY layer and enhancement of MAC for mmWave system proposal," IEEE P802.15 Working Group for Wireless Personal Area Networks, IEEE802.15-07-0934-01-003c, Nov. 2007.

4. Hiroshi Harada, et al., "SC-PHY MCS updates of the baseline document," IEEE P802.15 Working Group for Wireless Personal Area Networks, IEEE802.15-08-0056-01-003c, Jan. 2008.

Patents

1. 原田博司, 木村亮太, 船田龍平, "基地局および通信方法," 特許第 3806763 号.

2. 木村亮太, 原田博司, 船田龍平, "信号復号装置, 信号復号方法, プログラム並びに情報記録媒体," 特許公開 2007-134911.

Others

1. Ryota Kimura and Shigeru Shimamoto, "A proposal of orthogonal frequency division duplex scheme towards flexible and efficient wireless networks," The Annual Symposium on the 21st Century COE Program in Waseda University: Productive ICT Academia Program, March 2006.

2. Ryota Kimura and Shigeru Shimamoto, "A new wireless duplex scheme based on the multi-carrier technique towards flexible radio resource management," Wireless Technology Park 2006, April 2006.

(February 12, 2008.)